PhD degree in Molecular Medicine

European School of Molecular Medicine (SEMM),

University of Milan and University of Naples "Federico II"

Faculty of Medicine

The role of the B cell antigen receptor in a mouse model of Non-Hodgkin lymphoma

Gabriele Varano

IFOM-IEO Campus, Milan

Registration Number R08394

Supervisor: Dr. Stefano Casola

IFOM-IEO Campus, Milan

Academic year 2011-2012

Table of Contents

1 List of abbreviations

2-NBDG	2-(N-(7-Nitrobenz-2-oxa-1,3-diazol-4-yl)Amino)-2-Deoxyglucose
Abs	Antibodies
AID	Activation-Induced cytidine Deaminase
BAFFR	B-cell-activating factor receptor
BCL-10	B-cell lymphoma 10
BCL-6	
BCR	B cell antigen receptor
BER	Base excision repair
BIM	BCL-2-interacting mediator of cell death
BM	Bone marrow
BrdU	5-bromo-2'-deoxyuridine
BTK	Bruton tyrosine kinase
CARD11	caspase recruitment domain 11
CBs	Centroblasts
CCN	Cyclin
CCR7	Chemokine receptor 7
CCs	Centrocytes
cDNA	Complementary DNA
CDR	Complementarity determining regions
CDRs	Complementarity-determining regions
CFSE	5-(and-6)-carboxyfluorescein diacetate, succinimidyl ester
C_H	IgH chain constant region
CLPs	common lymphoid progenitors
CSR	Class Switch Recombination
D	Diversity region
DG	Diacylglycerol
EBV	Epstein-Barr virus
ER	Endoplasmic reticulum
ERK	Extracellular signal-regulated kinase
Fab	Fragment antigen-binding
FACS	Fluorescence-activated cell sorting
FCCP	protonophore carbonylcyanide-4-(trifluoromethoxy)-phenylhydrazone
FDCs	Follicular dendritic cells
FITC-VAD-FMK	carbobenzoxy-valyl-alanyl-aspartyl-[O-methyl]-fluoromethylketone
FO	Follicular
FSC	Forward Scatter
GC	Germinal Center
GSK3β	Glycogen synthase Kinase 3 beta
H	Heavy Chain
HCV	Hepatitis-C Virus

HSCs	Hematopoietic stem cells
IEF	Isoelectric focusing
Ig	Immunoglobulin
IL-7R	interleukin-7 receptor
IP_3	Inositol-1,4,5-trisphosphate
IPA	Ingenuity enrichment pathway analysis
ITAMS	Immunoreceptor tyrosine-based activation motifs
J	Joining region
L	Light chain
LDH	Lactate dehydrogenase
LMPPs	lymphoid-primed multipotent progenitors
MACS	Magnetic activated cell sorting
MALT	Mucosal associated lymphoid tissue
MFI	Median fluorescent intensity
MHCII	Major histocompatibility complex class II
miRNA	Micro-RNAs
MLN	Mesenteric lymph node
MMR	Mismatch repair
MZ	Marginal zone
NFAT	Nuclear factor of activated T-cells
NFkB	Nuclear factor kB
NHEJ	Non homologous end joining
NHL	Non Hodgkin Lymphoma
PCR	Polymerase chain reaction
PCs	Plasma cells
PDK1	3-phosphoinositide-dependent protein kinase 1
PH	Pleckstrin-homology domain
PI	Propidium Iodide
PI3K	Phosphatidylinositol-3-Kinase
PIP_2	Phosphatidylinositol-4,5-bisphosphate
PIP_3	Phosphatidylinositol-3,4,5-trisphosphate
PKB	Protein Kinase B
PKC	Protein Kinase C
PLCγ2	Phospholipase C-γ2
Pro59	Proline-59
PTKs	Protein tyrosine kinases
RAG	Recombination activation gene
RLB2	Retinoblastoma-like 2
RM	Rapamycin
RT	Room temperature
RT-qPCR	Real-time quantitative PCR
S	Switch sequence
SD	Standard deviation
Ser62	Serine 62
SH2	Src-homology-domain
SHM	Somatic Hypermutation
SILAC	Stable Isotope labeling with Aminoacid in cell culture
SLP65	SH2-domain-containing leukocyte protein of 65 kDa
SPL	Spleen
SSC	Side Scatter

SYK	Splen tyrosine kinase
TAK1	TGFb-activated kinase 1
T_{FH}	T follicular helper
Thr58	Threonine 58
TRAIL	TNF-related apoptosis-inducing ligand
V	Variable region
WHO	World Health Organization

2 Figures index

3 Table index

4 ABSTRACT

The B cell antigen receptor (BCR) plays a central role both in early B-cell development and in mature B cells, where it controls survival and allows the organism to mount protective immune responses against foreign antigens. Surface BCR expression is retained in most types of Non-Hodgkin B-cell lymphomas (NHL), where it has been proposed to participate to tumor initiation, maintenance and progression. This study has provided for the first time an *in vivo* genetic proof for the role of the BCR in B-cell lymphomagenesis.

Using the λ-MYC Burkitt lymphoma (BL) mouse model, in which conditional ablation of the BCR can be induced in c-MYC transformed B cells through the Cre/loxP recombination system, I provide evidence for the essential role of the BCR in tumor maintenance. Acute BCR ablation in λ-MYC lymphomas delayed cell cycle progression and augmented apoptosis, causing the rapid disappearance of BCR^- tumor cells when these cells were grown both *in vitro* and *in vivo* in competition with their BCR^+ counterparts. Similar results were obtained using the human Burkitt lymphoma cell line, RAMOS.

This study has also elucidated crucial effectors of tonic BCR signalling that influence the survival and growth of BL cells. BCR inactivation led to a reduction in GSK3β phosphorylation, leading to an increase in its enzymatic activity. Importantly, treatment of lymphoma cells with a GSK3β small molecule inhibitor restored the ability of BCR-deficient lymphomas to compete with their BCR^+ counterparts. I could also show that c-MYC transformed B cells acquired exquisite sensitivity to the mTOR inhibitor rapamycin upon BCR inactivation.

Using a combination of quantitative proteome and whole transcriptome analyses we have started to shed light on the contribution of the BCR to the maintenance of c-MYC

transformed B cells. In λ-MYC lymphomas, the BCR regulated a substantial number of MYC targets genes. Notably, the majority of these shared targets were normalized in BCR^- tumor cells upon pharmacological inhibition of GSK3β. These result point to the tempting hypothesis that the BCR supports MYC-driven lymphomagenesis, by the inhibition of GSK3β-mediated phosphorylation and hence degradation of c-MYC protein.

Finally, our study demonstrates that the failure of c-MYC transformed B cells to grow *in vivo* is strictly dependent on the concomitant presence of their BCR^+ counterparts. This result has important implications for the design of clinical trials limited to the use of inhibitors of the BCR signalling pathway for the treatment of BL and other forms of aggressive NHL. To avoid the outgrowth of BCR^- escape variants in response to such treatments, we propose the integration in the therapeutic protocol of the mTOR inhibitor rapamacyin that showed high efficacy in the killing Ig receptor-less lymphoma cells.

5 INTRODUCTION

Every year, around 350000 new cases of Non-Hodgkin-Lymphomas (NHL) are diagnosed worldwide, accounting for over 190000 cases of death, and with an incidence which has been constantly increasing in the past 2 decades (Boffetta, 2011). Around 95% of NHL are of B-cell origin, and represent a very heterogeneous group of malignancies with different clinical behaviours, therefore requiring diverse treatment strategies. This heterogeneity depends on the combination of genetic events causing malignant transformation of B lymphocytes at defined stages of their differentiation.

A great effort has been made in the past 10 years to identify the cell of origin of human B-cell lymphomas, the identification of key transforming events and the definition of promising therapeutic targets for lymphoma treatment. Importantly, it's becoming clear that key factors, crucial for normal B-cell differentiation and survival, are also required for the growth of most B-cell lymphomas (Küppers, 2005). Among them, the B cell antigen receptor (BCR), whose expression is retained in virtually 100% of B-cell NHL, represents a promising target, as the survival signals supplied in normal B cells might have a similar role on the malignant counterparts.

5.1 B cell development

Generation of B-lymphocytes is a highly regulated process whereby functional subsets of mature B cells are generated from hematopoietic stem cells, in fetal liver during embryogenesis, and in the bone marrow during post-natal life (Hardy and Hayakawa, 2001). Our knowledge of B cell lymphopoiesis has significantly improved over the past two decades through the identification of a combination of surface markers and molecular events associated with specific stages of B-cell development.

5.1.1 Early B-cell development

In postnatal life, the production of B cells is a lifelong process that occurs in the bone marrow (BM) as a result of the differentiation of multipotent hematopoietic stem cells (HSCs). A strictly regulated and hierarchical process promotes the differentiation of HSC into lymphoid-primed multipotent progenitors (LMPPs) that in turn develop into common lymphoid progenitors (CLPs), a highly committed population of lymphoid precursors.

The progression of B-cells through the early stages of development can be tracked using a unique combination of surface markers and through the analysis of the status of the immunoglobulin (Ig) variable (V) region gene loci (Rajewsky, 1996). CLPs give rise to $B220^{+}CD43^{+}c\text{-}kit^{+}IgM^{-}$ pro-B cells, that express the Recombination Activation Genes (RAG)-1 and -2, to promote Ig V-gene rearrangements. In pro-B cells, Ig heavy (H) chain V-genes are assembled through the joining first of D_H and J_H segments (on both IgH alleles), followed by mono-allelic recombination of a single V_H segment to D_HJ_H rearrangements (Alt et al., 1984). Cells carrying a productive IgH V-gene rearrangement differentiate into $B220^{+/lo}CD43^{-}CD25^{+}IgM^{-}$ pre-B cells. Pre-B cells express a pre-B cell receptor consisting of a functional IgH chain paired to V-preB and λ5 surrogate light chains, respectively (Karasuyama et al., 1990; Tsubata and Reth, 1990). Signalling through the pre-BCR and the interleukin-7 receptor (IL-7R) triggers clonal expansion of pre-B cells, at a time when RAG proteins are temporarily down regulated. The switching from proliferation to differentiation signals triggers cell-cycle arrest of pre-B cells and re-activation of the RAG genes, which ultimately promote V_L to J_L gene rearrangements at the IgL chain locus. Expression of a functional IgL chain, and consequently its pairing to the IgH chain, allows the expression on the surface of a B-cell receptor (BCR). Bone marrow B cells expressing a *de novo* BCR on the surface are identified as $B220^{lo/+}CD43^{-}CD25^{-}IgM^{hi}IgD^{-}$ immature

B cells. Before exiting the BM, newly generated B cells are tested for auto reactivity. Depending on the strength of the signal emanating from auto-reactive BCRs, immature B cells: i) undergo secondary IgL chain rearrangements through a process called IgL receptor editing), ii) die through apoptosis, or iii) become unresponsive to cognate antigen (a process also called *anergy;* Goodnow et al., 1988; Retter and Nemazee, 1998; Tiegs et al., 1993). Immature B cells expressing functional, non-autoreactive BCRs exit the bone marrow and through the blood stream home to secondary lymphoid organs, where they complete their development (Allman et al., 1993).

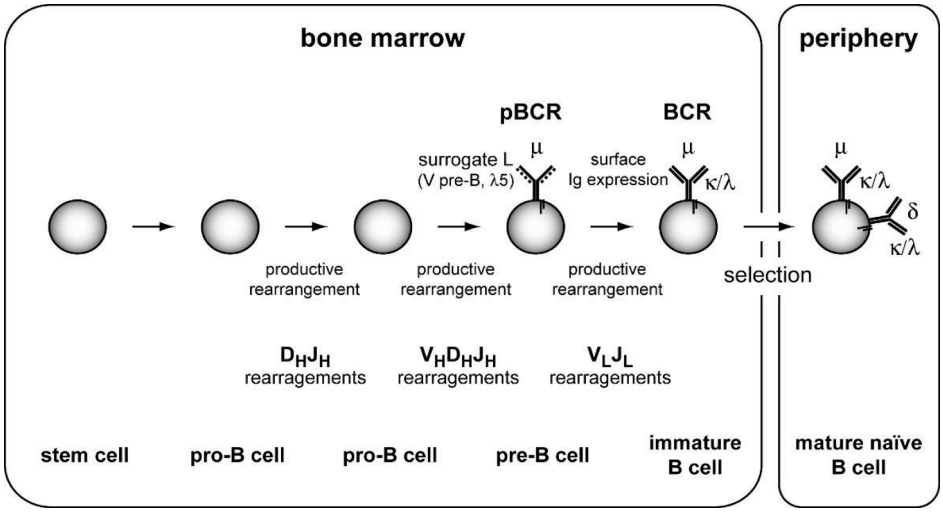

Figure 1: Schematic view of B cell development

Hematopoietic stem cells give rise to pro-B cells through a series of sequential developmental steps. Specific stages of stages of early B-cell lymphopoiesis are defined through the analysis of Ig V-gene rearrangements. When successful VDJ recombination occurs at the IgH locus, a functional IgH chain pairs to surrogate IgL chains to give rise to the pre-B cell receptor (pBCR). Signalling through the pBCR promotes first clonal expansion of pre-B cells and later the rearrangement of Ig L chain V-gene segments. Productive V_L to J_L rearrangements, followed by IgH/IgL chain pairing leads to surface expression of a functional BCR. Newly generated B cells are selected on the basis of their BCR specificity to eliminate autoreactive clones. Only B-cells expressing "innocent" BCRs are allowed to leave the bone marrow and continue their differentiation in secondary lymphoid organs (adapted from (Rajewsky, 1996).

5.1.2 Peripheral B cell differentiation

Newly generated, short-lived $B220^{+}IgM^{hi}IgD^{-}$ immature B cells reach the spleen where they continue their development as transitional B cells identified through a unique combination of surface markers (Allman et al., 2001; Loder et al., 1999). Transitional T1 cells ($B220^{lo}IgM^{+}CD23^{-}$ $AA4.1^{+}$) corresponding to the earliest BM emigrants, give rise to T2 cells ($B220^{lo}IgM^{hi}CD23^{+}$), which ultimately differentiate into the major subsets of mature B cells. Only a limited number of T2 cells is ultimately recruited in the compartments of mature B cells.

According to their origin, function and localization, mature B cells are divided into three main subsets represented by follicular (FO)/B2, marginal zone (MZ) and B1 B cells.

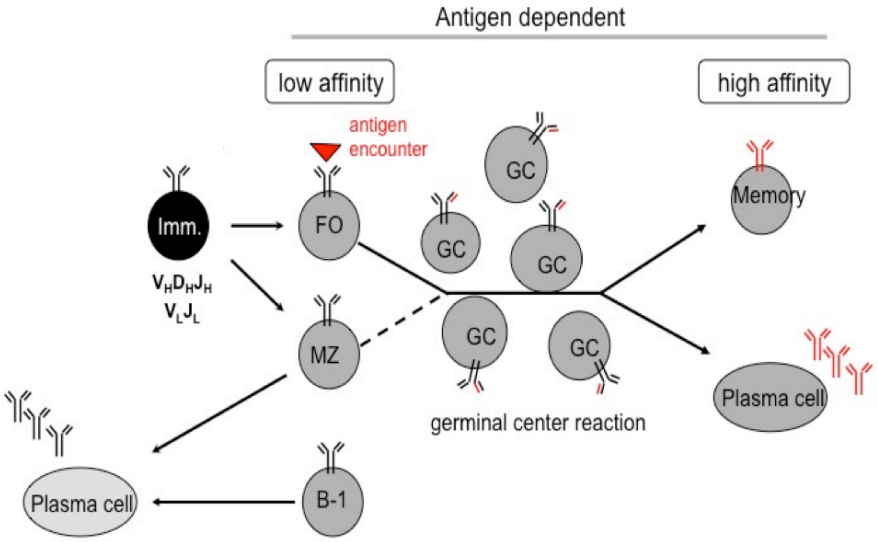

Figure 2: Peripheral B cell development

Bone marrow-derived immature B cells, express a functional BCR on the surface and migrate to secondary lymphoid organs such as spleen and lymph nodes. Here, they complete their differentiation to become respectively follicular (FO), marginal zone (MZ) or B1 B cells. Upon recognition of foreign antigen, in the presence of T-cell help, FO (and in some instances MZ) B cells are recruited to form germinal centers (GC). In GCs, B cells undergo secondary diversification of the antibody repertoire through the process of Ig somatic hypermutation. Only few GC B cells expressing high affinity BCRs are selected to differentiate into long-lived memory and antibody-secreting (ASC) plasma cells. B1 and MZ B cells differentiate directly into ASC in response to antigen recognition, in T-cell independent immune responses.

5.1.2.1 Follicular B cells

FO B cells ($IgM^{hi}IgD^{hi}CD21^{mid}CD23^{+}$) represent the major population of mature B cells present in secondary lymphoid organs. They express both IgM and IgD on the cell surface. The life span of FO B cells ranges from weeks to months (Fulop et al., 1983; Hao and Rajewsky, 2001). FO B cells reside within primary follicles of the white pulp of the spleen and in the cortical area of lymph nodes. FO B cells represent also the primary B-cell subset found in mucosal associated lymphoid tissue (MALT). B2 B cells participate to both T cell-dependent and -independent immune responses. In T-cell dependent immune responses, antigen recognition through the BCR promotes the recruitment of B2 B cells into the germinal center (GC) reaction (see below, 5.1.2.4). As a result of the GC reaction, B2 B cells differentiate into high affinity antibody-secreting plasma cells (PCs) or memory B cells. In T-cell independent immune responses B2 B cells give rises directly to short-lived, low affinity PCs (MacLennan et al., 2003).

5.1.2.2 B-1 B cells

B-1 cells ($IgM^{hi}IgD^{-}B220^{low}CD23^{low}CD43^{+}CD11b^{+}$) are a population of self-renewing B cells, predominantly located in body cavity serosa. According to the Ly-1/CD5 marker, B-1 cells are classified as B-1a ($CD5^{+}$) and B-1b ($CD5^{-}$) B cells (Stall et al., 1992). B-1 B cells originate mainly from fetal liver HSCs that are distinct from those giving rise to B-2 and MZ B cells (Montecino-Rodriguez et al., 2006). B-1 B cells are responsible for the production of so-called *natural* antibodies reactive against a plethora of microbial antigens. These antibodies represent the first line of defence of the organism against invading pathogens (Su and Tarakhovsky, 2000).

5.1.2.3 Marginal Zone B cells

MZ B cells ($IgM^{hi}IgD^{low}CD21^{hi}CD23^{low}$) are exclusively found in the spleen, in close proximity with the marginal sinus, surrounding B cell follicles. MZ B cells are provided with self-renewal capacity (Hao and Rajewsky, 2001) and are recruited into both T cell-dependent and -independent immune responses, in response to blood-borne pathogens (Martin and Kearney, 2002). MZ B cells can rapidly differentiate into IgM- and IgG_3-secreting plasma cells in response to T-cell independent antigens, or alternatively, get efficiently recruited into the GC during a T-cell dependent immune response, given the efficient presentation of antigens via major histocompatibility complex class II (MHCII) molecules (Lopes-Carvalho et al., 2005).

The identification of the precursor cell as well as the signalling pathway(s) driving MZ versus FO B cell differentiations are a matter of active investigation (Allman et al., 2006). Activation of the Notch pathway as well as signalling through the BCR have been proposed as central determinants of MZ versus FO B cell (Casola et al., 2004; Pillai et al., 2004; Radtke et al., 2010).

5.1.2.4 The germinal centre reaction

In secondary lymphoid organs, lymphocytes are segregated into adjacent B- and T-cell zones, defined by gradients of chemokines (Cyster, 2010).

During a T-cell dependent immune response, B cells recognize protein antigens through the BCR, followed by internalization of the BCR/antigen complex. Proteolytic cleavage of the antigen is followed by the loading of short peptides onto MHC-II molecules. B cells primed with the antigen, up regulate specific chemokine receptors (CCR7) that attract them to the boundary with the T cell zone. Here, B-cells present antigens to cognate $CD4^+$ T follicular helper (T_{FH}) cells. B and T cells contact each other via MHC class-II/TCR pairing, in the presence of co-stimulatory signals (CD40/CD40L and CD80 (and CD86)/CTLA4). These events are crucial for the full

activation, survival and further differentiation of antigen-specific B cells (Klein and Dalla-Favera, 2008). Once activated by T-cells, antigen-specific B cells follow one of two developmental paths: i) they differentiate directly into short-lived low-affinity antibody secreting PCs (Smith et al., 1996), or ii) they return to the B cell zone where they give rise to a germinal center reaction nucleated around follicular dendritic cells (FDC) loaded with immune complexes (Kosco-Vilbois and Scheidegger, 1995). GCs represent a polarized structure consisting of an area (the dark zone) densely packed with proliferating B cells (also called centroblasts, CBs), separated by the light zone consisting of resting B cells (centrocytes, CCs) positioned in close proximity with FDCs, T_{FH} cells and macrophages (Allen et al., 2007; Victora et al., 2010; Victora and Nussenzweig, 2012).

During clonal expansion, CBs undergo diversification of their IgH and IgL V-gene repertoires through a process called somatic hypermutation (SHM). SHM is dependent on Activation-Induced cytidine Deaminase (AID), an enzyme identified in 1999 by the Honjo group. (Muramatsu et al., 2000; Revy et al., 2000). GC B cells undergo Ig SHM at very high rate (1 mutation/10^3bp/cell division) thus contributing to a further diversification of the primary antibody repertoire. Ig SHM creates B cells expressing novel BCR specificities, from which only a very limited subset is selected on the basis of their binding with high affinity to cognate antigen. The latter cells are destined to leave the GC, however not before completing their differentiation into long-lived memory B cells or PCs (Klein and Dalla-Favera, 2008; Wagner and Neuberger, 1996). In contrast, the majority of GC B cells die in situ by programmed cell death. CBs express indeed high levels of pro-apoptotic proteins including CD95/FAS, whereas they lack expression of most anti-apoptotic factors (Klein et al., 2003a; Klein et al., 2003b). The high sensitivity of GC B cells to pro-apoptotic stimuli allows the rapid elimination of GC B cells that fail to receive survival signals from the

engagement of their BCR. Indeed, in the light zone, the persistence of centrocytes is strictly dependent on the ability of such cells to capture, through their BCRs, the antigen in the form of immune complex from FDC and to present it to a limiting number of T_{FH} cells (Allen et al., 2007; Schwickert et al., 2007) (McHeyzer-Williams et al., 2009; McHeyzer-Williams and Nussenzweig, 2009)

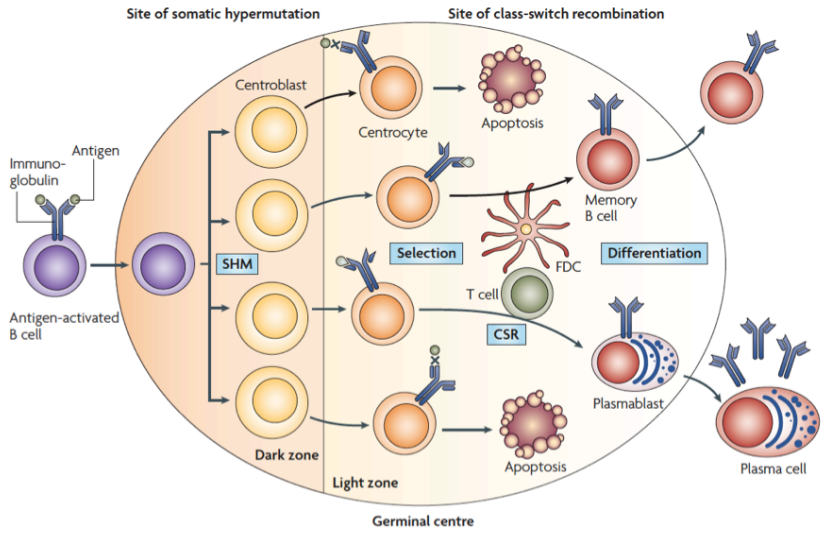

Klein U., Dalla-Favera R., Nat. Rev. Imm. 8, 2008

Figure 3: The germinal center reaction

During T-cell dependent immune response, antigen-specific B cells participate to the GC reaction. The GC reaction is characterized by an initial phase of clonal B-cell expansion that is coupled to Ig SHM, followed by the selection of B cells for the ability to recognize cognate antigen with high affinity through their "mutated" BCRs. The selection process requires FDCs, presenting the antigen, and follicular T-helper cells which provide the necessary co-stimulatory signals to support further rounds of Ig SHM, selection and differentiation into memory B cells and ASC plasma cells. Only few high-affinity B cells survive the GC reaction, with the majority instead dying *in situ* by apoptosis. GC B cells also replace the effector domain of their BCR through the process of Ig isotype switching (a process also known as Ig class switch recombination).

The net result of a GC reaction is the generation of few highly selective memory B cells and PCs, expressing high affinity immunoglobulins. GC–derived PCs home to the BM where they provide a lifelong resource of high-affinity antibodies. On the other hand, memory B cells represent a restricted pool of highly selected, antigen-specific

long-lived resting B cells ready to be recruited into secondary immune responses once the organisms enters again in contact with the same antigen. Reactivation of memory B cells leads to either terminal differentiation into PCs or recruitment into GCs, to generate B cells with a progressively higher affinity for the antigen.

5.1.2.5 Ig somatic hypermutation and class switch recombination

Ig SHM and class switch recombination (CSR) represent somatic rearrangements occurring at Ig gene loci in antigen-activated B cells (Figure 4). In particular, SHM targets rearranged Ig variable region genes, while CSR promotes the replacement of the IgH Cμ constant region gene with that of another isotype (for example, γ, ε or α)

During the process of SHM, single nucleotide substitutions (or deletions) are introduced within rearranged IgH and IgL V genes at high frequency (1 mutation every 10^3 nucleotides/cell division) (Kocks and Rajewsky, 1988; McKean et al., 1984), within a window of 2Kb downstream of the V-gene promoter (Neuberger et al., 1998). Analysis of the mutation pattern has revealed a preference of AID to target a WRCY consensus sequence (where W = A/T, R = A/G, and Y = C/T) (Petersen-Mahrt et al., 2002; Pham et al., 2003). AID deaminates cytidine to uridine, generating therefore an U:G mismatch. Upon DNA replication, in the absence of mismatch repair, SHM causes thus C to T transitions. All other nucleotide substitutions within Ig V-genes that result from AID action depend on the recognition/resolution of the U:G mismatch by either base excision repair (BER) or mismatch repair (MMR) pathways (Di Noia and Neuberger, 2002; Di Noia and Neuberger, 2007).

CSR occurs during both T cell-dependent and -independent immune responses. It is an irreversible recombination event by which B cells replace the coding exons of Cμ and C∂ with that of a distinct Ig isotype. The IgH chain constant region (C_H) locus consists of an ordered set of C_H exons (Cμ, Cδ, Cγ3, Cγ1, Cγ2b, Cγ2a, Cε and Cα in the mouse), each preceded by an upstream GC-rich switch (S) sequence. CSR takes place

between two S regions, resulting in the deletion of the intervening DNA segment (Iwasato et al., 1990; Matsuoka et al., 1990). Transcription through S regions generates long stretches of single-stranded DNA, (Bottaro et al., 1994; Harriman et al., 1996; Jung et al., 1993; Zhang et al., 1993), and the formation of stable RNA-DNA structures (termed R-loops), that displace the non-coding DNA strand (Reaban et al., 1994; Yu et al., 2003). The R-loops are thought to assist in the targeting of AID. DNA double strand breaks that occur in the S regions are joined by the NHEJ pathway (Manis et al., 1998). As a result of CSR, the intervening DNA fragment is excised as a circle and the 3' and 5' ends of the IgH locus are finally juxtaposed (Figure 4b).

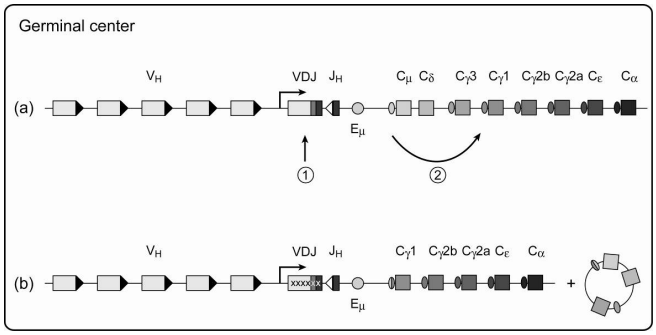

Figure 4: Ig somatic hypermutation and class switch recombination

Schematic view of the IgH locus before (a) and after (b) onset of Ig SHM and CSR. SHM (1) targets the variable region gene leading to the single-nucleotide substitutions or deletions (represented as x). (2) CSR acts on the IgH constant (C_H) region gene, promoting the replacement of Cμ with that of another isotype (Cγ3, Cγ1 etc).

5.2 The B cell antigen receptor

The B-cell antigen receptor (BCR) provides B lymphocytes with the capacity to recognize foreign antigens, thereby allowing B cells to neutralize potentially lethal pathogens.

5.2.1 The BCR: from structure to function

The BCR is a transmembrane protein complex comprised of two IgH chains covalently linked by disulfide bonds to two IgL chains of the kappa (κ) or lambda (λ) type. The amino-terminus of both IgH and IgL chains consists of the variable (V) region, featuring extensive sequence variability, as a result of VDJ recombination, N-nucleotide addition and SHM. The hypervariable regions within V_H and V_L regions are termed complementarity-determining regions (CDRs). They represent the antigen-binding site of the BCR and define its specificity and ligand binding affinity. The carboxy-terminus invariable portion of the IgH chain, termed constant (C) region, confers the effector functions to the BCR. There exist five different immunoglobulin isotypes (IgM, IgD, IgG, IgA and IgE). IgM and IgD are expressed by naive B-cells, whereas the other isotypes are typically expressed upon B-cell activation in response to antigen recognition (Brezski and Monroe, 2008). Each BCR complex consists of a single Igα/Igβ heterodimer (also called CD79a and CD79b, respectively) that represents the signal transduction component of the Ig receptor. The BCR complex is assembled within the endoplasmic reticulum (ER) and is transported through the Golgi to the plasma membrane. A schematic representation of the BCR is shown in Figure 5.

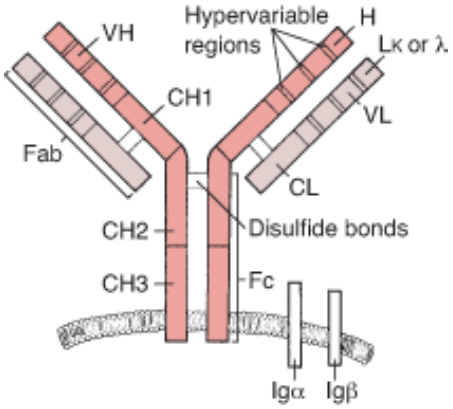

Figure 5: Structure of the BCR signalling complex.

Pairs of Ig heavy (H, pink) and light (L, grey) chains are kept together by disulfide bonds (thin lines joining the two types of Ig chains). CH: Ig heavy chain constant region; CL: Ig light chain constant region; Fab: antigen-binding fragment; Fc: fragment to crystallize; VH: Ig heavy chain variable region; VL: Ig light chain variable region. The BCR complex is completed by a single Igα/Igβ heterodimer.

5.2.2 The BCR signalling pathway

Antigen-specific B cell responses depend on the engagement of the BCR that leads to the activation of several downstream signalling cascades (Rajewsky, 1996). Upon antigen binding, the BCR complex, through its signalling subunits Igα and Igβ (Brezski and Monroe, 2008), triggers B cell effector functions that include cell-cycle progression, antigen presentation and up-regulation of co-stimulatory molecules and homing receptors. The initiation of signalling pathways downstream of the BCR depends on immunoreceptor tyrosine-based activation motifs (ITAMs) present in the cytoplasmic portion of Igα and Igβ (Reth et al., 1991). Receptor engagement promotes ITAM phosphorylation mediated by Lyn, a member of Src-family protein tyrosine kinases (PTKs). Phosphorylation of ITAM-associated tyrosine residues creates docking sites and recruits Src-homology-domain (SH2) containing proteins, such as the Spleen tyrosine kinase (SYK). The role of SYK in promoting B-cell proliferation is confirmed by the failure of SYK-deficient pre-B-cells to undergo clonal expansion (Turner et al., 1995). SYK activation results in the phosphorylation of downstream targets and in the initiation of several signalling cascades.

5.2.2.1 PLCγ2 regulates Ca_2^+ flux and ERK activation

A crucial SYK target is SLP65/BLNK, a B cell adaptor that fine-tunes BCR signals by connecting kinases to downstream BCR signalling effectors. Upon SYK-mediated phosphorylation, SLP65 recruits the Bruton tyrosine kinase (Btk) and phospholipase C-γ2 (PLCγ2). The latter becomes phosphorylated by SYK and BTK, and thereby is activated to catalyse the second messengers diacylglycerol (DAG) and inositol-1,4,5-trisphosphate (IP_3) from phosphatidylinositol-4,5-bisphosphate (PIP_2) (Kurosaki, 2011). IP_3 binds to IP_3-gated intracellular Ca^{2+} channels present on the ER membrane, thereby leading to the release of Ca^{2+} from the ER storage. Signalling mediated by Ca^{2+} fluxes activates transcriptional pathways (such as those centred on NFAT and NFκB) involved in proliferation and immune effector functions (Jun and Goodnow, 2003). In addition, DAG facilitates the recruitment of both PKC β and nucleotide exchange factors (GRP3 or Sos) to the plasma membrane, leading to Ras activation and its binding to Raf1. The latter, in turn, phosphorylates and activates ERK1/ERK2 (Kurosaki et al., 2010). Phosphorylation of ERKs leads to their dimerization, followed by nuclear translocation and subsequent phosphorylation of transcriptional factors, including Fos, Jun, and Ets family members (Dong et al., 2002).

5.2.2.2 The NF-κB pathway is central to BCR function

The NF-κB family comprises the DNA binding members NF-κB1 (p50) and NF-κB2 (p52) that are generated by proteolysis of larger precursors. NF-κB1 and NF-κB2 induce gene transcription via hetero dimerization with the other NF-κB-family members, RelA (p65), RelB and c-Rel that have transactivation functions (Li and Verma, 2002). In steady state conditions, NF-κB proteins are sequestered in the cytoplasm in an inactive state, bound to Inhibitory κB (IκB) proteins (Thome, 2004). The canonical pathway, which leads to the activation of NF-κB1, is tightly controlled

by the IκB kinase (IKK) complex, composed of two catalytically active kinases (IKK-α and IKK-β) and the regulatory subunit, IKK-γ (also known as NEMO) (Li and Verma, 2002). Activation of the IKK complex leads to phosphorylation and hence ubiquitylation and proteolytic degradation of IκBα, and allows NF-κB to translocate to the nucleus to activate gene transcription (Li and Verma, 2002). A second, so-called alternative pathway of NF-κB activation is induced by Tumor Necrosis Factor (TNF) receptor superfamily, including the receptor for lymphotoxin-β, B-cell-activating factor receptor (BAFFR), and CD40 (Pomerantz and Baltimore, 2002). In contrast to the classical pathway, triggering of TNF receptors activates IKK-α that promotes the phosphorylation and subsequent proteolytic processing of NF-κB2/p100 to p52, and the formation of transcriptionally active NF-κB dimers, composed of p52 and RelB.

BCR-induced NF-κB activation proceeds through the classical NF-κB pathway (Ruland and Mak, 2003). A recent breakthrough in our understanding of this signalling pathway has been the identification of three physically and functionally interacting proteins known as CARD11 (caspase recruitment domain 11), BCL-10 (adaptor protein B-cell lymphoma 10) and MALT1 (mucosal-associated lymphoid tissue 1) that act as crucial signaling components connecting the antigen receptor to the IKK complex (Jun and Goodnow, 2003) (Thome and Tschopp, 2003). PKCβ has been found to be important for the activation of the canonical NF-κB pathway (Shinohara et al., 2005). Phosphorylation of CARD11 by PKCβ promotes the generation of the CARD11-Bcl10-MALT1 ternary complex. Acting as a molecular scaffold, CARD11 brings the TGFβ-activated kinase 1 (TAK1) in close proximity with the IKK complex, thus allowing its activation (Figure 6, from Thome, 2004).

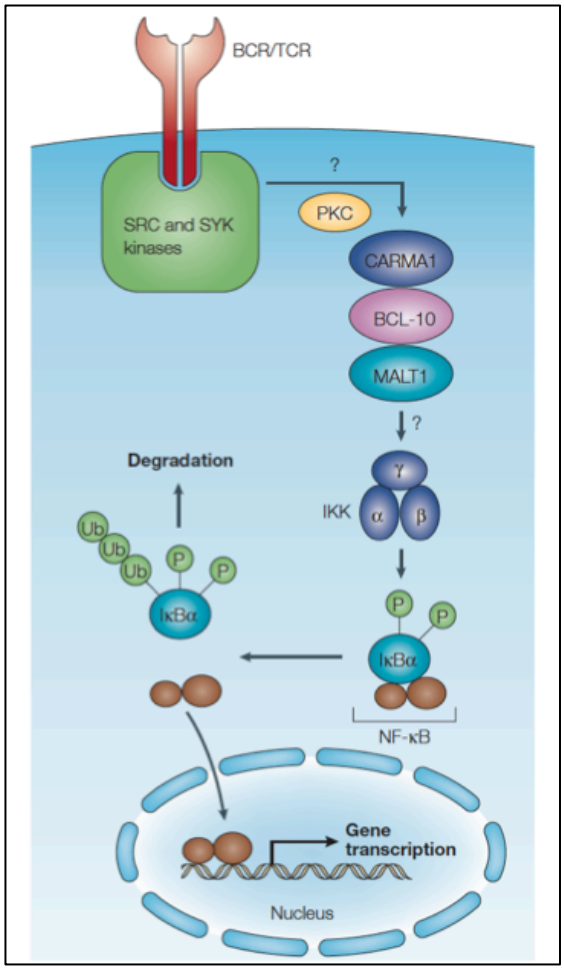

Figure 6: BCR signalling triggers NF-κB activation

The activation of NF-κB by the BCR depends on SYK-mediated PKC-β activation and association of a tri-molecular complex consisting of CARMA1/CARD11, BCL-10 and MALT1. These proteins have a crucial role in the subsequent activation of the IKK complex (IKK), which regulates the activation of NF-κB1 (p50)–RelA/p65 heterodimers through the phosphorylation of **IκBα.** Phosphorylated **IκBα** is ubiquitylated (Ub) and degraded by the proteasome machinery, allowing NF-κB to translocate to the nucleus and activate target gene expression.

5.2.3 BCR controls the Phosphoinosititide 3-kinase/FOXO pathway

The Phosphoinosititide 3-kinase (PI3K) represents a crucial effector of BCR signaling. It has been shown that SYK induces phosphorylation and hence activation of PI3K, which regulates diverse biological processes, including cell growth, survival, proliferation, migration and metabolism (Deane and Fruman, 2004). Activation of SYK and SRC family PTKs in response to BCR signalling, induce phosphorylation of the BCR co-receptor CD19 and the adaptor protein BCAP (also known as PIK3AP1), leading to the local recruitment and activation of PI3K (Aiba et al., 2008; Deane and Fruman, 2004). Subsequently, PI3K phosphorylates its substrate PIP_2, thereby generating the second messenger phosphatidylinositol-3,4,5-trisphosphate (PIP_3) (Okkenhaug and Vanhaesebroeck, 2003). Several signalling proteins, including the serine/threonine kinase protein kinase B (PKB; also known as AKT) and

3-phosphoinositide-dependent protein kinase 1 (PDK1), contain a pleckstrin-homology (PH) domain that binds PIP_3, which allows their recruitment to the plasma membrane. AKT, which becomes activated by PDK1-mediated phosphorylation, is thought to be the main mediator of the PI3K signaling pathway and induces cell proliferation through the inhibition of multiple downstream targets that are involved in the control of the cell cycle (Manning and Cantley, 2007).

AKT kinase regulates a variety of proteins involved in metabolism (such as GSK3β), proliferation and survival (Manning and Cantley, 2007). Among the targets of Akt there is the family of FOXO transcription factors. FOXO proteins are transcriptional regulators promoting cell death and inhibition of cell-cycle progression. FOXO proteins are tightly regulated through post-translational modifications (Vogt et al., 2005). Most importantly, AKT-mediated phosphorylation of FOXO proteins inhibits their transcriptional activity by promoting their translocation from the nucleus to the cytoplasm, where these molecules are rapidly degraded (Coffer and Burgering, 2004). Among FOXO family members, FOXO1 has been identified as a crucial factor in the regulation of B cell development. Conditional FOXO1 inactivation at the pro-B-cell stage results in a complete block in B-cell development (Coffer and Burgering, 2004; Dengler et al., 2008). In the absence of BCR-dependent PI3K/AKT signaling, FOXO proteins promote transcriptional activation of genes inducing cell-cycle arrest (RBL2, or p27) and apoptosis (BIM, BCL6 or TRAIL). Thus, the PI3K/AKT module is a crucial node in BCR signaling as it supports B-cell survival through the inhibition of FOXO activity (Coffer and Burgering, 2004; Srinivasan et al., 2009). A schematic representation of PI3K signaling downstream of BCR is shown in Figure 7.

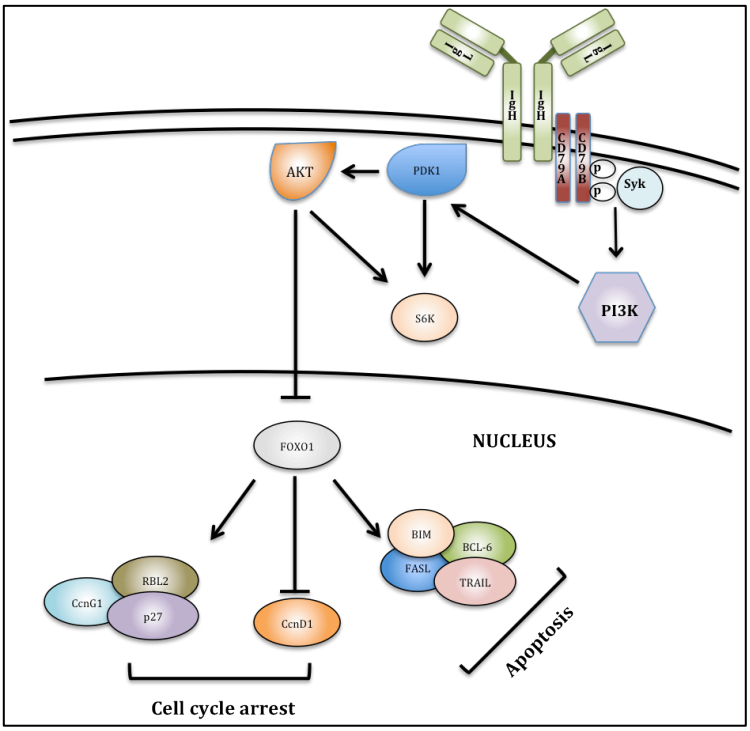

Figure 7: PI3K activation in response to BCR signalling

Schematic representation of PI3K-mediated regulation of FOXO transcription factors in B cells. Activation of PI3K/AKT prevents nuclear localization of FOXO proteins. Nuclear FOXO1 regulates the expression of genes involved in apoptosis (FASL, BIM, and TRAIL) and cell cycle progression (RBL2, CCNG1, p27 or CCND3).

5.2.3.1 The BCR "tonic" signal

While signal transduction through the BCR is generally thought to be initiated by antigen-induced crosslinking, the BCR signals also in a ligand-independent manner. Ligand-independent signalling through the BCR (also called *tonic signal*) has an important role in directing appropriate fate decisions during B cell development (Brezski and Monroe, 2008) and to sustain the survival of mature B cells (Lam et al., 1997). The existence of a tonic BCR signal was shown through elegant genetic experiments performed in mice by the Rajewsky group. Conditional deletion of the BCR in mature B cells led to a severe interference with B cell survival, thus suggesting the requirement for a constant BCR signaling to support mature B cell maintenance (Lam et al., 1997). This study was followed by the demonstration that BCR signalling competence is crucial to support the survival of resting mature B cells (Kraus et al.,

2004). Indeed, conditional deletion of the BCR signalling component Igα in mature B cells resulted in a severe loss in peripheral B cell numbers. Additional studies have since then confirmed the existence of a low-strength/*tonic* signal emanating from the BCR in the absence of cognate antigen recognition (Bannish et al., 2001; Grande et al., 2007). A first elucidation of the biochemical basis of the tonic BCR signal came again from the Rajewsky lab. Using conditional gene targeting, it was demonstrated that, against all expectations, the NF-κB signaling cascade was not responsible for transmitting the tonic BCR signal. Instead, signalling through the PI3K/AKT pathway was shown to be essential to sustain survival of resting mature B cells (Srinivasan et al., 2009). Moreover, in the same study it was shown that specific inactivation of FOXO1 was sufficient to rescue BCR-deficient resting B cells from death, highlighting the importance of the PI3K/AKT signaling pathway to inhibit FOXO1 to promote mature B-cell survival. Thus, activation of the PI3K pathway downstream of the BCR is critical both during B cell development (Aiba et al., 2008; Herzog et al., 2008; Verkoczy et al., 2007) and in resting mature B cells, where it is essential to sustain their survival (Srinivasan et al., 2009).

5.3 Non-Hodgkin lymphoma: the dark side of B-cell activation

The immune system preserves our body on a daily basis from infections caused by harmful pathogens. Nevertheless, this protective role has a price. B cell differentiation can indeed be compared to a clocking bomb, waiting to explode. Every day, millions of B lymphocytes put their genomic integrity in danger as a result of the genetic rearrangements occurring during the processes of primary (VDJ recombination) and secondary (Ig SHM and CSR) antibody diversification.

5.3.1 The germinal center reaction: a lymphoma prone environment

Ig CSR is a processes characterized by the generation of double stranded DNA breaks occurring at IgH chain constant region loci (Honjo et al., 2002; Papavasiliou and Schatz, 2002). Occasionally, such breaks are aberrantly resolved and promote the occurrence of chromosomal translocations. These genetic alterations are more frequently observed in B cells recruited into the GC reaction during a T-cell dependent immune response, due to the extremely high frequency of double strand breaks occurring at Ig loci in these cells as a result of AID activity. Chromosomal translocations resulting from aberrant CSR can lead to the juxtaposition of IgH *cis* regulatory regions to proto-oncogenes, leading ultimately to their deregulated expression. Indeed, recurrent chromosomal translocations found in B-cell lymphomas are commonly associated to aberrant expression of proto-oncogenes including c-MYC (Burkitt lymphoma), BCL2 (Follicular Lymphoma) and BCL6 (Diffuse Large B cell Lymphoma).

Another mechanism through which AID contributes to lymphomagenesis is represented by aberrant SHM. Despite a high preference for Ig V-genes, recent work has shown a striking promiscuity in AID binding to the genome. Several high throughput data have recently confirmed initial observations by the Dalla Favera

group showing the accumulation of somatic mutations affecting a variety of non-Ig genes in GC B cells. Importantly, these genes are often found mutated in GC-derived B cell malignancies, and possibly contribute to the transformation process (Richter et al., 2012; Schmitz et al., 2012).

From these considerations, it emerges that the GC reaction represents a tumorigenic environment, where the attempt to generate protective, high affinity neutralizing antibodies by mean of SHM and CSR is counterbalanced by the frequent occurrence of gross genetic aberrations or point mutations. The accumulation of the latter lesions in a highly proliferative compartment is expected to facilitate the selection of rare mutants, which ultimately will overcome tumor suppressor mechanisms to give rise to clonal B-cell malignancies (Kuppers et al., 1999; Stevenson et al., 1998; Klein and Dalla-Favera, 2008).

5.3.2 Most lymphomas derive from B cells transiting through the germinal center

Depending on histological appearance, B cell lymphomas are classified as Hodgkin and Non-Hodgkin (NH) lymphomas. NH lymphomas include the most common and aggressive forms of B-cell lymphomas. According to the World Health Organization (WHO), more than 80 percent of B cell malignancies (including both Hodgkin and most NH lymphoma subtypes) derive from B cells that have transited through the GC reaction. This is witnessed by the finding that clonal malignant B cells have undergone Ig SHM and/or CSR and display a gene expression profile closely related to that of activated mature B cells, or more specifically GC B cells (Alizadeh et al., 2000; Kuppers, 2005).

The most common forms of GC-derived NHL feature reciprocal chromosomal translocations that juxtapose proto-oncogenes to one of the Ig loci, resulting in their de-regulated expression (Kuppers and Dalla-Favera, 2001; Willis and Dyer, 2000). Classic examples include the t(14;18) *BCL2*/IgH translocation in follicular lymphoma

(Jager et al., 2000; Tsujimoto et al., 1985), the t(3;14) *BCL6*/IgH translocation in diffuse large B cell lymphoma (Baron et al., 1993; Ye et al., 1993), the t(11;14) CCND1/IgH translocation in multiple myeloma (Avet-Loiseau et al., 1998; Gabrea et al., 1999) and the t(8;14) c-MYC/IgH translocation in Burkitt lymphoma (Dalla-Favera et al., 1982; Taub et al., 1982).

The genes target of recurrent chromosomal translocations and point mutations in NHL affect in most cases the survival, proliferation and differentiation of GC B cells. As a result of the interference with the physiology of the GC reaction, malignant B cells are "frozen" in a stage that favours the acquisition of additional mutations by AID, possibly contributing to tumor progression and ultimately to render these cancers often incurable.

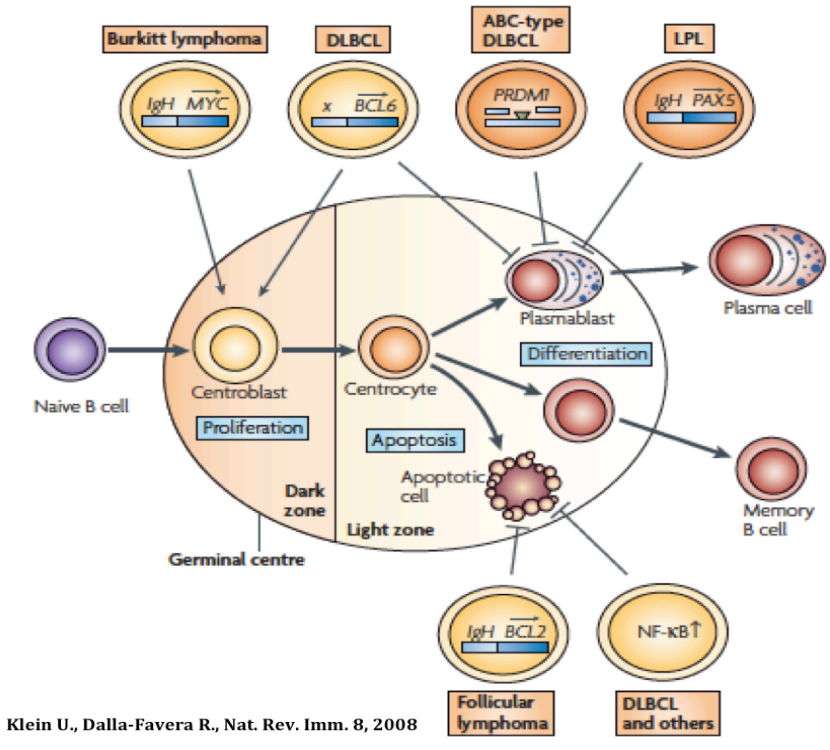

Figure 8: Most Non-Hodgkin B-cell lymphomas derive from GC B cells

Schematic representation of the main types of NHL, highlighting the molecular hallmark and derivation from B cells at defined stages of their transit though the GC reaction.

5.3.3 Burkitt Lymphoma

Burkitt lymphoma (BL) was first described in Uganda in 1958, when it was initially diagnosed as a sarcoma of the jaw (Burkitt, 1958). Shortly after, it was recognized as a distinct form of NHL (Burkitt, 1962). With a worldwide dissemination, BL is a hematopoietic tumor, affecting in particular the lymphoid system. There exist three forms of BL: (1) the endemic form, mainly distributed in subequatorial Africa, (2) the sporadic form, mainly occurring in the Western world and (3) a form affecting immuno-compromised patients (Blum et al., 2004).

The endemic form of BL is clinically characterized by jaw or kidneys involvement, whereas abdomen localizations are typical of the sporadic and immunodeficiency-associated forms. Symptoms include abdominal pain, nausea, vomiting, bowel obstruction and gastrointestinal bleeding. Over 95 percent of endemic BL cases are associated with Epstein-Barr virus (EBV) infection. In contrast, between 15 and 70 percent of sporadic BL cases display the presence of EBV in the tumor cells, with an incidence influenced by the socio-economic status and the age at which patients get infected with the virus (Jaffe and Pittaluga, 2011). Despite several studies have proposed an active role of EBV in BL pathogenesis, it remains still unclear how the virus contributes to the onset of this malignancy (Casola et al., 2004; Kelly et al., 2009; Rowe et al., 2009; Vereide and Sugden, 2011).

The genetic hallmark shared by all forms of BL is represented by the occurrence of a reciprocal chromosomal translocation that juxtaposes the c-MYC oncogene on chromosome 8, to the IgH locus on chromosome 14 (most cases), or, in 20 percent of the cases, to the Igκ or Igλ loci on chromosome 2 and 22, respectively (Dalla-Favera et al., 1982; Hecht and Aster, 2000b; Taub et al., 1982). Interestingly, the analysis of chromosomal breakpoints observed in endemic and sporadic BL cases revealed the involvement of either the IgH J_H region or the IgH switch region. These data point to

alternative mechanisms responsible for the occurrence of double strand breaks at Ig loci, including SHM and CSR, that are responsible for the t(8;14) translocation (Hecht and Aster, 2000a; Pelicci et al., 1986).

At the histological level, BL appears as a tumor composed of largely uniform cells with minimal cytological variation. The cells are of medium/large size with round nuclei, moderately clumped chromatin, and multiple (2-5) basophilic nucleoli. The cytoplasm is deeply basophilic. BL cells contain cytoplasmic lipid vacuoles, which are probably a manifestation of the high rate of proliferation (as shown by positivity to the Ki67 proliferation marker) and of spontaneous cell death. A "starry sky" appearance is a typical feature of BL and reflects the numerous benign macrophages that have infiltrated the tumor to engulfe apoptotic tumor cells (Jaffe and Pittaluga, 2011). BL tumor cells display a mature B-cell immunophenotype, expressing surface IgM, CD10, CD20, CD22 as well as CD43 in nearly all cases (Jaffe and Pittaluga, 2011). The absence of BCL-2 expression is helpful in ruling out "double-hit" lymphomas with dual translocations affecting MYC and BCL2 (Blum et al., 2004). Importantly, BL cells carry somatically mutated Ig genes, frequently associated to intra-clonal heterogeneity, pointing to a germinal center origin and to ongoing AID activity in the tumor cells (Chapman et al., 1996; Klein et al., 1995).

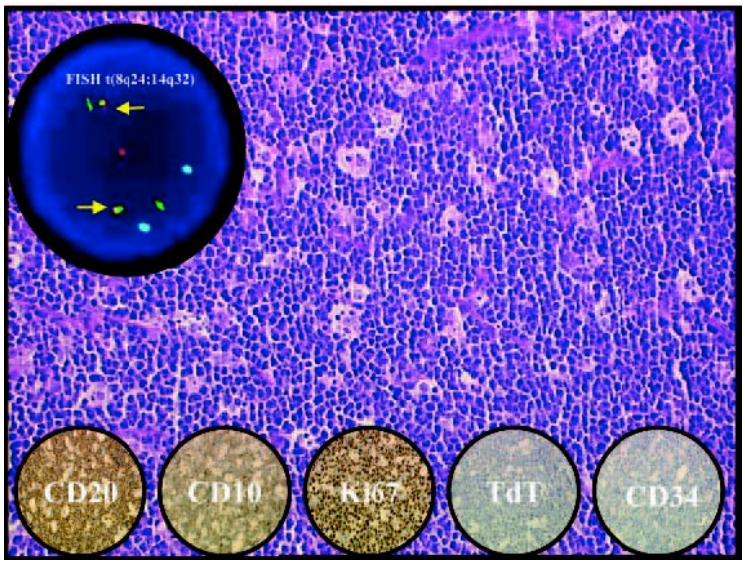

Figure 9: Typical morphology of a lymph node in BL

Histological appearance of human BL. Hematoxylin-eosin staining was performed on a lymph node section. Diffusely infiltrated lymphoid cells with small round nuclei and distinct nucleoli are visible. Numerous benign macrophages containing ingested apoptotic tumor cells generate the typical "starry sky" pattern. Insets: immunohistochemical analysis for the indicated markers in BL cells. Translocation involving c-MYC and immunoglobulin heavy chain genes can be visualized by FISH analysis with probes for IgH (green) and MYC (red). t(8;14)(q24;q32) are indicated by yellow arrows. (Adapted from Blum et al., 2004)

5.3.4 Management and outcome of BL

BL is a very aggressive malignancy due to the high proliferative rate. This property renders however BL particularly sensitive to cytostatic drugs including cyclophosphamide, vincristine, prednisolone, or doxorubicin, that are given at doses that are proportional to the stage of the disease. The use of rituximab (anti-CD20) (or improved variants of anti-CD20 antibodies, such as Veltuzumab or Ofatumumab) in primary therapy has been assessed with encouraging results (Foon et al., 2012). With the current therapeutic protocols, the outcome for sporadic BL is excellent, with an overall cure rate of roughly 90%. However, treatment has pronounced haematological toxic effects and mucositis, as well as high risk of severe infections. Moreover, relapse of BL, even though not very common, occurs on average 6 months after the end of the treatment, and has a very poor prognosis, probably because of the selection of particularly aggressive chemoresistant clones (Molyneux et al., 2012).

5.3.5 λ-MYC: a mouse model of Burkitt lymphoma

The translocation of c-MYC into Ig loci, leading to aberrant over expression of the proto-oncogene in B cells, represents the molecular hallmark of BL. Several attempts have been made in the past 30 years to reconstruct BL in the mouse model, all centered on B-cell specific over-expression of the c-MYC proto-oncogene. The first mouse transgenic line with targeted MYC over-expression to B cells was established by Adams, Cory and colleagues in 1985. In this line (Eμ-MYC), expression of the c-MYC gene was placed under the control of the IgH intronic enhancer (Adams et al., 1985). The main limitation of this strain is represented by the premature expression of c-MYC in B-cell progenitors. Indeed, the majority of tumors arising in Eμ-MYC mice represent aggressive IgM^- proB/preB lymphoblastic lymphomas. In 2000, the Morse lab described the λ-MYC strain carrying the human c-MYC gene and its promoter sequence (cloned from a human BL-cell line) under the control of Igλ light chain regulatory sequences (λ–MYC strain, Kovalchuk et al., 2000). This strategy was predicted to post-pone onset of c-MYC expression to mature B cells expressing IgL chains. Indeed, λ–MYC transgenic mice develop in most cases aggressive IgM^+ B cell lymphomas with immunophenotypical features shared with human BL ($IgM^+CD19^+B220^+CD43^+$ $CD5^-CD23^-$). Moreover, histological analysis of lymphoid organs infiltrated with λ-MYC tumor cells revealed a typical starry sky pattern. The main difference between hBL and λ-MYC lymphomas is represented by the accumulation in the latter tumors of the required combination of genetic mutations, before the entry of transgenic B cells in the GC reaction. Indeed in most cases, Ig V-gene rearrangements cloned from λ-MYC lymphomas lack signs of SHM. This limitation has been very recently overcome in a novel mouse BL model established by the Rajewsky group, in which expression of c-MYC was specifically induced in GC B cells (Sander et al., 2012). Importantly, deregulated c-MYC expression was not

sufficient to initiate BL, as tumors appeared only upon concomitant activation of the Phosphoinositide 3-kinase pathway.

5.4 The c-MYC proto-oncogene

c-MYC is a highly pleiotropic transcription factor that controls cell proliferation, metabolism, differentiation and apoptosis (Albihn et al., 2010; Nasi et al., 2001). It is therefore not surprising that its expression is commonly altered in variety of human tumors.

5.4.1 c-MYC: structure and function

The *c-MYC* gene maps on human chromosome 8 and consists of 3 exons. Translation of the *c-MYC* transcript can be initiated at 3 different sites: i) the AUG in the second exon, giving rise to the canonical 64kDa MYC protein; ii) a non-AUG codon (CAG) near the 3′ end of exon 1, generating a longer c-MYC isoform (p67) (Hann et al., 1988), and iii) an internal AUG codon in exon 2, downstream the first AUG, resulting in the expression of a shorter protein called MYCS (Blackwood et al., 1994). The MYC protein, translated from the canonical AUG, consists of a N-terminal transcriptional regulatory domain, followed by a nuclear localization signal and a C-terminal region with a basic DNA-binding domain tethered to a helix-loop-helix-leucine zipper (HLH-Zip) dimerization motif. To bind DNA, MYC dimerizes with Max, identified in 1991 as a c-MYC obligate partner protein (Amati et al., 1993; Amati et al., 1992). The MYC-Max heterodimer locks onto and bends DNA through binding motifs (5'- CACGTG -3') termed E boxes (Park et al., 2004), where it mainly acts as inducer of gene transcription. Although the mechanism of MYC-induced transcription is progressively emerging (Lin et al., 2012; Nie et al., 2012), its contribution to transcriptional repression is still unclear. Several observations indicate that MYC inhibits gene expression through different modalities that are mainly linked to regulatory loops. For example, it has been proposed that the inhibitory effect of MYC on gene transcription is the result of the induction of repressive factors, and/or the regulation

of specific micro-RNAs (miRNA) (Chang et al., 2008). An interaction with other transcription factors to repress gene expression has been also proposed (Eilers and Eisenman, 2008).

Finally, several studies have provided a link between MYC and genomic instability as an indirect consequence of its transcriptional activity (Wade and Wahl, 2006). However, evidence proposed by Domininguez-Sola and colleagues indicated a non-transcriptional role for MYC in the initiation of DNA replication (Dominguez-Sola et al., 2007). In fact, despite its conventional definition as transcription factor, MYC can interact with components of the pre-replicative complex, and localizes at early sites of DNA replication. These observations indicated that MYC might directly control the initiation of DNA synthesis and progression through S phase. Moreover, MYC-related genomic instability might result from the induction of DNA replication stress, rather than being dependent on the transcriptional activation of S-phase promoting genes (Cole and Cowling, 2008).

5.4.2 MYC regulation

Lying at the crossroad of many different pathways including proliferation, apoptosis, differentiation and metabolism, MYC expression is tightly regulated by a number of transcriptional and post-transcriptional mechanisms (Brooks and Hurley, 2010; Hurley et al., 2006; Levens, 2010).

The MYC mRNA is short lived. It is targeted by several miRNAs (let-7, miR-34, and miR-145) resulting in translational repression (Christoffersen et al., 2010; Kress et al., 2011). The MYC protein undergoes poliubiquitination and degradation by the proteosome, with a half-life in the order of 15–20 minutes (Gregory and Hann, 2000). Phosphorylation of 2 specific residues of the MYC protein influences MYC activation or degradation. Mitogen-activated signalling pathways (inducing the activation of the Ras/MAPK pathway) lead to phosphorylation of MYC at Serine 62 (Ser62), which

results in the stabilization of the protein. By contrast, phosphorylation at Threonine 58 (Thr58) destabilizes MYC and facilitates Ser62 de-phosphorylation. Thr58 is phosphorylated by glycogen synthase kinase-3 beta (GSK3β) (Gregory et al., 2003), which, in turn is inhibited by the PI3K pathway. GSK3β can phosphorylate MYC Thr58 only if Ser62 is already phosphorylated ("primed phosphorylation"). Phosphorylation of MYC in Thr58 promotes its recognition by the prolyl-isomerase PIN1, which in turn leads to the isomerization of MYC Proline-59 (Pro59) thus enabling protein phosphatase-2A (PP2A) to remove the phosphate residue from Ser62. The ubiquitin E3 ligase SCF^{FWB7} (FBW7) poly-ubiquitylates MYC in a Thr58-phosphorylation-dependent manner, and targets it for proteasomal degradation (Welcker et al., 2004a; Welcker et al., 2004b; Yada et al., 2004) (Figure 10 adapted from Adhikary and Eilers, 2005).

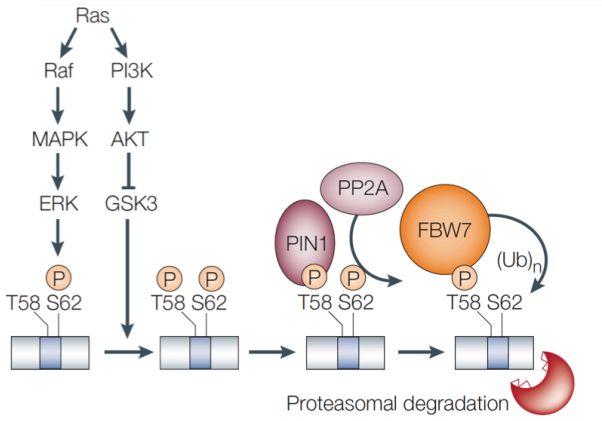

Figure 10: Post-translational modification of c-MYC in response to upstream signalling events

MYC Phosphorylation on serine-62 (S62), in response to Ras signalling, provides the docking site for GSK3β, which in turn phosphorylates MYC threonine-58 (T58). Phosphorylated MYC is recognized by the prolyl isomerase PIN1 that leads to isomerization of Proline-59 and thereby enables PP2A-mediated dephosphorylation of MYC S62. This allows the E3 ligase to recognize and poly-ubiquitylate T58-phosphorylated MYC, promoting ultimately its degradation by the proteasome machinery.

The selection for MYC Thr58 point mutations preventing its phosphorylation and thus degradation can be observed in human BL (Bahram et al., 2000).

Whereas high MYC protein levels represent a common feature of several human neoplasms, deregulation of MYC activity throughout the cell cycle may represent another important mechanisms leading to altered MYC function in tumor cells (Adhikary and Eilers, 2005).

5.5 The BCR in B cell lymphomas

The expression of a functional, non auto-reactive BCR on the surface of B cells represents a prerequisite to ensure a successful progression throughout B cell development. In early B cell development, the expression of the pre-BCR first, and the BCR later, represents a critical checkpoint to promote further B-cell differentiation (Kitamura et al., 1992; Kitamura et al., 1991; Torres et al., 1996). In secondary lymphoid organs, the survival of mature B cells is strictly dependent on surface BCR expression, as conditional ablation of the BCR, or its signaling component Igα, in genetically modified animals, have revealed a strict dependence on these determinants for B-cell survival (Kraus et al., 2004; Lam et al., 1997; Srinivasan et al., 2009).

Given that most mature B cell lymphomas retain BCR expression, it has been long suggested that the immunoglobulin receptor contributes to the survival and/or proliferation of malignant B cells, and the following evidences support this hypothesis.

First, in BL, the MYC translocation affects always specifically the Ig locus in germline configuration, or at most carrying a non-functional V gene rearrangement. This condition preserves in the tumor cells the ability to express a functional BCR and thus suggests the requirement of lymphoma cells for signals emanating from the antigen receptor both during tumor initiation and maintenance (Kuppers, 2005; Kuppers and Dalla-Favera, 2001).

Second, treatment of follicular lymphoma patients with anti-idiotypic antibodies led to an efficient treatment of the disease. Patients showing tumor relapses developed FL consisting of malignant B-cell clones that retained BCR expression but had a different BCR-specificity, thus eluding the anti-idiotypic treatment (Cleary et al., 1986; Meeker et al., 1985).

Finally, except for classical Hodgkin disease, most GC-derived B cell lymphomas (including the most common BL, FL and DLBCL types) with signs of ongoing Ig somatic hypermutation display a strong selective pressure to retain the structural integrity of the BCR, accumulating mutations in the CDR regions (Braeuninger et al., 1997; Lossos et al., 2000).

5.6 Objectives of the study

As previously described, numerous observations pointing to the requirement of the BCR for lymphoma cell survival and\or proliferation are currently available. Nevertheless, the direct contribution of the immunoglobulin receptor to the maintenance of B cell tumors has not been specifically addressed. In this view, the aim of the present work is to determine the role of the BCR to survival and proliferation of c-MYC transformed mature B cells in a mouse model of BL.

For this purpose, cell proliferation and survival of transformed B cells were evaluated both *in vitro* and *in vivo,* upon conditional deletion of the BCR by TAT-Cre transduction of primary lymphomas. Moreover, the molecular mechanisms underlying the requirement of the BCR for survival of lymphoma B cells will be addressed. Finally, the identification of molecules and\or signalling pathways, as crucial determinants for lymphoma survival, will provide novel therapeutic targets to be introduced in the treatment of MYC-driven mature B cell tumors.

6 Materials & Methods

6.1 Mice

C57BL/6 and C57BL/6 x BALB/c F1 (CB6F1) animals were purchased from Charles River or Jackson Laboratories. λ-myc and B1-8f mice were previously described (Kovalchuk et al., 2000; Lam et al., 1997). All animals were kept under specific pathogen free conditions. Mouse experimentations were performed under the protocol number approved by the Italian Ministry of Health and the IFOM IACUC Committee.

6.1.1.1 Histology

Tissue samples were fixed in PBS/1% formalin and embedded in paraffin. Haematoxylin and eosin stainings were performed in collaboration with Dr. C. Doglioni and M. Ponzoni (Department of Pathology, San Raffaele Scientific Institute, Milan, Italy) according to standard procedures.

6.2 Molecular Biology Techniques

6.2.1 Genomic DNA extraction from tail biopsy

Mouse tissue or cells were lysed o/n at 56°C in 400 µl lysis buffer (100 mM Tris-HCl pH 8; 5 mM EDTA; 200 mM NaCl; 0.2% SDS; 100µg/ml Proteinase K), shaking at 850 rpm, overnight in Thermomixer compact. Undissolved debris were pelleted and DNA in the supernatant was precipitated with 1 ml of isopropanol. The DNA was pelleted by centrifugation, air-dried and resuspended in 400 µl of milliQ water by incubation at 50˚C for 20 min.

6.2.2 Genotyping strategy

The genotypes of all mice offsprings were analyzed by polymerase chain reaction (PCR) performed on genomic DNA extracted from tail. For amplification, primers summarized in Table 1 and PCR reagents in Table 2 were used. PCR conditions are summarized in

Table 3. PCRs were run in automatic thermocycler GeneAmp PCR System9700 (Applied Biosystems).

6.2.3 Agarose gel electrophoresis and DNA gel extraction

Separation of DNA fragments by size was achieved by electrophoresis in agarose gels (0.7% - 2.5%; 1x TAE (Sambrook and Russell, 2001); 1x GelRed™, BIOTIUM). As a size marker for agarose gel electrophoresis 1kb plus ladder (NEB, USA) was used.

6.2.4 RNA and DNA extraction

Total RNA was extracted from 10^6 cells, using QIAGEN RNeasy kit following the manufacturer's protocol. A DNAse (QIAGEN) digestion step was added before elution to ensure the complete elimination of contaminant DNA.

6.2.5 cDNA synthesis

Complementary DNA (cDNA) was produced using SuperScript® VILO™ cDNA Synthesis Kit (Invitrogen) following the manufacturer's protocol. Specifically, master mix (containing 5X VILO™ Reaction Mix, 10X SuperScript® Enzyme Mix, water and RNA) was incubated for 10 min at RT. For increased yields of cDNA incubation time was prolonged to 120 min at 42°C. Reaction was terminated by 5 min incubation at 85°C. 25 ng of cDNA were used for real time PCR reaction.

6.2.6 Real-time quantitative PCR (RT-qPCR)

For gene expression analysis RT-QPCR was performed using 25 ng of cDNA, 500 nM primers mix and 10 µl of LightCycler® 480 SYBR Green I Master, containing Hot-start polymerase (Roche) in a final volume of 20 µl per reaction in 96-well format. Reaction conditions were: 95°C for 10 min, 45 cycles of 95°C for 1 sec, 60°C for 10 sec, 72°C for 1 sec. Accumulation of fluorescent products was monitored using a LightCycler® 480 Real-Time PCR System (Roche). Specificity of PCR reaction was controlled by the melting-temperature profiles of final products (dissociation curve). Ribosomal protein large p0 (Rplp0) gene was used as a control housekeeping gene for normalization (Akamine et al., 2007; Laborda, 1991). Primers are listed in Table 4. Transcript fold enrichment was calculated by ΔΔct method (Livak and Schmittgen, 2001).

6.2.7 Microarray analysis

Affymetrix GeneChip® Arrays were performed at GeneChip® Mouse Gene 1.1 ST Array platform. The GeneChip® Mouse Gene 1.1 ST Array with more than 750,000 unique 25-mer oligonucleotides covers the whole genome transcript. Each of the 28,853 covered genes is represented on the array by approximately 27 probes spread

across the full length of the gene. Data analysis is described in Statistical analysis section.

Table 1: Genotyping primers, annealing temperatures and amplicons

Primers		T_A	Product	
Human c-MYC			Amplicon	size
5'-GAGGCAGGCTCCTGGCAAAAGGTCA-3'	hMYC Fw	58°C	tg	400 bp
5'-GAAATGAGCTTTTGCTCCTCTGCTTG-3'	hMYC Rv			
B1-8F vs IgH				
5'-CCAAAGTCCAGGCTGAGCAAAAC-3'	B1-8f vs IgH Fw	56°C	wt	300 bp
5'-GATCATGAACAAAGTCACTGTAAATG-3'	B1-8f vs IgH rv		fl	340 bp
***Cdkn2a*\p19**				
5'-TTAACAGCGGAGCTTCGTACA-3'	Ink4a/Arf Fw	60°C	tg	150 bp
5'-CTGCACCGTAGTTGAGCAGAA-3'	Ink4a/Arf Rv			
Trp53				
5'-GGATGGTGGTATACTCAGAGCC-3'	Trp53 Fw	58°C	wt	450 bp
5'-AGCGTGGTGGTACCTTATGAGC-3'	Trp53 Rv			
V_kJ_k				
5'–GCGAAGCTTCCCTGATCGCTTCACAGG-3'	V_k Fw 1		VkJk1	800bp
5'-GCGAAGCTTCCCWGCTCGCTTCAGTGG-3'	V_k Fw 2		VkJk2	550bp
5'-GCGAAGCTTCCCAKMCAGGTTCAGTGG-3'	V_k Fw 3		VkJk3	250bp
5'-CTCAGAGCTCTAGGCCCCTCTTTGAT-3'	J_{k5} Rv	55°C	VkJk5	100bp

Table 2: Master mix used for PCR genotype

PCR master mix	µl
H2O	14.4
5x flexi buffer	5
MgCl2 25 mM	2
dNTPs 2.5 mM	2
primer Fw 50 µM	0.2
primer Rv 50 µM	0.2
GO Taq	0.2
DNA	1
total	25

Table 3: Conditions used for PCR genotype

PCR cycle	
Temperature(°C)	Time (min)
94	2:30
94	0:30
T_A	0:30
72	0:30
72	5:00
4-15	hold

] X35

Table 4: Primer sequences for quantitative PCR analysis

Primers	Sequence	Target
Rplp0 Fw	5'-TTCATTGTGGGAGCAGAC-3'	RNA
Rplp0 Rv	5'-CAGCAGTTTCTCCAGAGC-3'	RNA
B1-8-Cm Fw	5'-CTGCGGTCTATTATTGTGCAAG-3'	RNA
B1-8-Cm Rv	5'-GGAAGACATTTGGGAAGGAC-3'	RNA

6.3 Lymphoma Cell Culture

6.3.1 Preparation of cell suspension from lymphoid organs

Single-cell suspensions were obtained by grinding spleens and lymph nodes between slide glasses followed by filtering through 70 μm nylon meshes (Becton Dickinson, USA). Femurs were flushed using a syringe containing 5-10 ml of B-cell medium (DMEM supplemented with 10% heat-inactivated fetal bovine serum, 0.1mM non-essential amino acids, 1 mM sodium pyruvate, 50μM β-mercaptoethanol and 2mM L-glutamine; Invitrogen) to obtain bone marrow cells.

Erythrocytes lysis from spleen and bone marrow preparations was achieved incubating cell suspensions in 1 ml of a 9:1 (v/v) solution of 0.15M NH_4Cl and 0.17M Tris-HCl pH 7.65 for 3 min on ice. Red blood cell lysis was interrupted adding 10 volumes of B-cell medium. Cells were centrifuged at 1200 rounds per minute (rpm) at 4°C and re-suspended in B-cell medium before counting.

Live cells were counted using Trypan blue dye to distinguish live and dead cells.

6.3.2 B cell activation

Primary B cells were isolated from spleen of C57 BL6/J mice by magnetic activated cell sorting (MACS) purification (see below, 6.4.2, Magnetic Cell sorting). Briefly, spleen was processed as previously described (6.3.1, Preparation of cell suspension from lymphoid organs) and single cell suspension was labelled using anti-CD19 conjugated micro-beads, according to manufacturer's protocol (Milenyi Biotech, Germany). $CD19^+$ B cells were purified using LS columns (Milenyi Biotech, Germany) and activated by by cross-linking the BCR using polyclonal goat anti-mouse IgM bivalent antibody ($F(ab')_2$, 20 μg/ml, Jackson Immuno-Research), 3 to 5 minutes at 37°C. Cells were washed twice with ice cold PBS, by centrifuging for 5 minutes,

2000 rpm at 4°C. Cells were lysed as described below (6.5.1, Immunoblot analysis) and used for western blot analysis.

6.3.3 Establishment of cell lines from λ–MYC lymphomas

Primary lymphomas obtained from diseased animals were cultivated with B cell medium in 25 mm^2 or 75 mm^2 cell culture flasks at 37°C in a humid atmosphere with 5% CO_2. Cell density was adjusted to $2x10^5$ cells/ml and medium was refreshed every 48 hours. On average two weeks after initial seeding, over 50% of primary lymphomas gave rise to tumor cell lines adapted to grow under *in vitro* experimental conditions.

6.3.4 TAT-Cre transduction of primary lymphoma cells

Lymphoma cells were washed three times, re-suspended in serum-free media (Hyclone, USA) at a density of $5x10^6$ cells/ml and incubated for 45 min at 37°C with 37.5 µg/ml (final concentration) of recombinant TAT-Cre. Transduction was stopped diluting samples with 10 volumes of B-cell medium, cells were spun down, re-suspended in B-cell medium and cultured at a density of 2 x 10^5 cells/ml. Deletion efficiency was evaluated 24-48 hours later by flow cytometry.

6.3.5 Isolation of BCR^- lymphoma cells by limiting dilution

Upon Tat-Cre transduction, mixture of BCR^+ and BCR^- lymphoma cells were seeded at a density of 0.3 cells\well, in 96-well plates. Cells were incubated at 37°C, 5% CO_2, until colonies derived from single cells were visible in the plates. BCR status of each colony was analysed by flow cytometry.

6.3.6 Treatment of lymphoma cells with small molecule inhibitors

BCR^+ and BCR^- lymphoma cells were seeded at $5x10^5$\ml and incubated at 37°C, 5% CO_2, for 12-16 hours. Cells were washed with PBS and plated at a density of $4x10^5$\ml in B cell medium, in 24-well plate. 1 volume of 2x Rapamycin (10nM final

concentration) or CT99021 (1μM final concentration) was added to each well. DMSO was used as vehicle control. Cells were counted every 24-48 hours and analysed by flow cytometry (see below 6.4.1, Flow cytometry and cell sorting analysis). Rapamycin and CT99021 were purchased from ABCR (#AB253776) and Sigma-Aldrich (#53123-88-9), respectively.

6.3.7 BCR complementation of tumor cells by retroviral transgenesis

Phoenix packaging cells were transfected with either a pMIG-IRES-GFP empty vector or a pMIG-IRES-GFP vector, expressing an allotype b-marked IgH chain carrying a B1-8 V_H gene. Supernatant containing the viral particles was added to a BCR^+ λ-MYC;B1-8f lymphoma cell line, followed by three rounds of spin infection (2000 rpm, 30°C, 45 minutes). Infected cells were transduced with TAT-Cre and sorted (as described below, *6.4.1,* Flow cytometry and cell sorting) respectively as $GFP^+IgM_b^+IgM_a^-$ or $GFP^+IgM_b^-IgM_a^-$. IgM_b^+ and IgM^- sorted cells were mixed in equal numbers and cultured *in vitro* for 9 days or transplanted into recipient mice.

6.3.8 Adoptive transfer of λ-MYC lymphomas

Primary lymphomas were obtained as single cell suspensions from SPL, BM or MLN of 12 to 16 weeks-old diseased mice. After red blood cell lysis, tumor cells were counted and cultured for the following one to two weeks in B cell medium at a density of $2x10^5$ cells\ml. Before transplantation into secondary recipients, lymphoma cells were washed twice in PBS, re-suspended at $3x10^7$ cells/ml and 100 μl of cell suspension was injected into the tail vein of 16-20-weeks old immunoproficient CB6F1 mice.

6.4 Flow cytometry

6.4.1 Flow cytometry and cell sorting analysis

For flow cytometric analysis aliquots of $1x10^6$ cells were stained for 20 minutes on ice in 50 µl FACS buffer (1% PBS, 1% BSA, 0.01% Sodium Azide (N_3) containing the appropriate mixture of fluorescently labeled antibodies (Abs). Two-step staining was performed when biotinylated Abs were detected using fluorescently-labeled streptavidin as secondary reagent. Stained cells resuspendend in FACS buffer were acquired on a FACSCalibur (BD Pharmingen, USA) and data were analyzed using Flowjo software (Tree Star, USA). Dead cells were excluded from the analysis by labeling with propidium iodide or based on forward and side scatter parameters.

Sorting of labeled cells was performed with a FACS Vantage or FACS Aria (BD Pharmingen, USA). Monoclonal Abs were purchased from eBioscience. Anti-IgM monoclonal Abs R331.12 and R3324.12 were produced in house. Monovalent anti-IgM Fab polyclonal Abs were purchased from Jackson Immunoresearch.

List of Abs as well as working dilutions are listed in Table 5

6.4.2 Magnetic cell sorting

For B cell purification, splenic cells were magnetically labeled by using MicroBeads conjugated Abs anti-CD19, following manufacturer's protocol (MACS; Milenyi Biotech, Germany). This procedure allows the isolation of resting B cells from single cell suspensions of lymphoid tissues. For purification of BCR^- tumors, cells were stained with biotinylated anti-IgM (cl. R331.12) for 20 min on ice, washed twice with PBS/0.5% BSA/N_3 (FACS Buffer), and subsequently labeled by incubation with anti-biotin microbeads, for 30 min at 4°C. Finally, cells were applied onto LD columns under a magnetic field (Miltenyi et al., 1990). Flow-through IgM^- lymphoma cells

were spun down, re-suspended in B-cell medium and cultured at 37°C in a humid atmosphere with 5% CO_2

Table 5: List of antibodies used for flow cytometry

Antibodies and antigen (clone)	Source	Dilution factor
Monoclonal Rat–anti mouse CD5 (53-7.3)	eBiosciences	1/200
Anti mouse IgM (R331.12)	Home-made	1/400
Anti mouse Kappa (R331.18)	Home-made	1/800
Monoclonal Rat-anti mouse CD138 (281-2)	eBiosciences	1/200
Monoclonal Rat-anti mouse CD19 (eBio1D3)	eBiosciences	1/400
Monoclonal Rat-anti mouse CD21/CD35 (eBioD89)	eBiosciences	1/1000
Monoclonal Rat-anti mouse CD23 (B3B4)	eBiosciences	1/100
Monoclonal Rat-anti mouse CD25 (PC61.5)	eBiosciences	1/200
Monoclonal Rat-anti mouse CD38 (90)	eBiosciences	1/600
Monoclonal Rat-anti mouse CD43 (eBioR2/60)	eBiosciences	1/100
Monoclonal Rat-anti mouse/human CD45R (B220) (RA3-6B2)	eBiosciences	1/400
Monoclonal Rat-anti mouse CD69 (H1.2F3)	eBiosciences	1/200
Monoclonal Rat-anti mouse BP-1 (6C3)	eBiosciences	1/100
Monoclonal mouse-anti BrdU (PBR-1)	BD	1/5
Monoclonal mouse anti-human IgM (G20-127)	BD	1/1000
Streptavidin (APC)	eBiosciences	1/800
Streptavidin (FITC)	eBiosciences	1/400

6.4.3 CFSE labeling

Single-cell suspensions of primary λ-MYC lymphoma cells or their cell line derivatives were washed three times in PBS followed by labeling for 10 min at 37°C with serum-free RPMI media containing 0.5 μM (final concentration) 5-(and-6)-carboxyfluorescein diacetate, succinimidyl ester (CFDA); Molecular Probes, USA) (Lyons and Parish, 1994). The labeling reaction was stopped adding 10 ml DMEM/10% FBS. Subsequently, labeled cells were washed once in B-cell medium and

seeded at a density of $1x10^6$ cells/ml. 20 million tumor cells were injected into syngeneic recipients after CFSE-labeling for *in vivo* homing experiments.

6.4.4 Measurement of glucose uptake

Highly purified BCR^+ and BCR^- lymphoma cells were grown under normal conditions, plated at $5x10^5$/ml and incubated O/N at 37°C, 5% CO_2. For glucose uptake assays, 100 μM 2-NBDG (Invitrogen) was added to the media for 2 hr. Cells were washed with PBS, counted and BCR^+ and BCR^- cells were mixed in equal amount and stained for IgM expression as described above. Fluorescence was measured in a FACSCalibur Analyzer (BD).

6.4.5 Cell cycle analysis

BCR^+ and BCR^- lymphoma cells were plated at a density of $5x10^5$\ml and incubated O/N at 37°C, 5% CO_2. BCR^+ and BCR^- cells were mixed in equal amount and pulsed with 33 μM_f BrdU (Sigma), for 5 minutes, at 37°C, 5% CO_2. Cells were washed 3 times with cold PBS and surface stained for IgM was performed. $1x10^6$ cells were stained in 50 μl of FACS buffer, for 20 min at 4˚C in dark and subsequently washed twice with 200 μl of FACS buffer. Surface stained cells were fixed in BD Cytofix/Cytoperm™ buffer for 20 min at room temperature (RT) in U bottom 96 well microplate, washed by Perm/Wash™ Buffer (P/W) and re-fixed in BD Cytofix/Cytoperm™ Plus buffer for 10 minutes, at RT, light protected. Cells were washed with P/W and incubated 5 minutes with BD Cytofix/Cytoperm™ buffer, at RT, light protected, and washed again with P/W. Fixed cells were treated with 300 μg/ml DNAse for at least 1 hour, at 37°C, washed with P/W, and stained with anti-BrdU-FITC conjugated antibody, 30 minutes, RT. Stained cells were washed two times, re-suspended in 1 ml of cold PBS containing propidium iodide (50 μg/ml, Sigma) and RNase (250 μg/ml), and incubated overnight

at 4°C. Samples were acquired by FACSCalibur (BD) and analyzed using FlowJo software.

6.4.6 Apoptosis analysis

For detection of apoptotic cells CaspGLOW™ Fluorescein Active Caspase Staining Kit (Biovision) was used, with specific modifications in protocol. *In vitro* cultured cells were incubated in 100 μl of B cell medium containing 1 μl of FITC-VAD-FMK (carbobenzoxy-valyl-alanyl-aspartyl-[O-methyl]- fluoromethylketone), a cell-permeable pan caspase inhibitor that irreversibly binds to the catalytic site of caspase proteases, for 1 h at 37°C and 5% CO_2. Cells were collected by centrifugation (280 g for 5 min) and washed with 200 μl of wash buffer. If required cells were stained following the protocol of chapter 6.4.1 (*Flow cytometry and cell sorting analysis*), acquired by FACSCalibur (BD) and analyzed using FlowJo software.

6.4.7 Phospho flow cytometric analysis

10^6 cells BCR^+ and BCR^- were fixed in 2% paraformaldehyde, washed in PBS, and re-suspended in 90% ice-cold methanol at -20°C for at least 30 min. Cells were then washed three times in PBS/2% FCS before incubation with antibodies against surface markers as well as with a specific Rabbit anti-mouse phospho-GSK3β, for 30 min, at RT. Unconjugated phospho-GSK3β antibody was detected by subsequent incubation with Cy5-conjugated goat anti–rabbit antibody (30 minutes, RT). Cells were then washed twice and analyzed by flow cytometry using FACSCalibur (BD).

6.5 Biochemical techniques

6.5.1 Immunoblotting analysis

Cells were harvested by centrifugation for 5 min at 280 g and washed in cold PBS. For protein extraction cell pellet was resuspended in 8 M Urea lysis buffer (8 M Urea, 0.1 M NaH_2PO_4, 0.01 M Tris pH 8.0) or RIPA buffer (10 mM Tris-HCl, pH 8.0, 1% Triton, 0.1% SDS, 0.1% Deoxycholate, 140 mM NaCl, 1 mM EDTA, 1 mM DTT, 1 mM PMSF and protease inhibitor cocktail Set III (EDTA-free, Calbiochem,), and incubated 1 hour on ice. Sonication was performed in 2-3 cycles of 10 sec each. Lysates were centrifuged at maximum speed for 10 min to remove debris. Lysates were quantified with a protein assay reagent (Bio-Rad Laboratories). 20 - 50 µg of proteins, in Laemmli loading buffer (62.5 mM Tris-HCl pH 6.8, 2 % (w/v) SDS, 5 % (v/v) 2-mercaptoethanol and 10 % (v/v) glycerol) and 10 µl of NOVEX ® Sharp Pre Stained protein standard (Invitrogen) were run onto 10% SDS-polyacrylamide gel electrophoresis and transferred by dry iBlot® Dry Blotting Device (Invitrogen) to nitrocellulose membranes (iBlot® Transfer Stack, Invitrogen) in 6 minutes. After blotting, the membranes were stained with Ponceau S staining solution (0.1 % Ponceau S (w/v) and 5% acetic acid (w/v) to verify equal loading and transfer. Membranes were briefly washed in water and blocked for 1 h at RT in blocking solution 5% BSA, or 5% milk, in TBS-T (20 mM Tris HCl pH 7.4, 500 mM NaCl, 0,1 % Tween). After blocking, filters were incubated with primary antibodies (Table 6), diluted in blocking solution, for 1-2 hours at RT or overnight at 4°C. After three washes, of 5 min each in TBS-T, membranes were incubated with the appropriate horseradish peroxidase (HRP) conjugated secondary antibody diluted in blocking solution (Table 6), for 30 min, at room temperature. Membranes were washed three times for 5 min in TBS-T and the bound secondary antibody was revealed using the ECL (Enhanced Chemiluminescence) plus method (Amersham).

Table 6: Antibodies used for immunoblot protein detection

Primary Abs	Residue	Clone	Dilution factor	Source
Rabbit α p-Syk	Tyr 525/526	Polyclonal	1/1000 (BSA)	Cell signaling
Rabbit α-Syk		Polyclonal	1/1000 (BSA)	Cell signaling
Rat α phosho-tyrosine		4G10	1/1000 (BSA)	Millipore
Rabbit α-phospho-MYC	Thr 58	Polyclonal	1/500 (BSA)	Santa Cruz
Mouse α-Vinculin		hVIN-1	1/20000 (MILK)	Sigma
Mouse α-TP53		Polyclonal	1/1000	Santa Cruz
Secondary Abs				
Goat α mouse Ig	Polyclonal	170-6516	1/20000	BioRad
Goat α rabbit Ig	Policlonal	170-6515	1/20000	BioRad

6.5.2 Mitochondrial respiration

BCR^+ and BCR^- lymphoma cells were cultured at $2x10^5$\ml for 24 hours. Equal numbers of BCR^+ or BCR^- cells were loaded into an oxygraph chamber and oxygen consumption was measured. Baseline respiration was measured in the absence of exogenous substrates; cells were then stimulated with the protonophore carbonylcyanide-4-(trifluoromethoxy)-phenylhydrazone (FCCP; 0.05 mM) and uncoupled respiration was measured. Finally, antimycin A (2.5 μM) was used to inhibit cytochrome bc_1 complex (complex III), thus allowing non-mitochondrial respiration to be measured. Respiration rates were measured for each condition by an average value of the oxygen flux within a region of stable, consistent oxygen consumption. Respiration rates of each sample were normalized to the protein content.

6.5.3 Measurement of Lactate dehydrogenase activity

LDH activity in lymphoma cells was defined by measurement of NADH levels in supernatant of cultured cells. BCR^+ or BCR^- cells were seeded at $2x10^5$\ml and supernatant was collected 48 hours later. NADH levels were determined using Lactate Dehydrogenase Activity Assay Kit (BioVision), according to manufacturer's protocol. NADH binding to a specific probes results in a colorimetric reaction (λmax= 450 nm), and optical density (OD) was measured using a microplate reader (WALLAC VICTOR^3, PerkinElmer) at time zero (A_1), and after incubating the reaction, light protected, at 37°C for 30 min (A_2) (or longer if the LDH activity was low). The difference between the two reads (ΔA450 nm = A_2 - A_1) was then calculated. Background values were subtracted from all readings. ΔA450nm of the sample was applied to a NADH standard curve to get "*B*" (the NADH amount that was generated between T_1 and T_2). LDH Activity was then calculated as following:

$$LDH\ activity = \frac{B}{(t2 - t1) * V} * sample\ dilution = \ nmol/min/ml \ = \ mU/ml$$

Where:

- **B** is the NADH amount that was generated between t_1 and t_2 (in nmol).
- t_1 is the time of first reading (A_1) (in min).
- t_2 is the time of second reading (A_2) (in min).
- V is the pre-treated sample volume added into the reaction well (in ml).

Unit definition: One unit of LDH is the amount of enzyme that generates 1.0 µmol NADH per minute at 37°C in the provided buffer system.

6.6 Stable Isotope Labelling Aminoacid in Cell Culture (SILAC)

6.6.1 Aminoacid Labeling of lymphoma B cells

BCR^+ and BCR^- lymphoma cells were grown in SILAC media, prepared as described previously (Ong et al., 2002). Briefly, cells were grown in lysine- and arginine-free DMEM/Ham's F12 (1:1), supplemented with 10% dialyzed fetal bovine serum (FBS, Invitrogen). "Heavy" and "Light" media were prepared by adding 0.146 g/L $^{13}C_6$, $^{15}N_2$ L-Lysine and 0.84 g/L $^{13}C_6$ $^{15}N_4$ L-Arginine (Sigma) or the corresponding non-labelled amino acids, respectively. Growth in SILAC media was carried out for eight replications, to ensure complete protein labelling. Equal numbers ($12x10^6$) of heavy and light labelled cell population were mixed and lysed in 300 µl RIPA buffer. Briefly, protein extracts were Trypsin digested in solution overnight. To maximize protein identification, sample complexity was reduced by peptide fractionation using isoelectric focusing (IEF) (See below*, 6.6.2 In solution digestion and off-gel separation of peptide mixtures*). Liquid chromatography was coupled with tandem mass spectrometry on a high-resolution instrument (LTQ-FT Ultra Thermo Scientific; for details see below 6.6.3, *Liquid chromatography and Mass Spectrometry*). The experiment was performed in triplicate.

6.6.2 In solution digestion and off-gel separation of peptide mixtures

Total protein extracts (150 µg) from BCR^+ and BCR^- lymphoma cells were dissolved in denaturation solution (6 M urea, 2 M thiourea in 20 mM ammonium hydrogen carbonate) for 30 min. After complete denaturation, extracts were supplemented with 1 mM DTT and incubated for additional 30 minutes. Thyols were carboxymethylated with 5 mM IAA for 20 minutes and the proteins were digested by addition of 1 µg LysC for 3 h. After 4-fold dilution with 50 mM ammonium bi-carbonate, 1 µg trypsin was added and the sample was incubated overnight at 37°C.

The digestion was terminated by acidifying the sample to pH<2 with 100% TFA. Product peptides were then separated according to their isoelectric point (pI) by isoelectrofocusing electrophoresis, using the Agilent 3100 OFFGEL Fractionation Kit (Agilent Technologies) (Hubner et al., 2008). Samples were prepared and separated according to the manufacturer's protocol. After separation, peptides mixtures focused at different pH were reconstituted with 1% TFA and desalted and purified on C18 STAGE tips (Rappsilber et al., 2007).

6.6.3 Liquid chromatography and Mass Spectrometry

Peptides eluted from C18 Stage-tips were analyzed by nano-liquid chromatography using an Agilent 1100 Series nano-flow LC system (Agilent Technologies), directly interfaced to a LTQ-FT Ultra mass spectrometer (ThermoFisher Scientific, Bremen, Germany). The nano-liter flow LC was operated in one column set-up with a 15 cm analytical column (75 lm inner diameter, 350 lm outer diameter) packed with C18 resin (ReproSil, Pur C18AQ 3 lm, Dr. Maisch, Germany). Solvent A was 0.1% FA and 5% ACN in ddH2O and 19 solvent B was 95% ACN with 0.1% FA. Samples were injected in an aqueous 0.1% TFA solution at a flow rate of 500 nl/min. We used 140 min gradient from 2% to 60% acetonitrile in 0.5% acetic acid. Nanoelectrospray ion source (Proxeon, Odense, Denmark) was used with a spray voltage of 1.5–2.0 kV. No sheath, sweep and auxiliary gasses were used and capillary temperature was set to 180°C. The mass spectrometer was operated in a data-dependent mode to automatically switch between MS and MS/MS acquisition. In the LTQ-FT Ultra, full scan MS spectra were acquired at a target value of 2,000,000 ions and with a resolution of 100,000 (FWHM) at 400 m/z. In the LTQ MS/MS, spectra were acquired using a target value of 5,000 ions and the five most intense ions were isolated for CID-fragmentation.

6.6.4 Analysis of proteomics data

Identification and quantification of proteins was carried out using the MaxQuant software package v. 1.2.2.5 (Cox and Mann, 2008; Cox et al., 2011). The integrated Andromeda algorithm was used to search the IPI Mouse protein sequence database (v.3.87, Sep 2011). A maximum of two missed cleavages were permitted. Oxidation of Methionine and acetylation of the protein N-terminus were used as variable modifications. Carbamidomethylation of cysteine was used as a fixed modification. A minimum peptide length of 6 residues was required and the maximum false discovery rates were set to 1% at both the protein and peptide levels. To determine at high confidence a qualitative proteome, each MaxQuant-defined proteinGroup required a minimum of three peptide matches, of which at least two were unique from all peptides identified. Therefore, to determine an accurate quantitative proteome, a minimum of three ratio counts (RC>2) was considered.

6.7 Statistical analysis

6.7.1 Student's t-test

Statistical analysis of normally distributed values (Gaussian) was performed by two-tailed unpaired Student's t-test. Differences were considered significant at *p-value*<0.05.

6.7.2 2-way ANOVA

Statistical analysis to compare two independent variables in grouped samples was performed using 2-way ANOVA test. Differences were considered significant at *p-value*<0.05.

6.7.3 Chi-square with Yates correction

Statistical analysis to test independence in contingency tables was performed using chi-squared test with Yates correction. Differences were considered significant at *p<0.05*

6.7.4 Statistical analysis of the microarray data

Microarray analysis was performed on Affymetrix Mouse Gene 1.1 ST arrays. Raw data (CEL files) were filtered and normalized with Affymetrix Power Tools (APT) Software Package, using the rma-sketch algorithm to generate Log2 transformed intensity values. Log2 transformed data were annotated and analyzed using the annotation "pd.mogene.1.1.st.v1" (Benilton Carvalho, Platform Design Info for Affymetrix MoGene-1_1-st-v1; R package version 3.6.0), "mogene11stprobeset.db" (Arthur Li, Affymetrix Mouse Gene 1.1 - ST Array Probeset Revision 4 annotation data (chip mogene11stprobeset); R package version 4.0.1.), "mogene11sttranscriptcluster.db" (Arthur Li, Affymetrix Mouse Gene 1.1-ST Array Transcriptcluster Revision 4 annotation data (chip mogene11sttranscriptcluster); R

package version 4.0.1.) and the "affy" (Gautier et al., 2004) package of R software version 2.16.0 (http://www.r-project.org). Genes with a cut-off of 1.5-fold change over the baseline, in at least two independent tumors, were defined as differentially expressed and were included in the gene ontology analysis.

6.7.5 Gene Ontology analysis

Gene Set Enrichment analysis was performed accessing the Gene Set Analysis Tool kit V2 (Zhang et al., 2005) (http://bioinfo.vanderbilt.edu/webgestalt/) on September 2012. A hypergeometric test was run to identify ten overrepresented Gene Ontology categories among Biological Process, Molecular Functions and Cellular Component. Adjusted *p values* were calculated applying Benjamini & Hochberg multiple test. Similarly a WIKIPathways Enrichment analysis was performed to identify overrepresented signaling pathways.

7 RESULTS

7.1 The λ-MYC lymphoma model

λ-MYC transgenic mouse strain (Kovalchuk et al., 2000) has been considered for several years the best mouse model for BL, given the close similarity in its genetic features, immunophenotype and histological appearance with the human BL. This strain was generated by cloning the c-MYC oncogene, derived from a human-BL cell line, under the control of the Ig λ light chain regulatory elements, thus restricting its overexpression in B cell compartment, and more precisely, from pre-B cell stage on. λ-MYC model overcomes the limitation of the Eμ-MYC mouse model, where c-MYC overexpression in pro-B cells resulted in the development of lymphoblastic lymphoma rather than BL. For this reason, the λ-MYC mouse model was used in the present study to investigate the role of the BCR in BL.

7.2 λ-MYC; B1-8f mice develop clonal Ig^+ B cell lymphomas

To delete the BCR in a conditional manner, λ-MYC transgenic mice (Kovalchuk et al., 2000) were bred to B1-8f knock-in animals, carrying a conditional pre-rearranged V_H gene inserted into the endogenous IgH locus (Lam et al., 1997) (Figure 11).

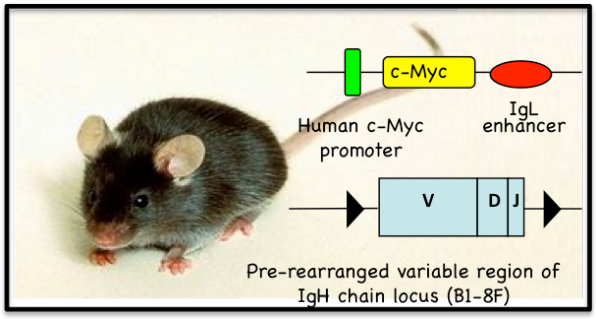

Figure 11: The λ–MYC; B1-8f lymphoma model

λ-MYC mice expressing a human c-MYC gene under the control of Ig light (igL) chain *cis* regulatory elements, were bred to conditional B1-8f knock-in mice carrying a pre-rearranged Ig heavy (IgH) chain variable region gene, flanked by loxP sites inserted into the IgH locus replacing the J_H segments.

λ-MYC;B1-8f double transgenic mice showed a median survival of 122 days (Figure 12). By this time, animals suffered of macroscopic lymphadenopathy, splenomegaly, decreased motility, shaggy fur and, at advanced stages of tumor, cachexia and limb paralysis.

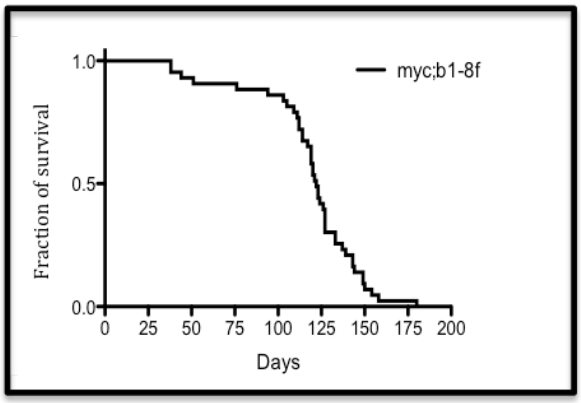

Figure 12: Survival of λ–MYC; B1-8f mice

Kaplan-Meier's plots representing the survival of λ-MYC; B1-8f mice. Median survival was 122 days (n=43).

Both male and female transgenic mice were equally affected. Histological analysis of the spleen of λ-MYC; B1-8f diseased animals revealed an expanded white pulp, and an infiltration of the red pulp by tumor cells. Tumors featured a "starry sky" appearance similar to human BL resulting from the presence of tissue macrophages clearing

apoptotic cell debris (Figure 13a). Upon dissection of diseased animals, flow cytometric analysis revealed the dissemination of large (FSC^{hi}) $CD19^{+}$ $CD43^{+}$ tumor B cells in spleen (SPL), bone marrow (BM) and lymph nodes (LN) where tumor cells frequently replaced the resident lymphocyte population (Figure 13b).

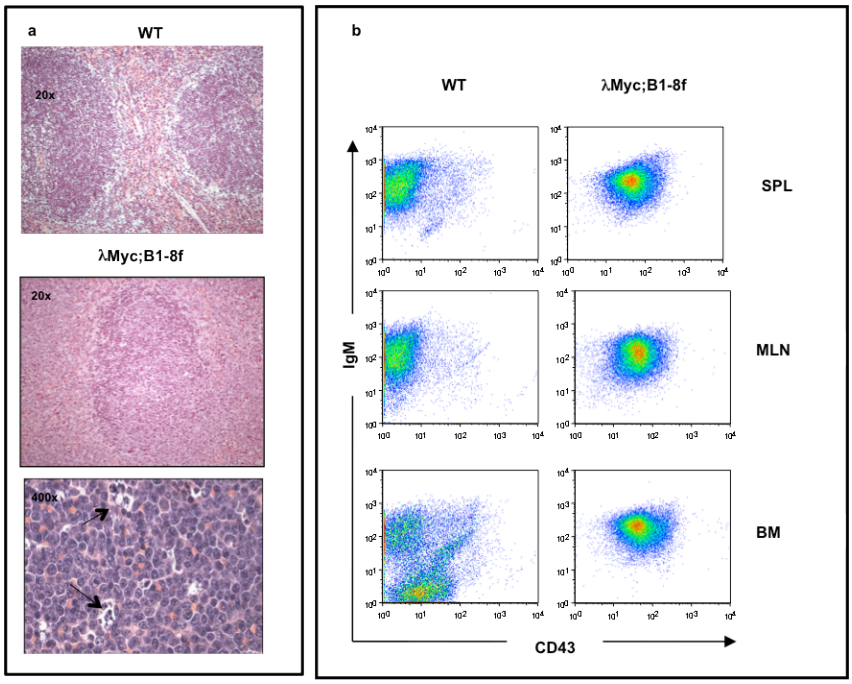

Figure 13: λ-MYC;B1-8f mice develop tumors resembling human Burkitt lymphoma by histological and immunophenotypic appearance

a) Hematoxylin and eosin staining of spleen sections from a representative λ-MYC;B1-8f diseased animal, revealing expanded red pulp and infiltrated white pulp (middle panel) and a characteristic starry sky appearance, comprised of sheets of neoplastic lymphoid cells with round to irregular nuclei and multiple distinct nucleoli, and numerous tingible body macrophages (400x, black arrows). Upper panel shows a representative spleen section from a C57BL6/J control mouse. Upper and middle picture: magnification X20, lower X400; **b)** Representative FACS analysis of single-cell suspensions from lymphoid organs of a representative λ-MYC;B1-8f diseased animal. Dot plots are gated on live $B220^{+}$ B cells. An aged-matched C57BL6/J wild-type (WT) animal was used as control.

Immunophenotypic analysis of B lymphoma cells revealed the expression of surface markers shared with B-cell progenitors (CD43 and AA4.1), immature/mature B cells (IgM, CD38) and most importantly with human BL (such as IgM, CD19, B220 and CD43).

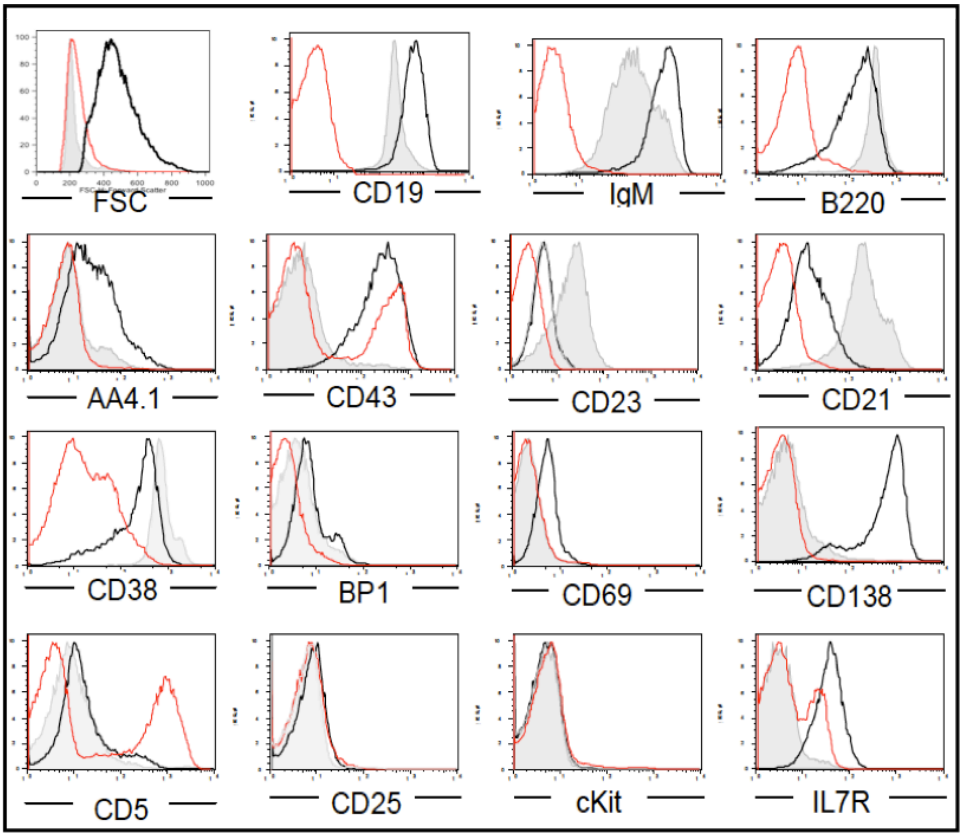

Figure 14: Immunophenotype of λ-MYC; B1-8f primary lymphoma B cells

Flow cytometric determination of surface expression levels of the indicated markers in $CD19^+$ splenic wild-type B cells (filled grey line), tumor B cells (thick black line) and $CD19^-$ non-B cells (red thin line).

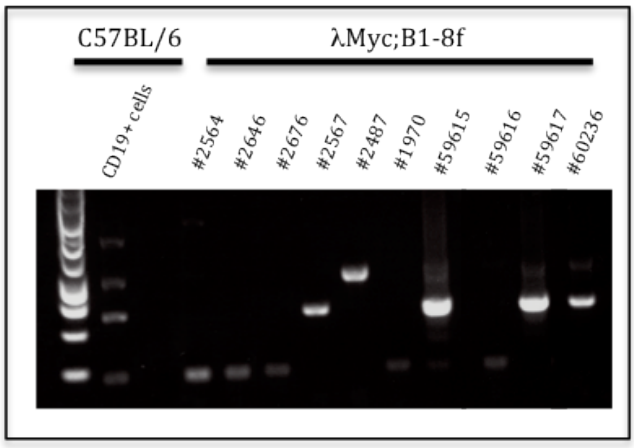

Figure 15: λ–MYC;B1-8f tumors are clonal

Analysis by genomic PCR of IgL VκJκ V-gene rearrangements in control (C57BL/6) $CD19^+$ B cells and in 10 independent primary λ–MYC;B1-8f lymphomas. The 4 PCR bands amplified in the control sample identify V_kJ_k rearrangements using respectively, J_k1, J_k2, J_k3, and Jk5 segments. In all tumor samples a single-PCR band was visible confirming the clonal nature of lymphomas. The 1Kb ladder size ladder (first lane) was used to determine the size of the PCR fragments.

A representative immunophenotypic analysis of λ-MYC;B1-8f lymphoma B cells is shown in Figure 14, and the repertoire of surface molecules expressed on λ-MYC;B1-8f tumor B cells pointed to an immature B cell phenotype.

Importantly, analysis of VJ rearrangements on the Igκ locus from 10 independent tumors confirmed the monoclonal nature of λ-MYC;B1-8f lymphomas (Figure 15).

7.2.1 Basal BCR signaling in λ-MYC; B1-8f lymphomas

The survival of resting mature B-cells is strictly dependent on a tonic, low-strength signal emanating from the BCR, since genetic deletion of the receptor, or its signalling components, represents a "sentence of death" for a lymphocyte (Kraus et al., 2004; Lam et al., 1997). BCR-dependent signalling is initiated by receptor-associated tyrosine kinases of the Src family (Lyn, Fyn, and Blk) (Saijo et al., 2003) and of the Syk family (Syk and Zap-70) (Rowley et al., 1995). Activated Syk and Src-family protein kinases phosphorylated specific proteins, such as CD19 or BCAP (B-cell PI3K adapter protein) that mediate the recruitment of PI3K to the plasma membrane, promoting its activation (Okkenhaug and Vanhaesebroeck, 2003). Concomitant depletion of BCR and activation of candidate signalling pathways in mature B-lymphocytes *in vivo* provided evidence that B cells without BCRs can survive and accumulate only in the presence of a constitutively active PI3K (Srinivasan et al., 2009). In fact, the establishment of either a constitutive mitogen-activated protein kinase (MAPK) pathway, a constitutive Rac1 pathway, or a constitutive non-canonical NF-κB pathway, was not able to rescue B cells, devoid of BCRs, from death. Interestingly, deletion of FOXO1 alone also rescued B cells without BCRs, suggesting that the PI3K-AKT-FOXO axis is crucial in supporting BCR-driven signals that mediate survival of B cells (Srinivasan et al., 2009).

The signal emanating from the BCR in resting B cells is weaker than that triggered in response to antigen recognition that leads to a robust activation of downstream

signaling pathways such as the NF-kB, PI3K and MAPK pathways, responsible for inducing cell proliferation and differentiation.

The activation status of the BCR signalling pathway in primary λ-MYC;B1-8f lymphomas was assessed by immunoblot analysis. The levels of total tyrosine-phosphorylated proteins, as well as phosphorylation of specific effectors of BCR-signalling, were compared between primary lymphoma cells and both resting and BCR-activated wild-type splenic B cells.

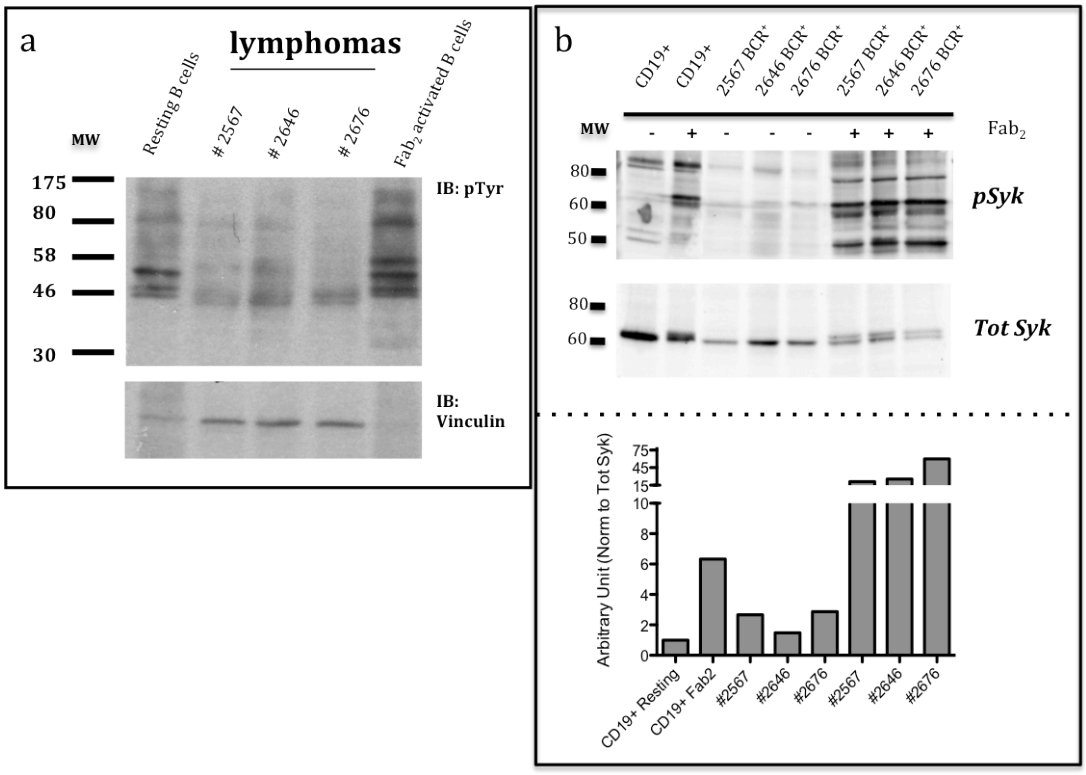

Figure 16: λ-MYC;B1-8f lymphoma B cells show basal, tonic BCR signalling

a) Immunoblot analysis to measure total levels of phosphotyrosine proteins in protein extracts from three independent primary B-cell lymphomas (#2567, #2646 and #2676, respectively). *Ex vivo* isolated CD19⁺ splenic B cells before (resting) and after (anti-F(ab)$_2$) BCR cross-linking were used as reference. Vinculin levels were measured to control for protein input b) Immunoblot analysis of phosphorylated Syk (pSyk) in three independent primary λ-MYC lymphomas (#2567, #2646 and #2676, respectively) before (-) and after (+) BCR crosslinking (α-IgM F(ab)$_2$ ab). Ex vivo isolated CD19⁺ splenic B cells were used as controls. Total Syk levels were measured to control for loading differences. Predicted Syk molecular weight (MW) is 72 kDa. Normalized phospho-Syk levels are shown in the lower panel. Bars indicate fold change in phospho-Syk levels compared to those measured in resting CD19⁺ splenic B cells.

As shown in Figure 16, the pattern of phospho-tyrosine proteins in three independent lymphomas closely resembled that of resting B cells. Moreover, phosphorylation levels of the Syk tyrosine kinase, an essential proximal effector of BCR signalling, were comparable between lymphoma and wild-type resting mature splenic B cells. These results indicate that λ-MYC;B1-8f tumor B cells receive a tonic low-strength signal from their BCR. Finally, I could show that crosslinking of the BCR in lymphoma cells led to a robust increase in total tyrosine-phosphorylated protein levels as well as Syk phosphorylation, pointing to a functionally competent BCR expressed by tumor B cells.

7.2.2 λ-MYC;B1-8f lymphomas expand in vitro and in vivo upon transplantation

Single cell suspensions of primary λ-MYC;B1-8f lymphoma B cells isolated from lymphoid organs of diseased animals, were cultured *in vitro* in complete B cell medium. An initial phase of cell death was followed by an exponential growth of lymphoma B cells that had adapted to the *in vitro* culture conditions. Lymphoma B cells showed a doubling time ranging between 12 to 24 hours (Figure 17). The establishment of stable cell lines was often associated with the property of lymphoma cells to shorten the doubling time.

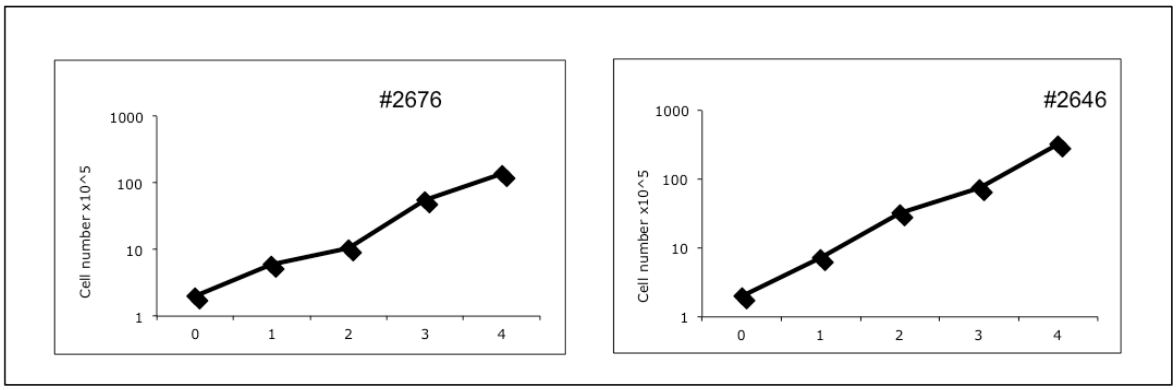

Figure 17: *Ex vivo* isolated lymphoma cells grow *in vitro*

In vitro growth curve of purified λ-MYC;B1-8f primary lymphomas (#2676 or #2646). Tumor cells were counted every 24 hours and diluted every second day. Each time point represents the average count of three replicates.

To determine the ability of lymphoma cells to give rise to secondary tumors, *ex vivo* isolated λ-MYC;B1-8f tumor cells were transplanted into non-irradiated, immunoproficient syngeneic recipients through tail-vein injection.

Recipient mice were sacrificed 20 days after transplantation and lymphoid organs analyzed for the presence of tumor cells. Lymphoma cells were identified by flow cytometry in all lymphoid organs on the basis of their size (FSC^{hi}) and their unique surface marker combination ($IgM^{+}CD43^{+}$) (Figure 18). Histological analysis confirmed the presence of aggressive B-cell lymphomas in the lymphoid organs of recipients, often associated to the identification of tumor cells in non-lymphoid organs including lung and liver.

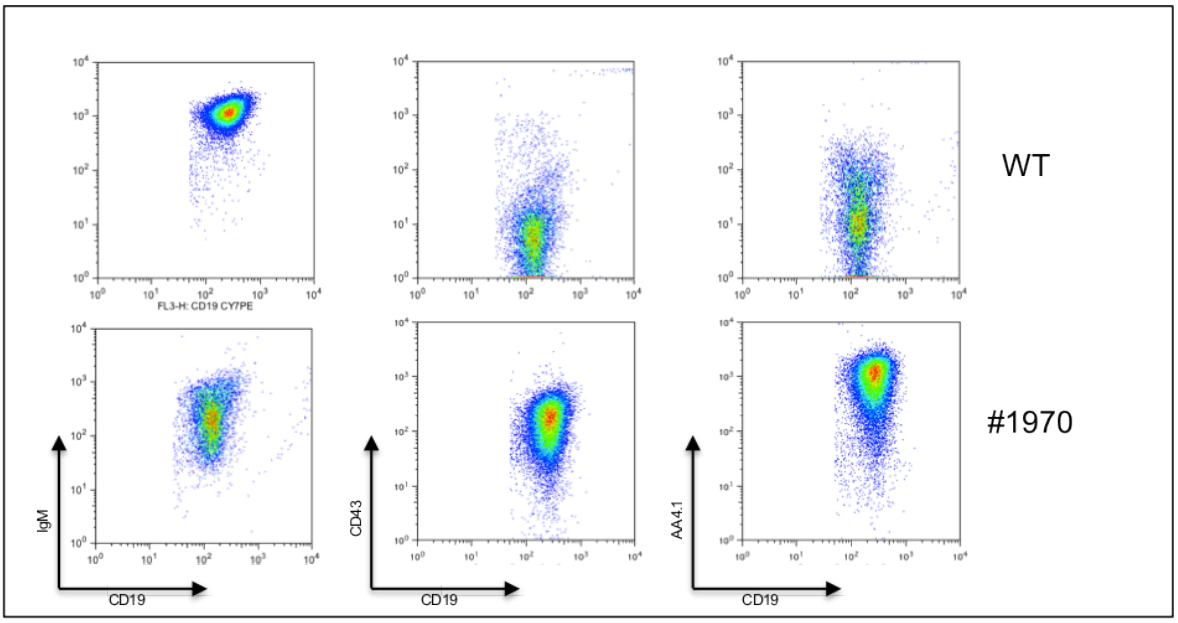

Figure 18: λ–MYC;B1-8f lymphoma B cells give rise to secondary tumors upon transplantation

Representative flow cytometric analysis of splenic cell suspensions obtained from wild-type (WT) CB6F1 mice and similar animals transplanted three weeks earlier with 3 million λ–MYC;B1-8f lymphoma cells (#1970). Immunophenotype of CD19-gated B cells are shown.

7.2.3 λ-MYC lymphomas retain surface BCR expression after prolonged in vitro and in vivo growth

The development of clonal B-cell malignancies in λ-MYC mice reflects the accumulation of secondary genetic alterations in B cells expressing the λ-MYC transgene. The most common alterations found in c-MYC transformed B cells include the loss of the tumor suppressor loci Trp53 and Cdkn2a (Schmitt et al., 1999). In accordance with published results, we found that the λ-MYC;B1-8f mice primary lymphomas suffered from either biallelic inactivation of *Cdkn2a* or accumulation of inactivating mutations affecting p53 protein stability (Figure 19 and (Mezzanzanica et al., 2004).

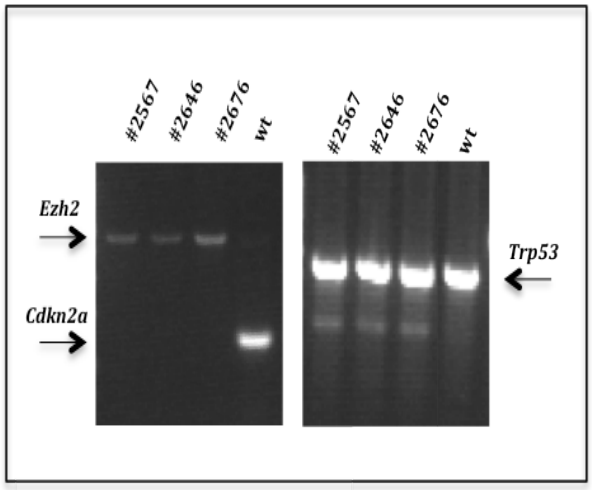

Figure 19: Status of *Cdkn2a* and *Trp53* loci in λ–MYC;B1-8f lymphoma B cells.

Measurement by genomic PCR of the status of Cdkn2a and Trp53 loci in three independent λ–MYC lymphomas. For the assessment of the Cdkn2a locus, I performed a competitive PCR using simultaneously primers annealing specifically to Cdkn2a and, as control, Ezh2. Arrows indicate the amplicons corresponding to the indicated genes. DNA from C57BL/6 wild type was used as control

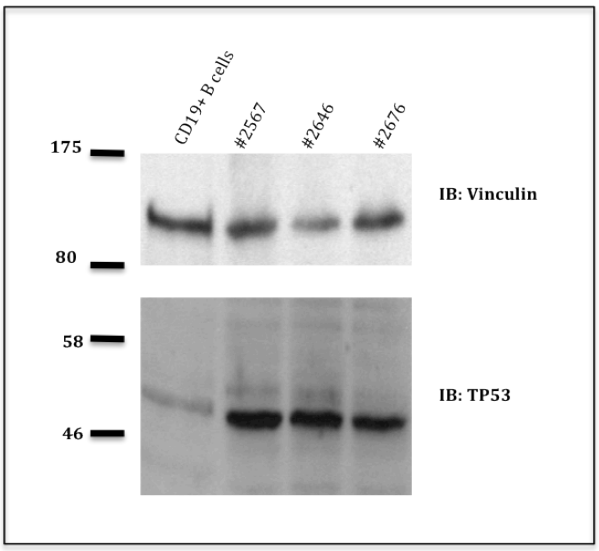

Figure 20: p53 protein is stabilized in λ–MYC;B1-8f tumor cells.

Immunoblot analysis of TP53 protein measured in protein extracts from *ex vivo* isolated resting B cells ($CD19^+$ B cells), and lymphoma cells derived from three independent λ–MYC;B1-8f mice (#2567, #2646 and #2676). Measurement of Vinculin levels was performed to control for protein input.

A previous report had shown that λ–MYC primary lymphomas and their cell line derivatives suffer from a high degree of genomic instability, including large-scale chromosomal aberrations (Rockwood et al., 2002). This condition may lead to the acquisition over time of additional genetic alterations that may render lymphoma cells independent of the BCR, and thus facilitate the isolation of BCR-less tumors. To test this possibility, *ex vivo* isolated lymphoma cells were cultured for prolonged time *in vitro* or serially transplanted into non-irradiated, syngeneic recipient mice, and monitored for BCR expression.

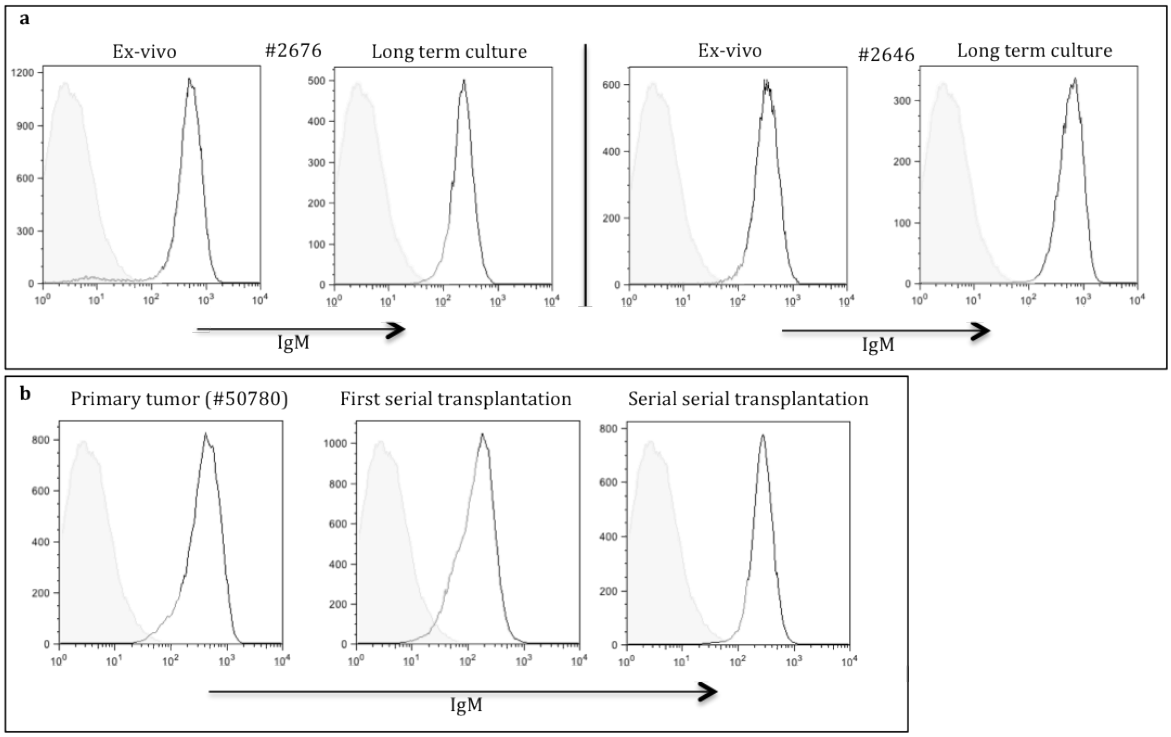

Figure 21: λ–MYC;B1-8f lymphoma cells retain BCR expression even after prolonged *in vitro* culture or serial transplantation

a) Flow cytometric analysis of surface IgM levels in *ex vivo* isolated primary lymphoma cells before (*ex vivo*) or after prolonged *in vitro* culture (over 50 passages). Two independent primary lymphomas #2676 and #2646) were assessed; b) Representative flow cytometric analysis of surface IgM levels in a primary λ–MYC tumor (#50780), and in lymphomas retrieved from the spleen of CB6F1 recipients after serial transplantations. Histograms indicated FSC^{hi} $CD19^{+}$ cells gated tumor cells; $CD19^{-}$ IgM^{-} cells (filled grey histograms) were used as negative control.

Extended growth both *in vitro* (Figure 21a) and *in vivo* (Figure 21b) of lymphoma cells was associated to the retention of surface Ig expression, thus suggesting a selective requirement for the antigen receptor to control lymphoma survival and/or proliferation

7.3 Inducible BCR inactivation in λ-MYC;B1-8f lymphomas

In this section, I will describe the effects of BCR inactivation on the *in vitro* and *in vivo* growth properties of λ-MYC;B1-8f B lymphoma cells.

To ablate BCR expression in transformed B cells, we took advantage of the Cre/*loxP* recombination technology. Specifically, *ex vivo* isolated B lymphoma cells were subjected to a Tat-Cre protein transduction protocol (Joshi et al., 2002; Peitz et al., 2002). Tat-Cre is a recombinant protein consisting of Cre-recombinase fused to a short peptide from the HIV Tat protein allowing passive diffusion through the plasma cell membrane (Schwarze et al., 2000). We developed a protocol that allowed efficient Cre-mediated recombination at the B1-8f allele, while minimizing the exposure time of tumor cells to Cre activity, preventing thereby possible toxic effects exerted by the recombinase (Schmidt-Supprian and Rajewsky, 2007).

Upon Tat-Cre transduction of primary lymphoma cells (or tumor cells grown in cultures for a limited number of passages), I monitored by flow cytometry analysis surface BCR expression of treated cells. A population of BCR^{low} tumor cells was already visible 24 hours after transduction and became clearly distinct from that of the BCR^{+} counterparts in the following day, ranging between 30 and 60 percent of all tumor cells (Figure 22a).

7.3.1 BCR ablation causes the disappearance of lymphoma cells in vitro

To study the impact of BCR deletion on lymphoma cells, *ex vivo* isolated primary λ-MYC;B1-8f tumor cells were cultured for few days, TAT-Cre transduced and BCR^{+} and BCR^{-} cells monitored over the following days by flow cytometry analysis. BCR^{+} tumor cells expanded exponentially *in vitro*, in contrast to their BCR^{-} counterparts that gradually disappeared from the cultures. Depending on the initial ratio between BCR^{+} and BCR^{-} lymphoma cells, from 5 to 10 days after Tat-Cre transduction Ig-negative

tumor cells were hardly detectable in culture. The disappearance *in vitro* of tumor cells following BCR inactivation has been observed in 4 independent lymphomas (Figure 22a).

The loss of BCR-negative cells was confirmed by Southern blot analysis. Specifically, the band corresponding to the B1-8 allele that had undergone Cre-mediated recombination (B1-8Δ) was no longer detected in tumor samples isolated starting from day 3 of TAT-cre transduction (Figure 22b).

This result excludes the possibility that the BCR^+ population contains tumor cells expressing a different BCR, as a result of secondary IgH gene rearrangements triggered by B1-8f inactivation.

7.3.2 BCR loss impairs lymphoma outgrowth in vivo under competitive conditions

I next assessed whether the loss of the antigen receptor interfered with the ability of lymphoma cells to grow *in vivo*. Primary λ–MYC;B1-8f lymphomas were *ex vivo* isolated, expanded in culture and subjected to TAT-Cre transduction to induce BCR inactivation. 48 hours after transduction, lymphoma cells were purified by magnetic cell sorting (MACS) on the basis of BCR expression, and allowed to grow for three to five days in culture. Finally, an equal number of BCR^+ and BCR^- tumor cells was co-injected through the tail vein into syngeneic immunoproficient mice (Figure 23 upper panels). I also injected highly purified (>95%) BCR^+ or BCR^--only tumor cells in another set of recipients. Recipients were sacrificed 18 to 21 days after transplantation, when signs of tumor outgrowth were clearly manifest. Cell suspensions were retrieved from lymphoid organs of recipient mice and analyzed by flow cytometry (Figure 23 lower panels).

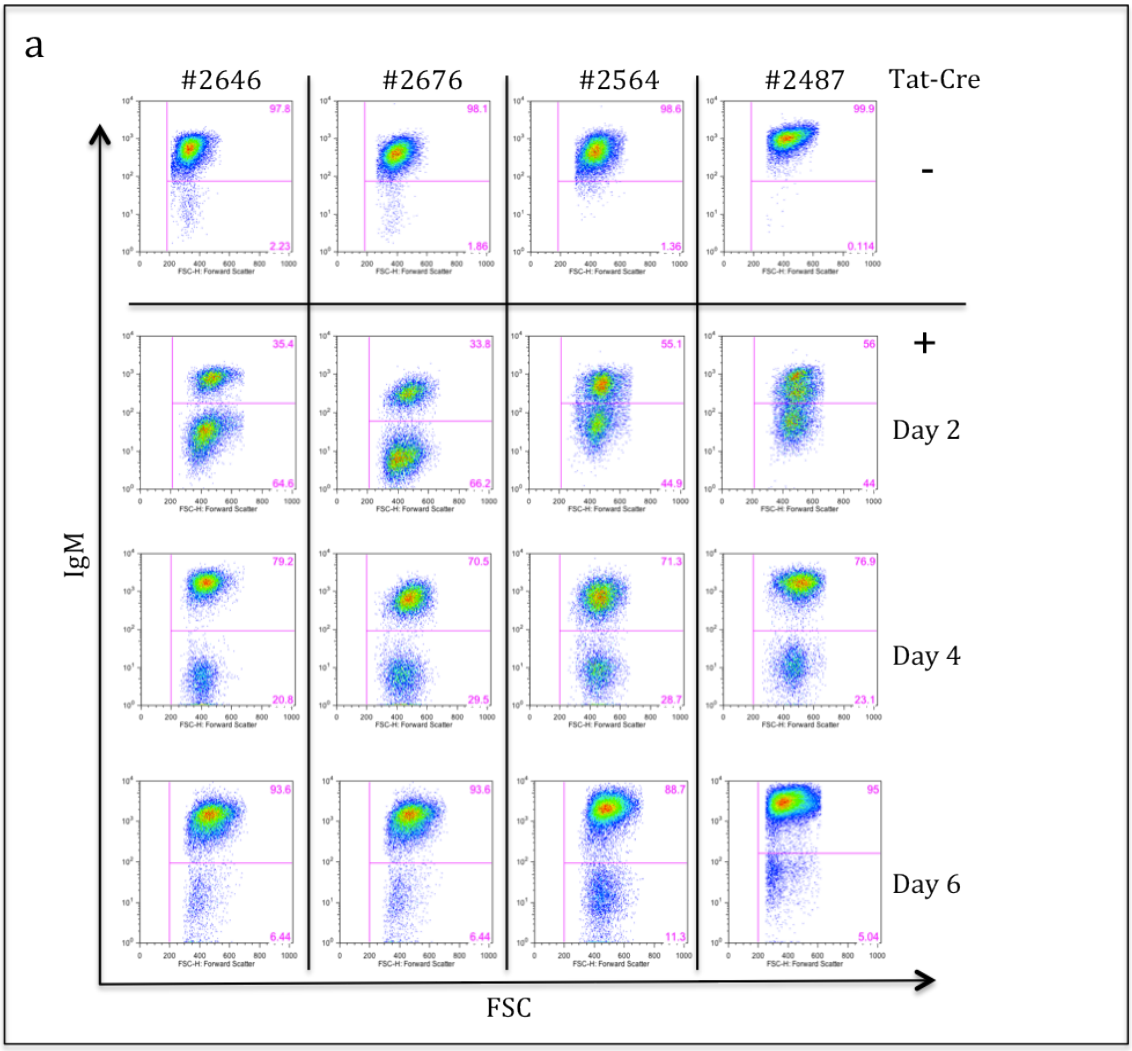

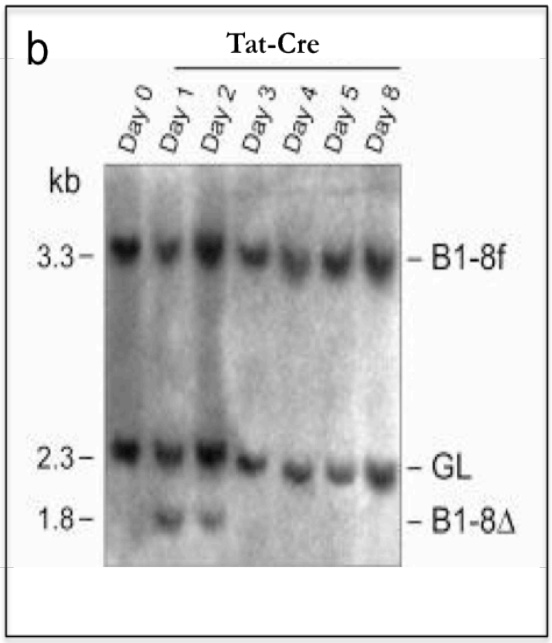

Figure 22: BCR ablation promotes the rapid disappearance of λ-MYC lymphomas *in vitro*

a) Flow cytometric analysis of *in vitro* cultures of 4 independent λ-MYC; B1-8f tumor B cells upon TAT-Cre transduction. Percentage of IgM^+ and IgM^- lymphoma cells at the indicated time points, before and after TAT-Cre transduction, are displayed. Dot plots are gated on live FSC^{hi} B cells; b) Status of the B1-8 allele in B lymphoma cell cultures at the indicated days after TAT-Cre transduction revealed by Southern blot analysis. Size and position of bands corresponding respectively to the conditional (B1-8f,) and Cre-deleted (B1-8Δ) B1-8 allele and the IgH germline (GL) gene are indicated. Note that mice are heterozygous for the B1-8f knock-in gene.

Mice that received only BCR$^+$ tumor cells displayed a sizeable fraction of tumor cells in primary and secondary lymphoid organs. In accordance with the *in vitro* data, lymphoma cells retrieved from mice transplanted with the mixture of BCR$^+$ and BCR$^-$ cells showed a consistent counterselection of Ig-negative lymphomas that were in all cases detected in very low amounts (tumor cell numbers obtained from the transplantation of four independent lymphomas is provided in Table 7).

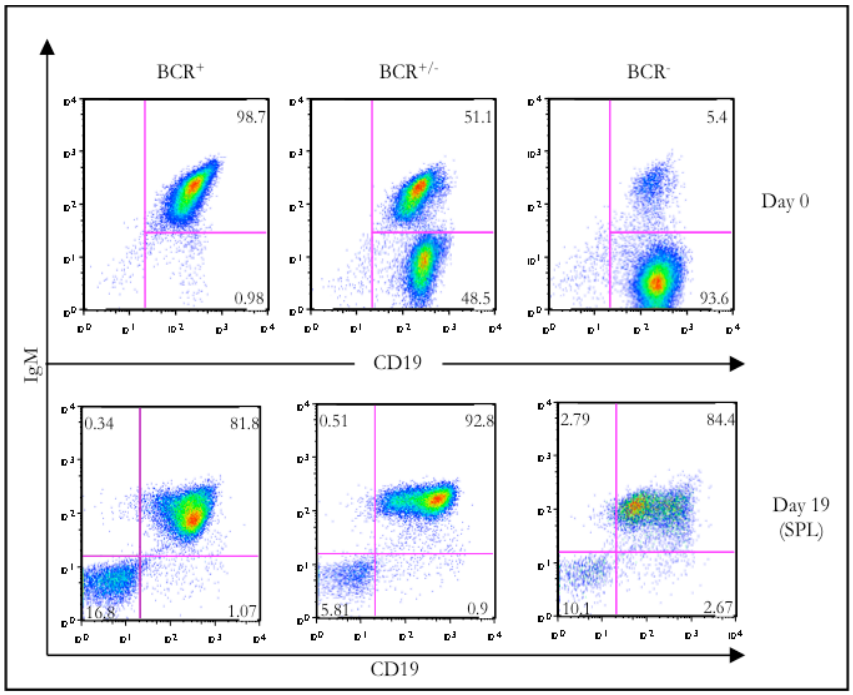

Figure 23: BCR ablation interferes with the tumorigenic potential of λ-MYC lymphomas *in vivo*

FACS analysis of single BCR$^+$ and BCR$^-$ primary lymphoma populations (#2567; left and right plots) or 1:1 mixtures (middle plot) derived from λ-myc;B1-8f mouse transduced *in vitro* with Tat-Cre, before (Day 0) or 19 days after their transplantation in syngeneic recipients. Cells in transplanted mice were retrieved from the spleen. Dot plots are gated on live FSC^{hi} cells. Numbers represent percentage of gated cells.

Noteworthy, tumor latency in mice transplanted with purified BCR$^-$ lymphoma cells was prolonged. This condition was often associated with reduced numbers of tumor cells infiltrating lymphoid organs of recipients. Strikingly, in most cases, tumor cells retained surface Ig expression, likely originating from the few contaminating BCR$^+$ tumor cells that remained in the BCR$^-$ lymphoma mixture that was injected.

Altogether, these results reveal a strict requirement for BCR expression for lymphoma cell survival/proliferation when tumors are grown under competitive conditions.

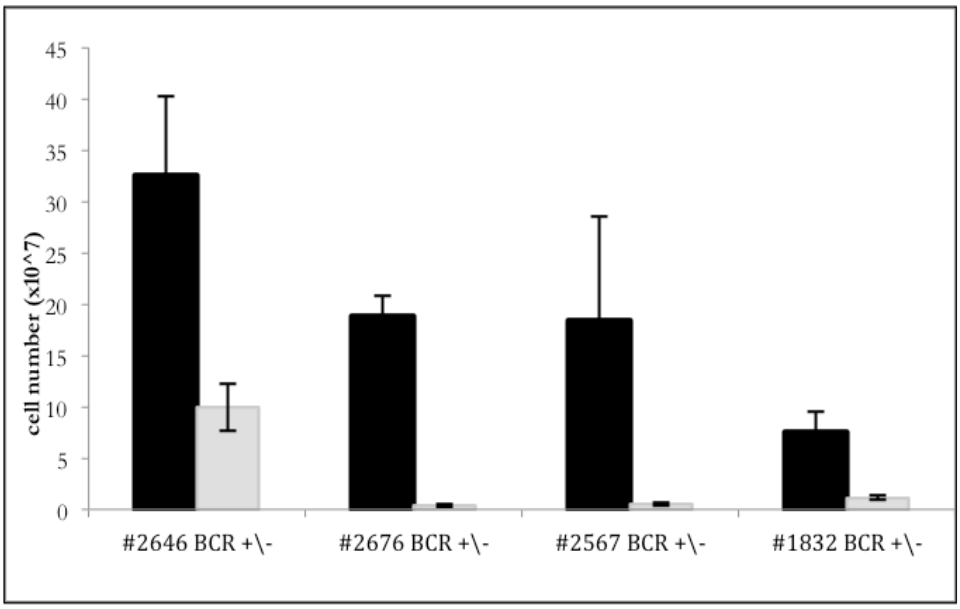

Table 7: Numbers of λ-MYC lymphoma cells retrieved after transplantations of BCR$^+$/BCR$^-$ 1:1 mixtures.

Summary of the data relative to absolute numbers of BCR$^+$ and BCR$^-$ lymphoma cells generated from four independent primary lymphomas, retrieved from the spleen of recipient animals after their injection as a 1:1 mixture. Each tumor competition was transplanted into 3 recipients, which were sacrificed between 18 and 21 days after transplantation. Average numbers of IgM$^+$ (black bars) and IgM$^-$ (grey bars) tumor cells (± SD) are shown.

7.3.3 λ-MYC lymphomas home primarily to the bone marrow regardless of Ig status

The failure of BCR-deficient lymphoma cells to expand *in vivo* could reflect the inability of the tumor cells to migrate to sites that support their growth. To test this possibility, two independent BCR$^+$ lymphomas (#2646 and #2676) and their BCR$^-$ derivatives (generated by TAT-Cre transduction), were labeled with the fluorescent cell tracker 5-(and-6)-Carboxyfluorescein Diacetate-Succinimidyl Ester (CFSE) and intravenously injected in equal amount into non-irradiated syngeneic mice (Figure 24a). Recipient animals were sacrificed respectively two and forty-four hours following transplantation, and lymphoid organs were analyzed by flow cytometry for

the presence of CFSE-labeled cells. Tumor cells first reached the bone marrow where they represented 0.2-0.6% of all CD19^{+} B cells two hours after transplantation (Figure 24b upper panel). Importantly, the ratio between BCR^{+} and BCR^{-} cells was comparable to that of the injected mixture, pointing to a normal migration of BCR-deficient lymphoma cells to lymphoid sites.

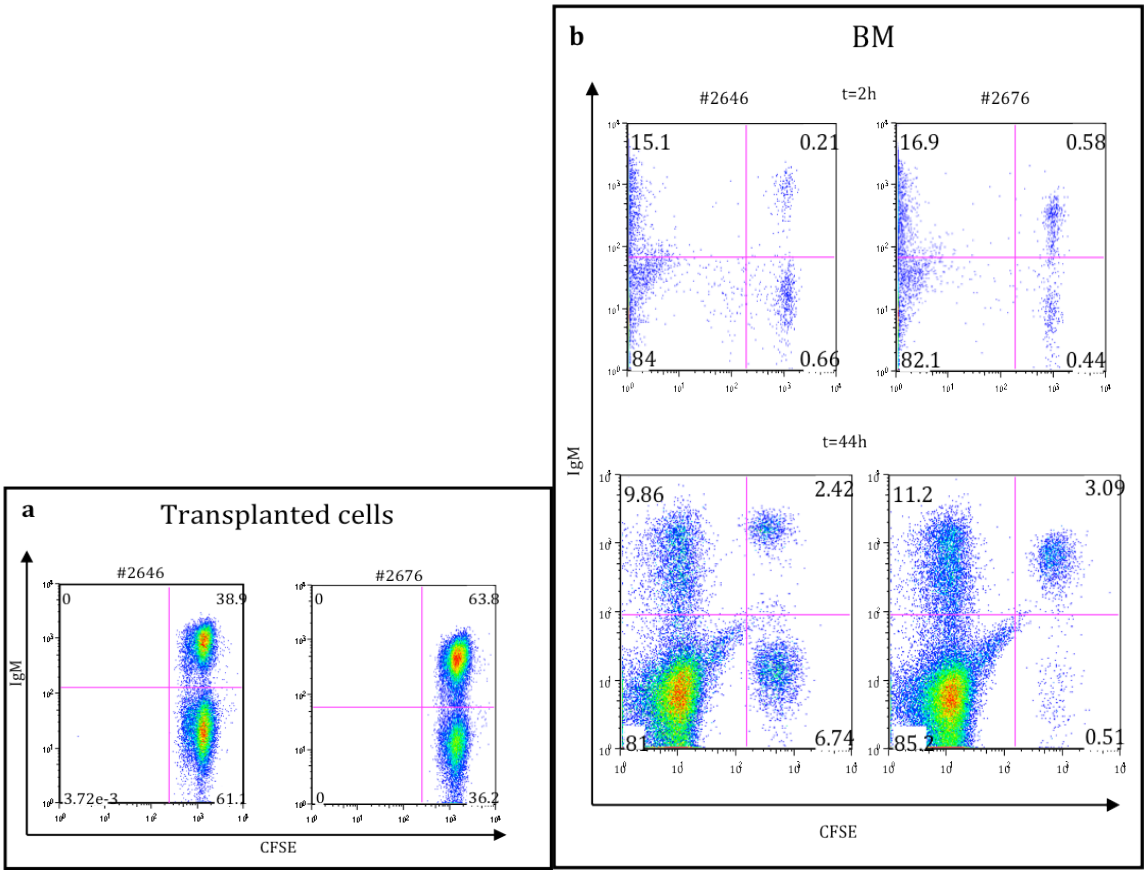

Figure 24: Normal homing to the bone marrow of BCR-less lymphoma cells

a) Flow cytometric analysis of IgM^{+} and IgM^{-} lymphoma cells, obtained after Tat-cre transduction of 2 independent primary lymphomas (#2646 and #2676), stained with CFSE at the time of their transplantation as a 1:1 mixture in syngeneic recipient; b) Flow cytometric analyses of bone marrow cells respectively 2 h and 44 h after transplantation are shown. Dot plots are gated on live CD19^{+} cells. Numbers indicate percentage of cells falling within the indicated quadrants.

Strikingly, by 44 hours post-transplantation, BCR^{+} tumor cells from lymphoma #2676 were largely overrepresented indicating a rapid loss of receptor-negative lymphoma cells (note: a BCR$^{+/-}$ ratio of 2:1 at the time of injection increased to 6:1, 44 hours after

transplantation; Figure 24b, lower panel). These results reveal a rapid clearance of BCR-negative tumor cells after reaching their niche.

7.3.4 Ig-deficient lymphomas gain growth competence upon BCR restoration

High levels of Cre expression can exert toxic effects on mammalian cells (Higashi et al., 2009; Schmidt-Supprian and Rajewsky, 2007; Silver and Livingston, 2001). To test whether the disappearance of BCR-deficient lymphoma cells was due to a toxic effect exerted by Cre recombinase, we generated a retroviral vector allowing the expression of a functional IgH chain consisting of the variable region encoded by the V_H186.2 (B1-8) gene that could be distinguished by flow cytometry using allotype-specific antibodies. Specifically, λ–MYC;B1-8f tumor cells (IgH_a^+) were infected with the retrovirus expressing IgH_b to become $IgH_a^+IgH_b^+$ double-positives. The latter were subsequently transduced with TAT-Cre to inactivate the B1-8f/IgH_a gene (Figure 25a). Cre-transduced, IgH_b-expressing tumor cells were mixed in equal amounts with BCR^- tumor cells infected with a control virus and allowed to grow in competition both *in vitro,* and *in vivo*.

If BCR^- cells suffered from genetic aberrations caused by Cre recombinase, complementation with a novel IgH chain will not improve their ability to outcompete IgM^- tumor cells. Instead, IgH-complemented tumor cells reacquired the ability to outcompete their receptor-less counterparts over a short period of *in vitro* culture (Figure 25b, upper panel). Moreover, transplantation of mixtures of IgH-complemented and BCR^- lymphoma cells led after three weeks to the preferential expansion of IgH-complemented cells both in the spleen and bone marrow of recipients (Figure 25b lower panel). These experiments rule out the possibility that the disappearance of BCR^- tumor cells depend on a toxic effect exerted by Cre recombinase.

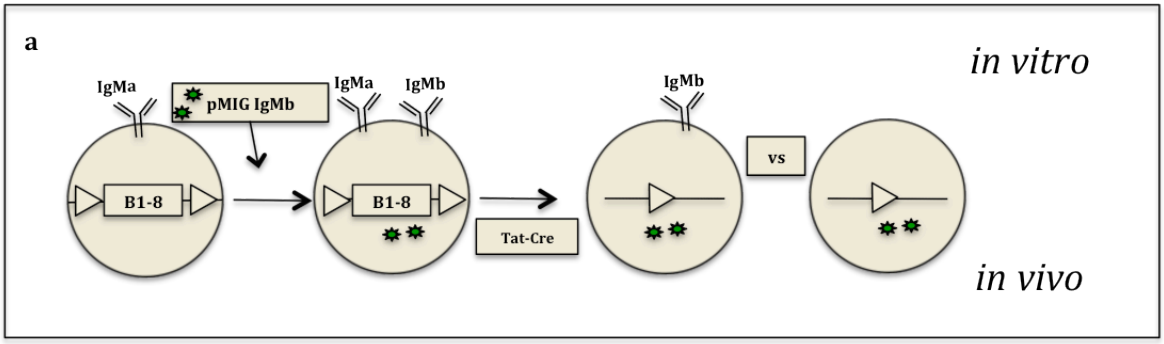

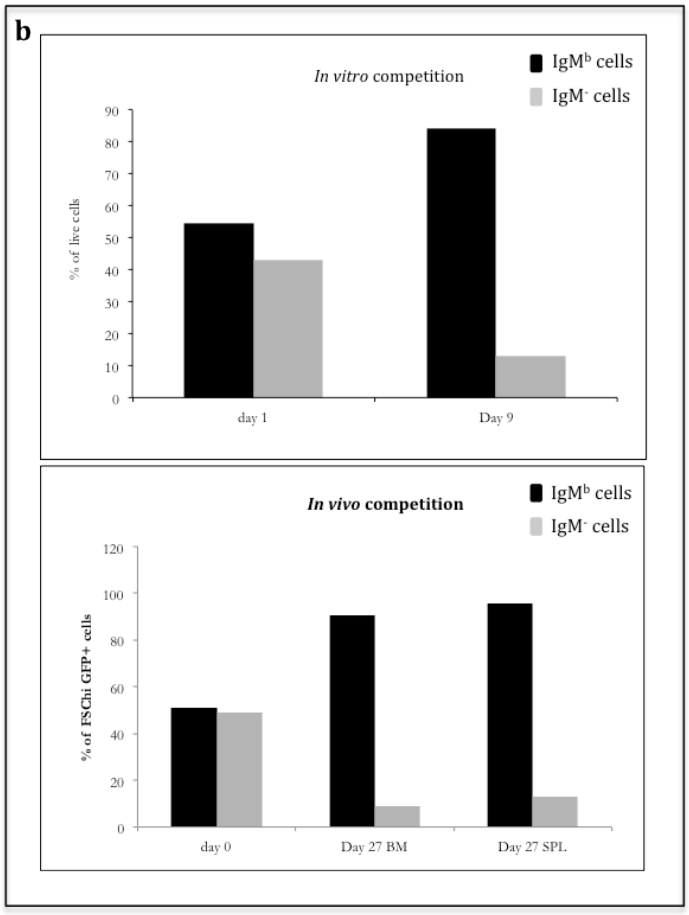

Figure 25: Expression of a novel IgH rescues BCR-deficient λ-MYC cells

a) Primary λ-MYC;B1-8f (IgM_a^+) lymphoma cells were infected with a retrovirus expressing allotype-b IgM (IgM_b) in combination with the GFP reporter (green stars). IgM_a;IgM_b double positive (GFP^+) cells were Tat-Cre transduced to induce the loss of IgM_a. $IgM_a^-IgM_b^+$ cells were finally mixed in equal amounts with BCR^- GFP^+ lymphoma cells (infected with a GFP control virus) and cultured *in vitro* for 9 days or transplanted *in vivo* into syngeneic mice. b) Summary table representing the average fraction of GFP^+ tumor B cells with the indicated surface Ig phenotype retrieved from bone marrow (BM) and spleen (SPL) of two transplanted mice before and 27 days after injection. A similar analysis was performed for tumor cells grown as 1:1 mixtures *in vitro* for 9 days.

7.3.5 BCR^- lymphoma cells expand in vivo in the absence of their BCR^+ counterparts

The evidences provided so far indicate that the BCR is critical for lymphoma cell survival and\or proliferation, under conditions of competitive growth both *in vitro* and *in vivo*. In order to investigate whether the BCR controls lymphoma survival in a cell autonomous fashion, tumor B cells isolated from two independent primary λ-

MYC;B1-8f mice (#2646 and #2676) were allowed to expand *in vitro* for few passages, TAT-Cre transduced, and cloned by limiting dilution.

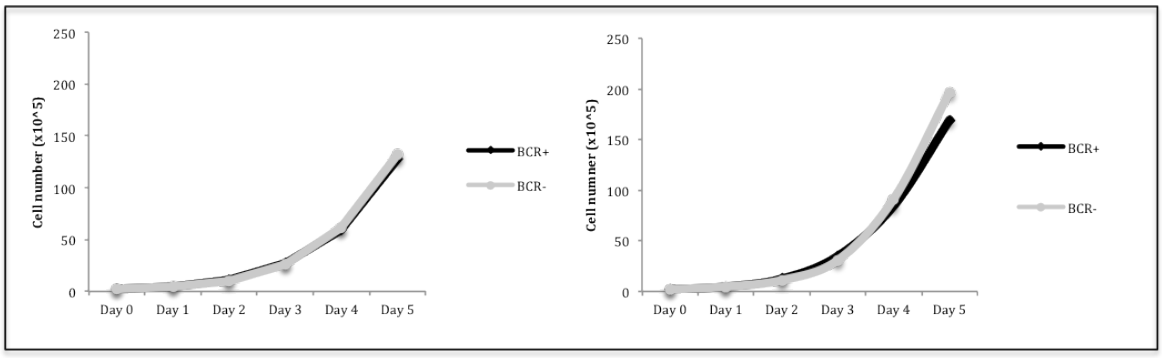

Figure 26: Pure BCR$^-$ cells grow *in vitro* as their BCR$^+$ counterparts

Growth curves of respectively BCR$^-$ (grey line) and BCR$^+$ (black line) tumor cells grown alone. Cells were obtained from primary λ-MYC;B1-8f lymphoma #2676 (left panel) and #2646 (right). Cells were counted and diluted every 24 hours. Each time point represents the average count of three replicates.

Surprisingly, purified BCR$^-$ tumor cells grew to the same extent as their BCR$^+$ counterparts (Figure 26), in striking contrast to their rapid disappearance when grown in competition. Interestingly, I identified few BCR$^-$ tumor clones that were no longer counterselected by BCR$^+$ tumors, pointing to the selection of cells that have accumulated additional genetic mutations overcoming the need for a functional BCR (Figure 27, left plots, #2567 clone).

In accordance with the *in vitro* data, BCR$^-$ tumor expanded successfully in lymphoid organs of recipients only in the absence of their BCR$^+$ counterparts (Figure 28a). However, whereas the injection of BCR$^+$ tumor cells killed recipients on average 17 days after transplantation, the same number of BCR-deficient lymphomas showed an appreciable delay in causing lethality of injected animals (23 days on average) (Figure 28b).

These data suggest that the contribution of the BCR to tumor growth becomes evident predominantly under conditions of inter-clonal competition both *in vitro* and *in vivo*.

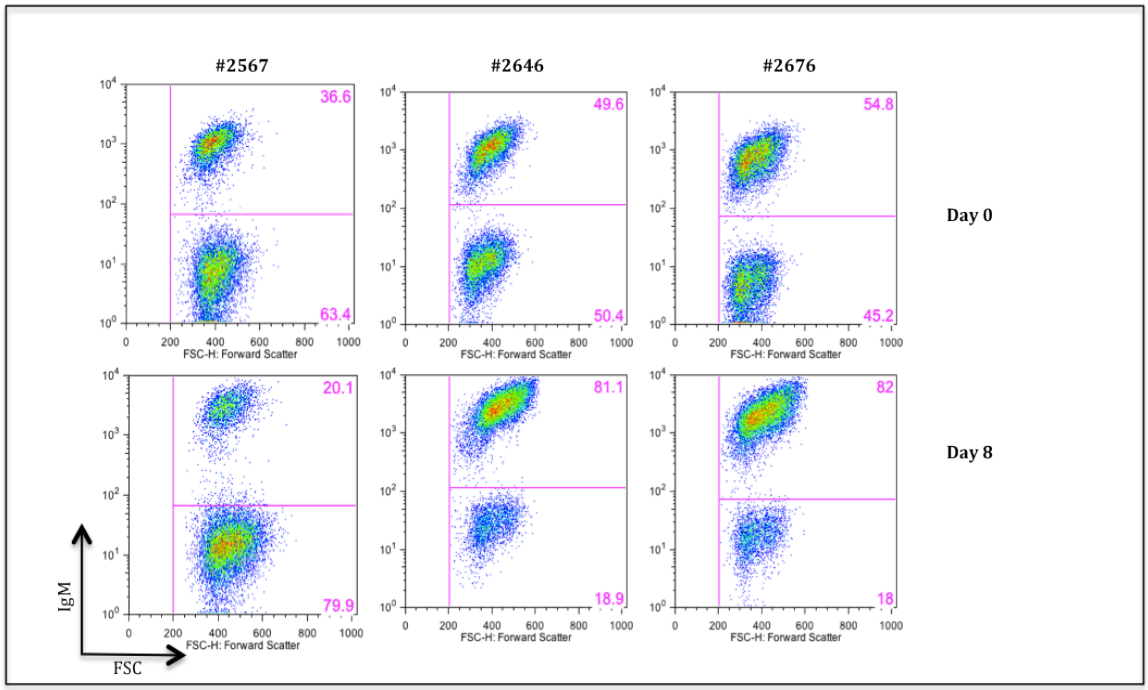

Figure 27: Prolonged cultures of receptor-less lymphomas selects clones that become BCR-independent

Flow cytometric analysis of BCR^+/BCR^- tumor mixtures. BCR^+ and BCR^- cells were cloned by limiting dilution of a mixture of Tat-Cre transduced λ-myc;B1-8f lymphoma cells from three independent tumors (#2567, #2646 and #2676). IgM expression was evaluated at the indicated time points. Dot plots are gated on FSC^{hi} live cells. Numbers represent percentage of displayed cells. Note the loss of BCR dependency of lymphoma #2567.

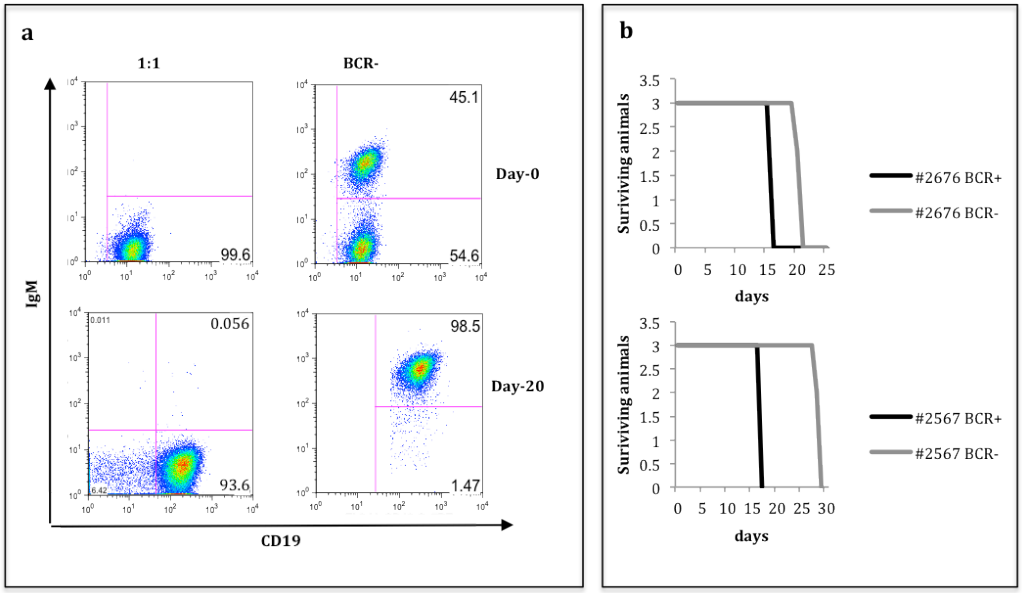

Figure 28: Pure BCR$^-$ lymphomas generate secondary tumors with longer latency

a) Flow cytometric analysis of BCR$^-$ tumor cells cloned by limiting dilution from primary cultures of Tat-Cre transduced #2676 λ-MYC;B1-8f lymphoma cells. Cells were transplanted as such or as a 1:1 mixture with BCR$^+$ counterparts. Upper dot plots show frequency of BCR$^+$ and BCR$^-$ at the time of transplantation. Lower plots display FACS analysis of tumor cell suspensions obtained from spleen of transplanted mice, sacrificed 20 days after transplantation. Dot plots are gated on FSC^{hi} live cells. Numbers represent percentage of cells; b) Cloned BCR$^-$ and BCR$^+$ tumor cells obtained after transduction of lymphomas #2676 or #2567 were transplanted into independent recipient mice. Survival of mice (n=3) receiving either BCR$^+$ (black curve) or BCR- (grey curve) tumors was compared.

7.3.6 BCR regulates G_1-to-S transition in c-MYC transformed B cells

To elucidate the basis of the competitive disadvantage of BCR$^-$ tumor cells, I compared the cell-cycle status of these cells to that of their BCR$^+$ counterparts. BCR$^+$ and BCR$^-$ cells from four independent lymphomas were allowed to transiently incorporate the thymidine analogue, 5-bromodeoxyuridine (BrdU) followed by staining of the cells with Propidium Iodide (PI). This approach allows through flow cytometry analysis, the precise determination of the fraction of cells falling in the various stages of the cell cycle, including those actively undergoing DNA replication (Miltenburger et al., 1987; Sasaki et al., 1989; Vanderlaan and Thomas, 1985).

Primary lymphoma cells were Tat-Cre transduced and BCR^+ and BCR^- lymphoma cells were cultured as 1:1 mixtures. At the stage when BCR^- cells were getting counter selected, the mixed tumor culture was pulsed with BrdU for 5 minutes. Staining of the cells with PI was coupled to incubation with fluorescent-labeled anti-BrdU and IgM staining. Three-color flow cytometric analysis revealed that lymphoma cells were mainly distributed between the G_o/G_1 and the S-phase, regardless of surface Ig status. On average, cultures contained 10% of cells in the G_2/M phases of the cell cycle. The comparison between BCR^+ and BCR^- cells revealed significant differences in the cell cycle profiles. Indeed, BCR-deficient tumors cells showed a higher fraction of cells in G_0/G_1 compared to their BCR^+ counterparts (Figure 29a). Conversely, the percentage of BCR^- lymphoma cells undergoing active DNA replication ($BrdU^+$) in S-phase was lower compared to that of the BCR^+ competitors. These results indicate that the BCR controls G_1-to-S transition in c-MYC transformed B-cell lymphomas (Figure 29a).

We next asked whether the cell cycle alterations observed in BCR^- tumor cells in competition assays was dependent on the presence of their BCR^+ counterparts. Therefore, BCR^+ and BCR^- lymphoma cells (obtained by subcloning, or as a result of cell sorting) were cultured separately for several days before performing BrdU/PI cell-cycle analysis. Interestingly, I failed to observe significant differences between the cell-cycle profiles of BCR^+ and BCR^- lymphomas (Figure 29b).

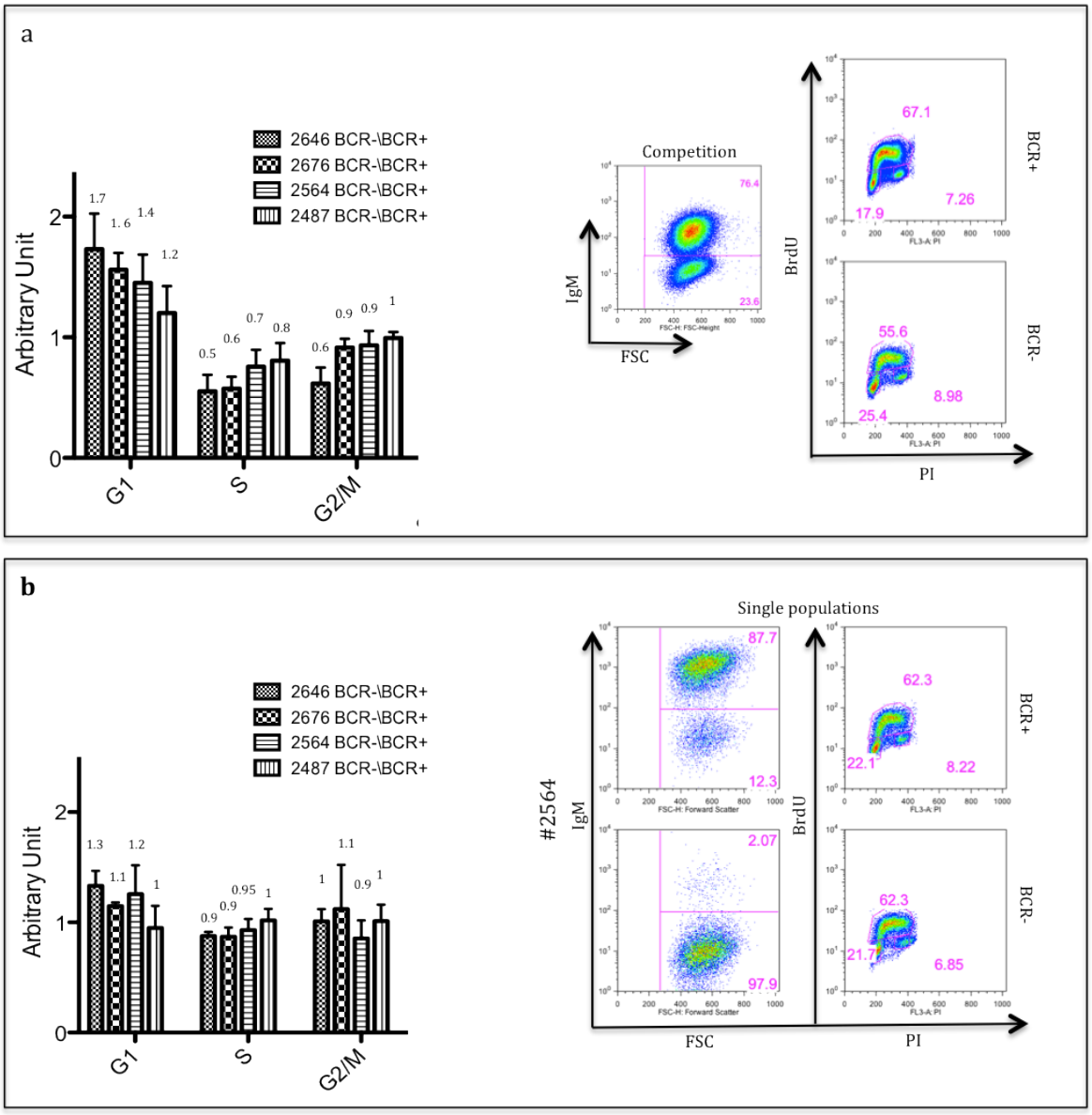

Figure 29: BCR regulates G_1-to-S transition in λ-MYC lymphoma B cells

a) Cell cycle analysis of BCR^+ and BCR^- lymphoma cells stained for BrdU incorporation and DNA content (propidium iodide, PI) were analyzed 4 days after a 1:1 in vitro competition assay (right panel). Summary of the data is shown on the left. The experiment was performed with lymphoma cells derived from 4 independent tumors (#2646, n=4; #2676 n=6; #2564, n=5; #2487, n=6); b) Flow cytometric analysis of BrdU incorporation in highly enriched cultures of BCR^+ and BCR^- tumors. Summary of the data obtained from 4 independent lymphomas is shown in the left panel (#2646, n=6; #2676 n=4; #2564, n=3; #2487, n=3). Numbers above each histogram indicate the ratio of the average percentage of BCR^- and BCR^+ tumor cells (± SD), in the indicated phases of the cell cycle. Cell doublets were excluded from the analysis. Numbers indicate percentage of cells.

This result points to a critical contribution exerted by the BCR^+ tumor population to the cell-cycle delay at the G_1-to-S transition suffered by BCR^- negative lymphomas.

7.3.7 Counter selection of BCR⁻ tumor cells is associated with increased apoptosis

I next tested whether aberrant cell death contributed to the disappearance of BCR$^-$ lymphomas grown in the presence of the BCR$^+$ counterparts. Flow cytometric determination of DNA content using PI staining revealed a substantial percentage of BCR$^-$ lymphoma cells with a hypodiploid (<2n) DNA content, representing cells undergoing apotosis (Figure 30a and b).

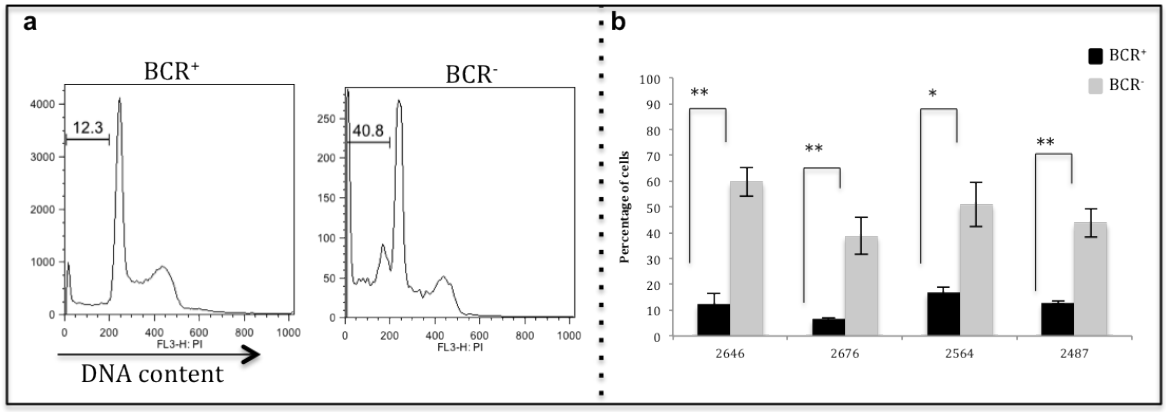

Figure 30: The BCR protects lymphoma cells from apoptosis

a) Representative flow cytometric analysis of IgM$^+$ and IgM$^-$ lymphoma B cells (#2487) 5 days after *in vitro* competition. Numbers in the histograms indicate frequencies of sub-G_1 apoptotic cells b) Frequencies of apoptotic BCR$^+$ (black bars) and BCR$^-$ (grey bars) lymphoma B cells, measured by flow cytometry according to DNA content (sub-G_1), at 5 days of *in vitro* competition. Tumor cells were from 4 independent lymphomas (#2646, #2676, #2564 and #2487). Bars represent the average of 3 replicates (± SD) (t-test: **p<0.001 or *p<0.05).

To confirm this result, the fraction of apoptotic cells was determined comparing the status of caspase activation in BCR$^+$ and BCR$^-$ lymphomas.

Activation of programmed cell-death is associated with the proteolytic cleavage of pro-caspases and the generation of active caspases (Durrieu et al., 1998). The fluorescent-labeled pan-caspase inhibitor peptide VAD-FMK (carbobenzoxy-valyl-alanyl-aspartyl-[O-methyl]-fluoromethylketone) binds with varying affinity to a spectrum of active caspases (caspase-1, -3, -4, -5, -7, -8 and -9) (Smolewski et al., 2002), representing therefore a suitable tool to assess by flow cytometry the fraction

of cells undergoing apoptosis. Flow cytometric analysis of 4 independent λMYC;B1-8f lymphomas transduced with Tat-Cre, revealed a two to three fold higher percentage of apoptotic cells within the population of BCR⁻ lymphomas as compared to the BCR⁺ counterparts present in the same *in vitro* culture (Figure 31a and b).

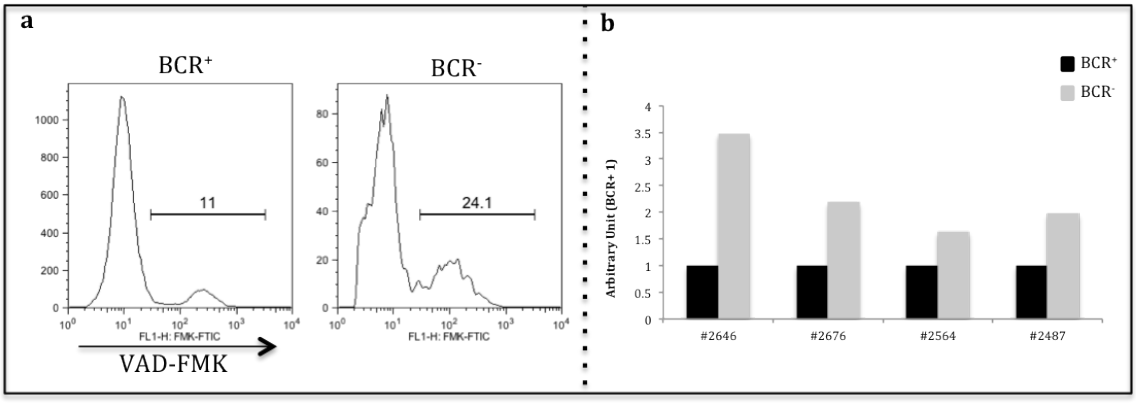

Figure 31: BCR inactivation triggers activation of caspases in λ-MYC lymphomas

a) Representative flow cytometric analysis of IgM⁺ and IgM⁻ B lymphoma cells (#2676) after 5 days of *in vitro* competition. Numbers within histogram plots indicate frequencies of apoptotic lymphoma cells expressing active caspases revealed through the staining with the caspase inhibitor VAD-FMK; b) Frequencies of BCR⁺ (black bars) and BCR⁻ (grey bars) lymphoma B cells expressing active caspase(s), measured by flow cytometry after 5 days of competition. Tumor cells were derived from 4 independent tumors (#2646, #2676, #2564 and #2487). Columns represent fold change over BCR⁺ caspase⁺ tumor cells.

These data, together with those on cell cycle analysis, are compatible with a scenario in which the competitive loss of BCR⁻ tumor B cells is the result of a combination of impaired proliferation and increased programmed cell death.

7.3.8 Human Burkitt lymphoma RAMOS cells require BCR for in vitro growth

To extend our findings to human BL, I analyzed the RAMOS BL cell line (Sale and Neuberger, 1998). RAMOS cells carry the t(8;14) translocation juxtaposing c-MYC to the IgH locus and, importantly, display ongoing Ig somatic hypermutation (Zhang et al., 2001). As a consequence of the latter, crippling mutations at IgH and/or IgL V-genes cause the continuous generation of a minute fraction (less than 0.1%) of BCR⁻

tumor cells, never expanding *in vitro*. I tested whether the failure of BCR-deficient RAMOS cells to overgrow *in vitro* was the result of a competitive disadvantage of these cells when cultured in the presence of their BCR$^+$ counterparts. To address this possibility, spontaneously generated BCR$^-$ RAMOS cells were purified by cell sorting and cloned by limiting dilution (Figure 32a). BCR$^+$ and BCR$^-$ RAMOS cells were then mixed in equal numbers and followed over time. By 8-12 days of culture, flow cytometry analysis revealed an over representation of RAMOS cells expressing a functional BCR (Figure 32b).

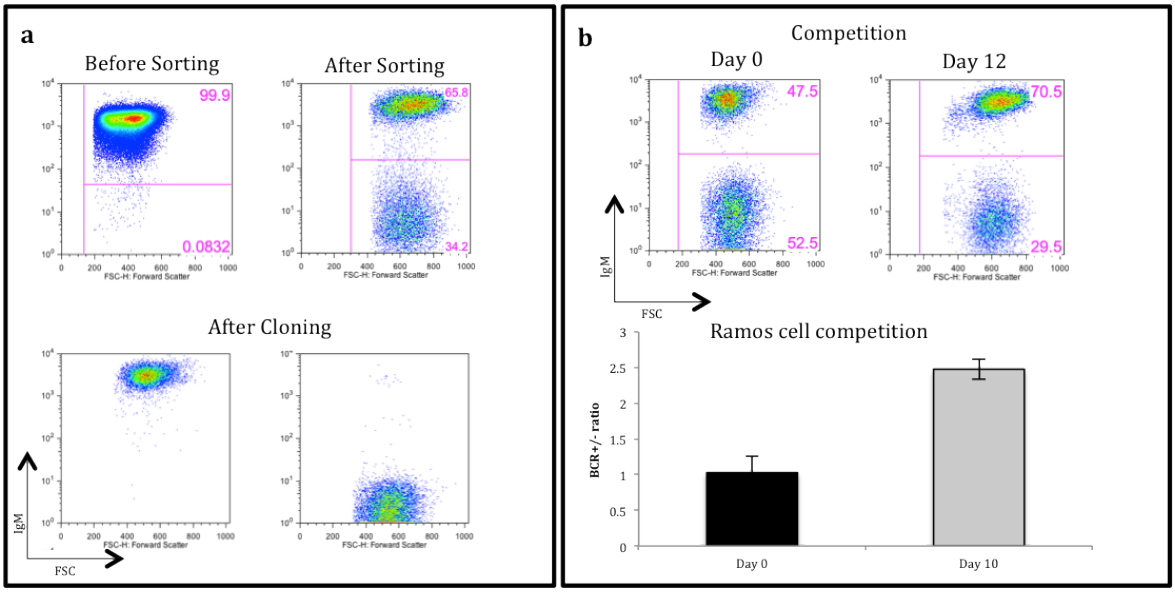

Figure 32: BCR provides a competitive advantage to the RAMOS human Burkitt lymphoma cell line

a) RAMOS cells were sorted according to surface IgM expression (upper left). Ig-negative tumor cells were enriched after cell sorting (upper right). Sorted cells were cloned by limiting dilution. We identified both BCR$^+$ and BCR$^-$ RAMOS clones (lower plots); b) Representative dot plot showing 1:1 mixtures of BCR$^{+/-}$ RAMOS cells at the start of the competition (Day 0) or 12 days later. Dot Plots are gated on FSC^{hi} live cells. Numbers represent percentage of cells in the corresponding quadrants. The lower part of the panel shows a summary of the data of three independent *in vitro* competition assays. Average ratios of BCR$^+$/BCR$^-$ lymphoma cells from 3 experiments are represented (±SD).

I next asked whether the BCR facilitates G_1-to-S transition and prevents apoptosis in human Burkitt lymphoma cells, as observed in the murine BL model. Therefore, BCR$^+$ and BCR$^-$ Ramos cells were cultured as independent populations or in competition for

8-12 days, and BrdU incorporation, as well as caspase activation, were studied. Interestingly, upon 8 days of competition I could score a partial increase in the percentage of BCR$^-$ lymphoma cells in G_1 phase, as compared to the BCR-proficient counterpart (Figure 33).

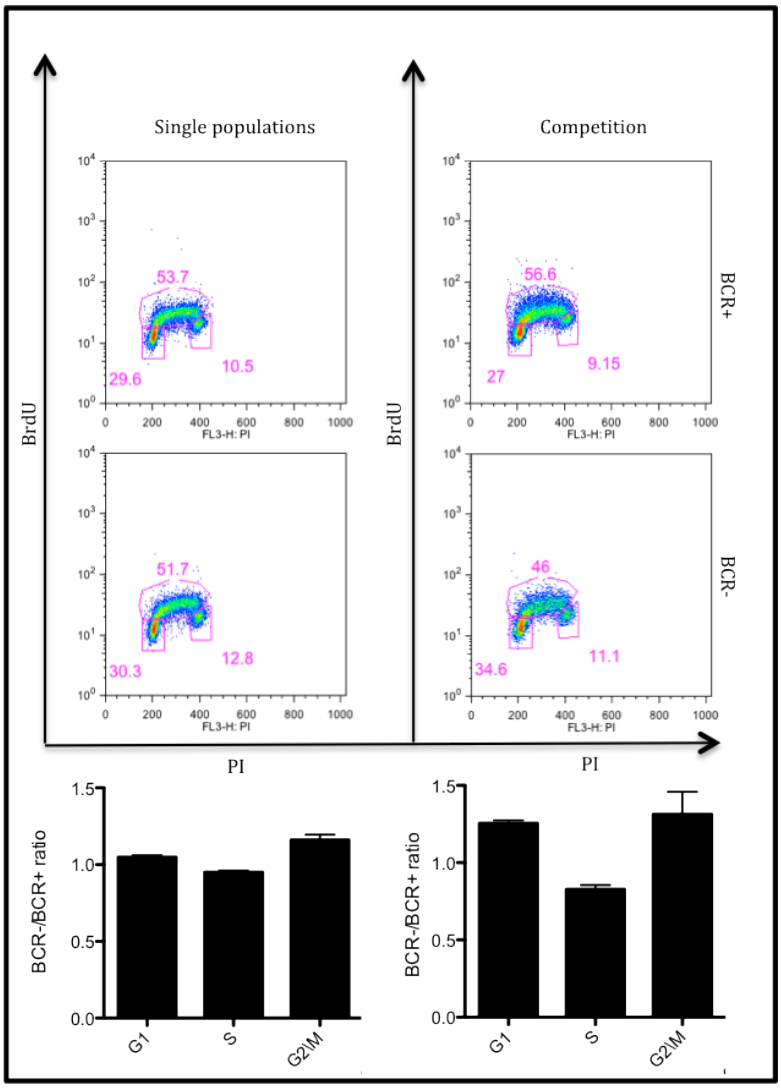

Figure 33: The BCR influences G_1-to-S transition in RAMOS cells in competition

a) Flow cytometric analysis of BrdU incorporation in BCR$^+$ and BCR$^-$ BL RAMOS cells, cultured as pure populations (left plots and histograms), or for 8 days in competition (right plots and histograms). Average ratio of frequencies of BCR$^-$ over BCR$^+$ cells in the indicated stages of the cell cycle (±SD) is shown in the lower histograms. Cell doublets were excluded from the analysis. Cells in dot plots were gated on the basis IgM status. Numbers in dot plots represent percentage of cells.

Indeed, the increased population at the G_1 stage was associated with a comparable reduction in the fraction of BCR$^-$ cells in S-phase. Similarly to the results from the

mouse model, the same increment was not observed when IgM$^-$ Ramos cells were cultured independently from the BCR$^+$ counterparts, thus suggesting a non cell-autonomous defect. Moreover, Caspase-glow staning identified a significantly higher fraction of apoptotic cells mainly in the BCR-deficient population.

However, programmed cell death appeared to be a cell autonomous defect in IgM$^-$ RAMOS cells, as no detectable difference were present between the competition and the independent cultures (Figure 34).

These results confirm the importance of the BCR in sustaining the growth of human BL and support a scenario where the continuous presence in the tumor of BCR-expressing tumor cells represents a limiting factor for the outgrowth of lymphoma cells loosing the BCR as a consequence of ongoing Ig SHM.

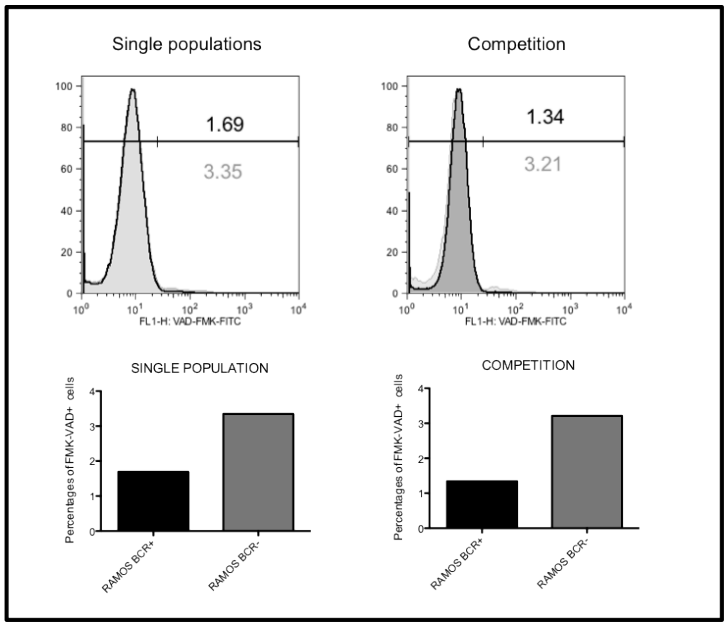

Figure 34: The BCR protects human Burkitt lymphoma from programmed cell death

Representative flow cytometric analysis of IgM$^+$ and IgM$^-$ RAMOS cells, cultured as single/pure populations, or for 8 days in competition. Numbers indicate frequencies of apoptotic cells among respectively IgM$^+$ (black numbers above the gate) or IgM$^-$ (grey numbers below the gate) BL cells, detected with caspase-glow staining; Frequencies of active caspase(s)$^+$ BCR$^+$ (black bars) and BCR$^-$ (grey bars) lymphoma B cells measured in pure cultures (left panels), or in competition for 8 days (right panels) are shown.

7.4 Mechanisms causing the loss of BCR$^-$ lymphomas

In this section I will describe a series of experiments that were performed in the attempt to dissect the molecular mechanism(s) responsible for the increased apoptosis and the impaired proliferation of tumor cells undergoing acute ablation of the BCR.

7.4.1 Quantitative proteome analysis of BCR$^+$ and BCR$^-$ lymphomas

To identify the pathways influenced by BCR deletion in lymphoma cells, in collaboration with the group of Tiziana Bonaldi (European Institute of Oncology, Milan) we established a quantitative proteome profile of B lymphoma cells before and after acute loss of the BCR, using Stable Isotope Labeling with Aminoacid in Cell culture (SILAC). This technology relies on the incorporation of isotope-labeled amino acids (like L-arginine containing six atoms of ^{13}C), in proteins synthesized by cells in exponential growth (Ong et al., 2002; Ong and Mann, 2007). In particular, cells are cultured in either "*light*" medium with amino acids of natural isotope abundance or "*heavy*" medium containing the labeled amino acid of choice. When proteins extracted from cells grown respectively in *light or heavy* medium are analyzed by mass spectrometry, pairs of chemically identical peptides of different stable-isotope composition can be differentiated owing to their mass difference (Figure 35).

BCR$^+$ and BCR$^-$ lymphoma cells, obtained after Tat-Cre transduction of the primary λ–MYC;B1-8f tumor #2567, were cultured in medium containing L-arginine and L-lysine, marked with either *light* or *heavy* isotopes. Cells were cultured for 4-5 days (corresponding to 8-10 generations) to allow efficient incorporation of labeled amino acids.

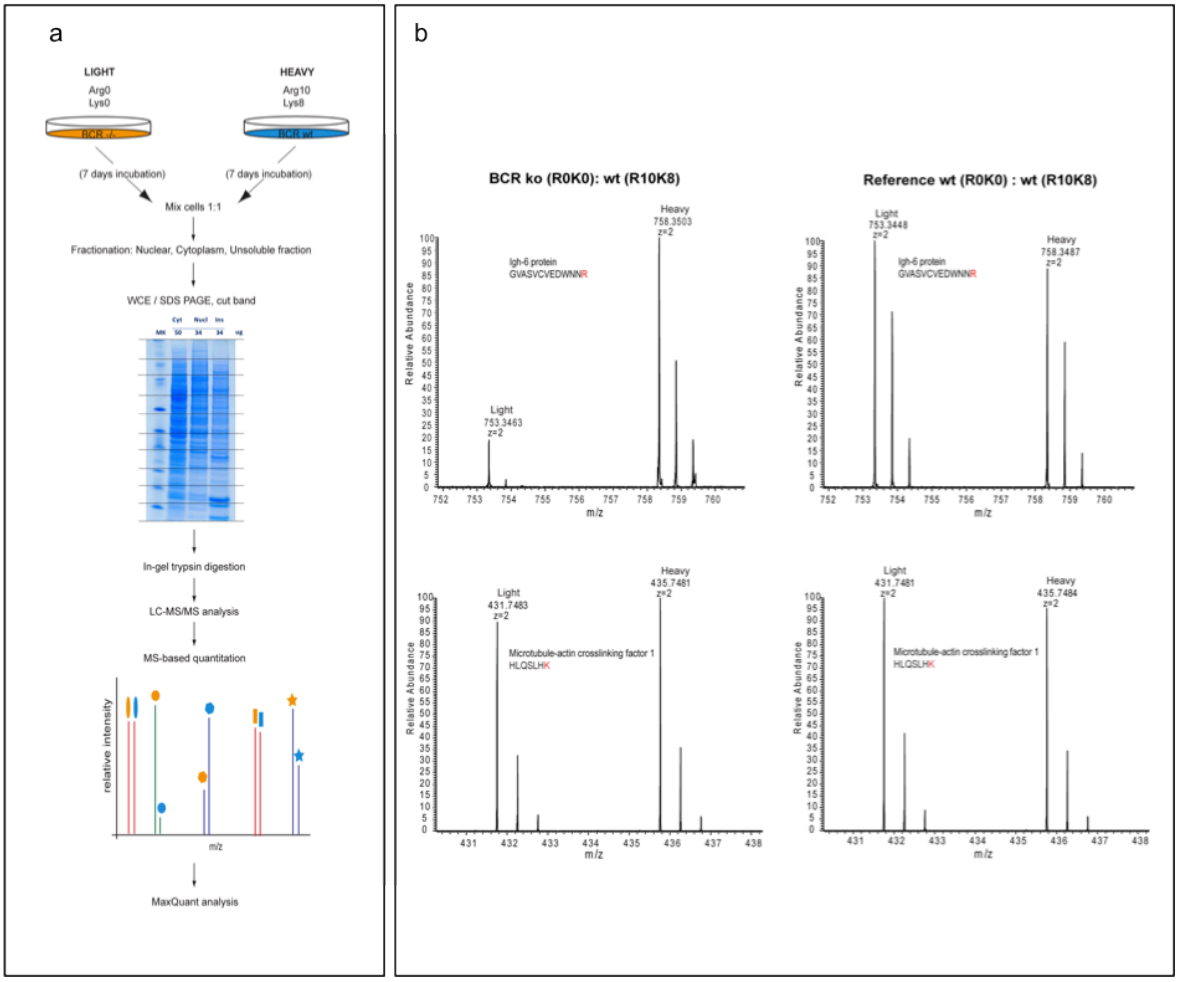

Figure 35: Schematic representation of SILAC methodology applied to BCR⁺ and BCR⁻ λ-MYC lymphomas

BCR⁺ or BCR⁻ lymphoma cells were cultured in medium containing labeled ("heavy" or "light") aminoacids for 7 days. Cells were harvested and BCR⁺ cells labeled with heavy aminoacids were mixed in equal amounts with their BCR- counterparts labeled with light aminoacids (the reciprocal experiment was also performed). Protein extracts were then processed for LC-MS/MS analysis. With this approach, the same protein derived from different samples can be differentiated according to the difference of the mass of its peptide composition. b) Representative example of protein quantification in BCR⁻ and BCR⁺ cells (left panels), labeled with light and heavy aminoacids, respectively. Ig heavy chain (Igh-6) and microtubule-actin crosslinking factor 1 are shown. As internal control, a comparison between BCR⁺ cells labeled respectively with heavy and light aminoacids labeled is shown (right panels).

The particular cell culture medium used for these experiments did not affect significantly the growth rate of both BCR⁺ and BCR⁻ cells (data not shown). Cells incorporating *heavy* or *light* amino acids into their proteins were mixed together in equal amount. Cytosolic, nuclear and insoluble protein fractions were extracted from

each sample and processed for liquid chromatography (LC)-mass-spectrometry (MS)/MS analysis. We quantified with a high confidence over 4000 proteins in both BCR^+ and BCR^- tumor cells (*ratio counts>2*). Importantly, 5% of cellular proteins were significantly regulated by BCR expression in lymphoma cells ($p<0.01$) (Figure 36).

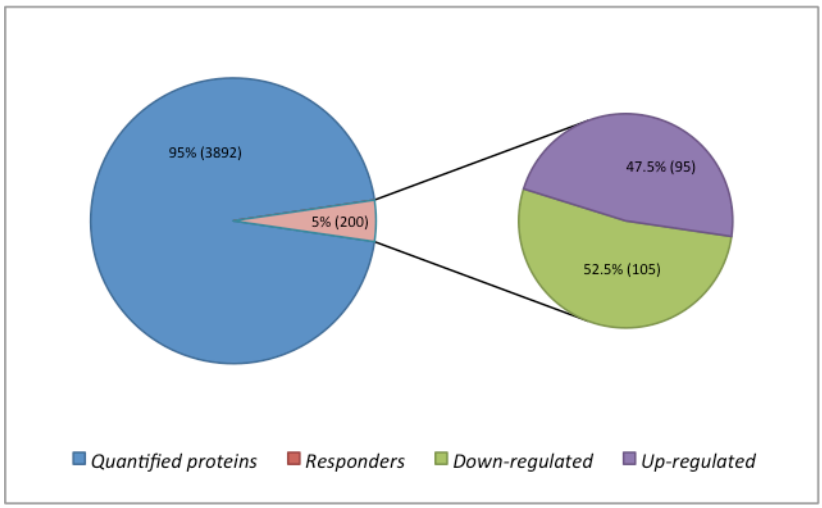

Figure 36: Quantification of proteins regulated by the BCR in λ-MYC lymphomas

Pie chart representation of proteins quantified with a good confidence (*ratio counts>2*) through SILAC technology. Percentage (and absolute number) of quantified proteins controlled by the BCR is indicated in pink (responders; $p<0.01$). Differentially expressed proteins between BCR^+ and BCR^- lymphoma cells are divided in up- (purple) and down (green)-regulated in BCR^- cells.

7.4.2 BCR regulates metabolism of λ-MYC;B1-8f lymphomas

The comparison of proteomes of BCR^+ and BCR^- lymphoma cells revealed 200 proteins differentially expressed between the two tumor subsets. This group of genes was further divided into two subgroups consisting of genes respectively up- (48%) and down- (52%) regulated in BCR-deficient lymphomas (Figure 36). Ingenuity Pathway enrichment Analysis (IPA) performed on statistically significant ($p<0.01$) down-regulated responders in BCR-deficient tumors, identified enzymes involved in key metabolic processes including glycolysis, gluconeogenesis, pyruvate and galactose metabolism (Figure 37). Interestingly, several enzymes of the same metabolic pathway such as glycolysis were at the same time down regulated in a

modest, yet significant, fashion in response to BCR inactivation. This result suggests an influence of the BCR on the efficiency of lymphoma cells to exploit glucose breakdown for both energetic and anabolic processes. Loss of the antigen receptor had also consequences on steady state levels of key BCR signalling effectors, including Cd79a, PLCγ2 and Vav1, suggesting a positive feedback mechanism supporting BCR function in lymphoma cells (Figure 38). Interestingly, among the proteins whose expression increased in response to BCR inactivation, we found components of the NRF2-mediated oxidative stress response and signaling pathways associated to mitochondrial dysfunction. These results warrant further validation to determine whether they contribute to the loss of BCR$^-$negative lymphomas.

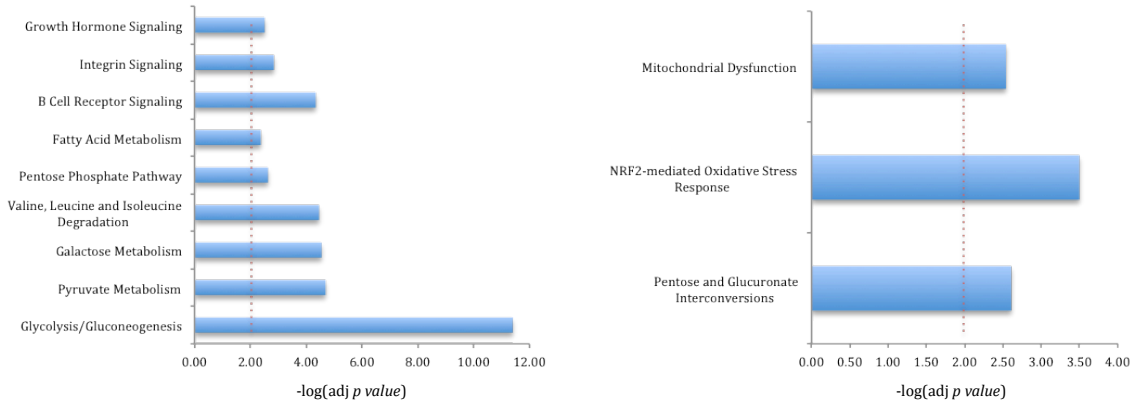

Figure 37: The BCR influences metabolism and its own signalling of c-MYC transformed B cells

Ingenuity pathway enrichment analysis on proteins respectively down- (left panel) and up- (right panel) regulated in BCR$^-$ lymphoma cells (#2567). Only significantly enriched pathways are shown (p<0.01, red dashed line indicates threshold of significance)

	Normalized H/L ratio	Ratio H/L (count)	Ratio H/L (significance)
Glycolysis			
Phosphoglucomutase-1	1,18	50	8.62E-06
Hexokinase-1	1,78	6	1.27E-08
6-phosphofructokinase	1.4	9	1.14E-06
Fructose-bisphosphate aldolase	1.15	421	2.58E-05
Triosephosphate isomerase	1.13	225	0.00036058
Glyceraldehyde-3-phosphate dehydrogenase	1.17	15	0.0023722
Phosphoglycerate kinase 1	1.18	596	5.94E-07
Phosphoglycerate kinase 2	1.22	14	1.60E-07
β-enolase	1.51	116	1.22E-33
Pyruvate kinase (Isoform M2)	1.15	1151	2.01E-05
L-lactate dehydrogenase A chain	1.1	937	0.0061961
Glucose uptake			
Phosphoinositide 3-Kinase-C2-α	1.61	84	7.17E-22
Galactose metabolism			
Galactokinase 1	1.13	178	0.00028304
Galactokinase 2	1.62	8	4.12E-08
BCR signalling			
Phospholipase C-gamma-2	1.14	177	0.00010835
Vav1	1.15	66	0.0019863
Hcls1	1.14	20	0.00023631
Rac2	1,094	69	0.0083523
CD79a antigen	1.62	24	6.22E-18
Igκ constant region	1.21	51	3.54E-07
IgH constant region	8.4	70	8.71E-252

Table 8: The BCR modulates sugar metabolism and its own signalling effectors in lymphoma cells

Main pathways down regulated in response to BCR ablation as revealed through Ingenuity Pathway enrichment Analysis. Normalized H/L ratio indicates the degree of down regulation of the indicated proteins upon BCR ablation (for example, levels of Hexokinase-1 are 78% down regulated in BCR^- cells). Ratio H/L count indicates number of times each protein was counted. Significance of the data is shown in the last column.

7.4.3 BCR protects lymphoma cells from starvation

To investigate whether BCR expression influenced the growth of tumor cells under conditions of limited nutrient supply, BCR^+ and BCR^- lymphoma cells generated upon Tat-Cre transduction of independent primary tumors were co-cultured in medium containing limiting amounts of fetal bovine serum (FBS), a major source of nutrients

and growth factors. 1:1 mixtures of BCR$^+$ and BCR$^-$ lymphomas were cultured under serum-restricted conditions for 24 hours. BCR-deficient lymphomas showed a higher sensitivity to nutrient deprivation than their BCR$^+$ counterparts, as confirmed by the acceleration in the counter-selection when mixtures of tumor cells were cultured in low serum (0.1% FBS) (Figure 38).

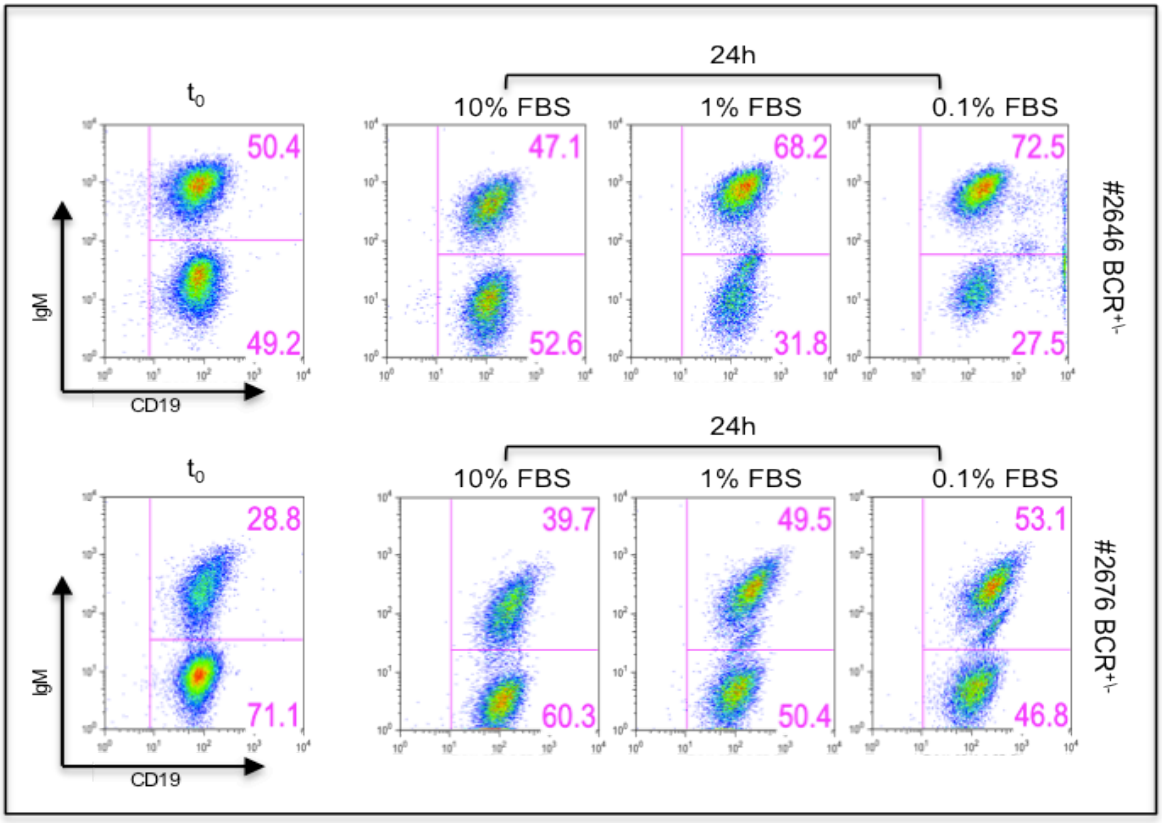

Figure 38: BCR$^-$ lymphoma cells are preferentially counter selected in response to serum deprivation

Flow cytometric analysis of BCR$^+$ and BCR$^-$ tumor cells cultured in competition, for 24 hours, in B-cell medium complemented with the indicated percentage of fetal bovine serum (FBS). Dot plots are gated on live FSC^{hi} lymphocytes. Numbers indicate percentage of BCR$^+$ and BCR$^-$ tumor cells. Tumor cells derived from two independent lymphomas (#2646 and #2676) are shown.

To further address the involvement of the BCR in the regulation of lymphoma anabolic metabolism, BCR$^+$ and BCR$^-$ tumors were cultured in competition in the presence of Rapamycin, a specific inhibitor of the mTOR (mammalian Target Of Rapamycin) kinase, which is an essential regulator of nutrient uptake (Peng et al., 2002). Strikingly, treatment with Rapamycin of 1:1 mixtures of BCR$^+$ and BCR$^-$

transformed B cells (from two independent lymphomas) led to a significant (3-fold) acceleration in the counter selection of receptor-negative tumors *in vitro* (Figure 39a-c).

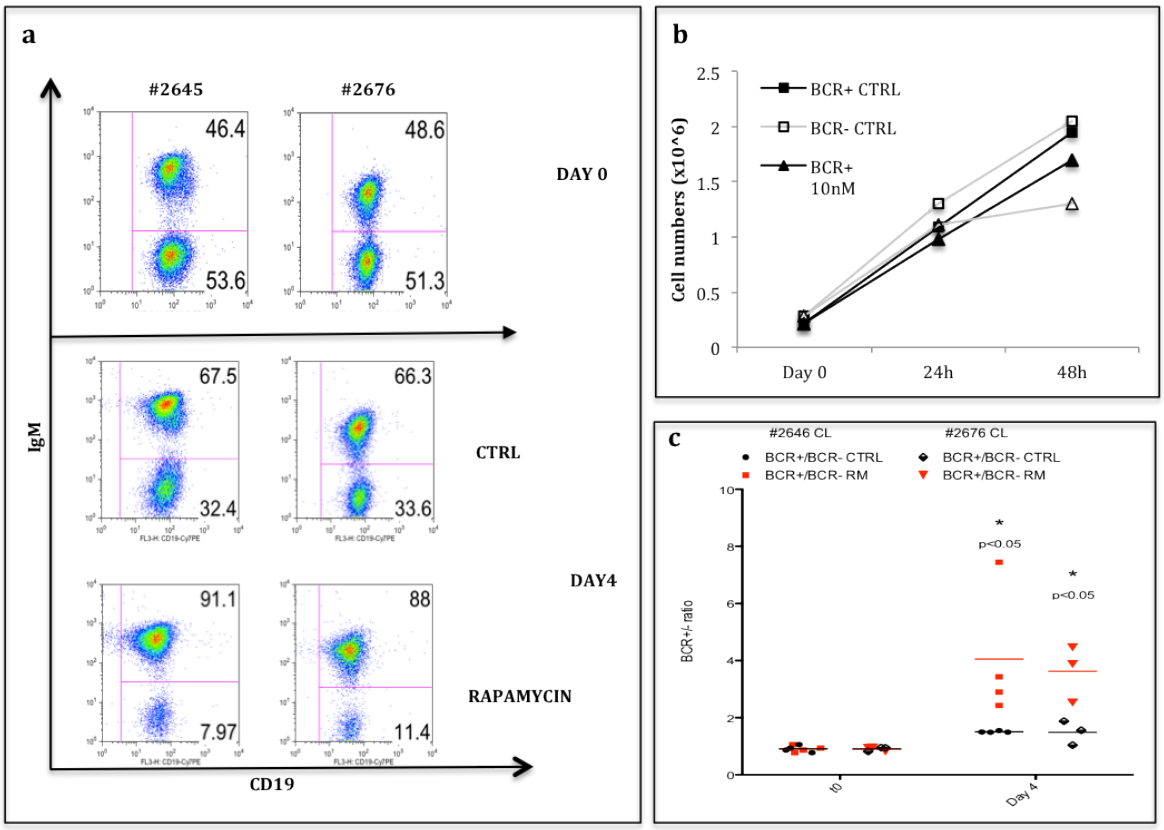

Figure 39: BCR⁻ lymphoma cells are more sensitive to Rapamycin treatment than their BCR⁺ counterparts

a) Representative flow cytometric analysis of BCR⁺ and BCR⁻ tumor cells co-cultured for 4 days in the presence (RM) or absence (CTRL) of 10nM Rapamycin. Dot plots are gated on live FSC^{hi} lymphocytes. Numbers represent percentage of BCR⁺\⁻ tumor cells. Tumor cells derived from two independent lymphomas (#2646 and #2676) are shown; b) Growth curves of BCR⁺ (black lines) and BCR⁻ cells (grey lines), derived from lymphoma #2646, cultured in competition for 2 days in the presence (triangles) or absence (rectangles) of 10nM Rapamycin (RM); c) Summary of competition assays between BCR⁺ and BCR⁻ lymphoma cells derived from two independent λ-MYC lymphomas (#2646 and #2676), cultured in presence (RM, red symbols) or absence (CTRL, black symbols) of 10nM Rapamycin. Ratio of BCR⁺/BCR⁻ cells at the indicated time points of the competition are shown. Bars represent average of 4 and 3 replicates, in #2646 and #2676 tumors, respectively (2way-Anova: *$p<0.05$).

Moreover, cell cycle analysis of Rapamycin treated cells showed an increase in apoptotic cells (with a hypodiploid (<2n) DNA content) mainly in the BCR⁻

compartment, whereas cell cycle of both BCR$^+$ and BCR$^-$ populations was slightly affected (Figure 40).

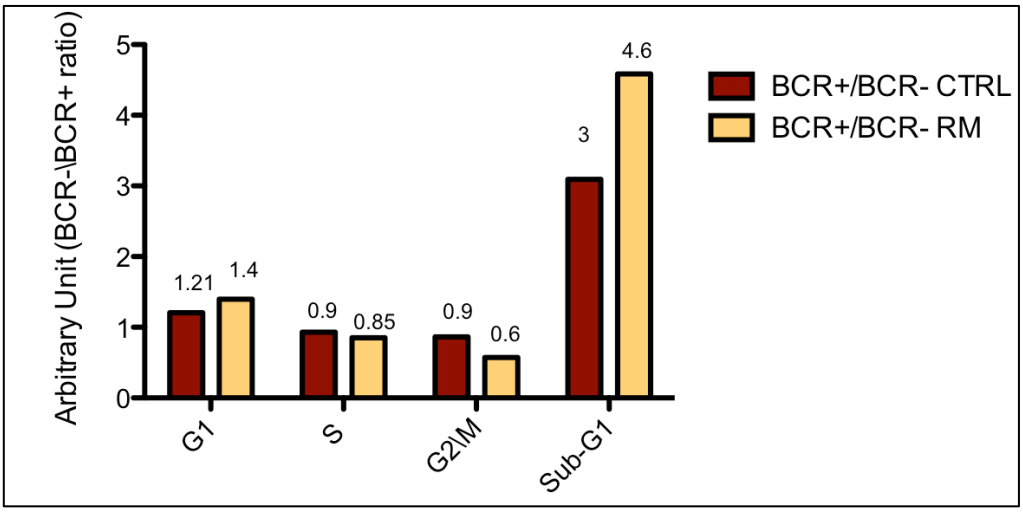

Figure 40: Rapamycin induces cell death preferentially in BCR-deficient lymphoma cells

Cell-cycle analysis (BrdU/PI) of BCR$^+$ and BCR$^-$ lymphoma cells (#2564 λ–MYC;B1-8f tumor), co-cultured for 3 days in the presence (RM, yellow histograms) or absence (CTRL, red histograms) of 10nM Rapamycin. Numbers above each histogram represent ratios of frequencies of BCR$^-$ and BCR$^+$ lymphoma cells at the indicated stage of the cell cycle. Apoptotic cells (in either IgM$^+$ or IgM$^-$ gates) were detected according to DNA content (PI), as hypodiploid (<2n) cells.

Interestingly, Rapamycin treatment of independent cultures of BCR$^+$ and BCR$^-$ tumors resulted in a significant difference in cell numbers between the two populations (Figure 41). In particular, cell viability of both BCR$^+$ and BCR$^-$ tumors was affected, as shown by a reduction in cell number regardless of BCR expression, after 2 days of treatment; nevertheless, Rapamycin-induced toxicity was significantly more pronounced in BCR$^-$ lymphoma cells ($p<0.001$) (Figure 41).

Altogether, these results reveal a higher sensitivity of lymphoma cells loosing BCR expression to undergo cell death when grown under condition of limiting nutrient supply, as well as upon Rapamycin treatment.

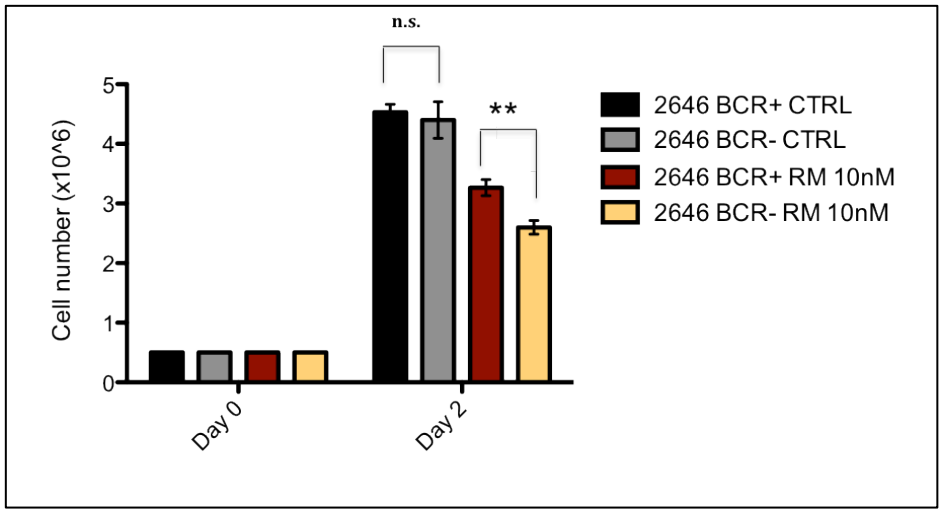

Figure 41: The BCR exerts a mild protective effect against Rapamycin-induced cell death

Numbers of BCR^+ (black and red bars) and BCR^- (grey and yellow bars) lymphoma cells (#2646 λ–MYC;B1-8f tumor) grown in separate cultures, in the presence (red and yellow bars) or absence (black and grey bars) of 10nM Rapamycin (RM) for 2 days. Histograms represent average of triplicates for the indicated time points (±SD) (2way-Anova: ***p-value<0.001*). *ns*= not significant.

7.4.4 Contribution of the BCR to energy metabolism in c-MYC transformed B cells

One of the hallmarks of tumor cells is the shift in glucose metabolism from oxidative phosphorylation to aerobic glycolysis, also known as the Warburg effect (Warburg, 1956). The shift to a more inefficient glucose metabolism (catabolism of one glucose molecule leads to only two ATP molecules instead of 38 molecules obtained through oxidative phosphorylation) is counteracted by the increase in anabolic processes that rely on glycolysis intermediates to support the rapid growth of tumor cells. I therefore tested whether BCR expression influenced glucose metabolism and thereby lymphoma growth.

7.4.4.1 Normal glucose uptake in λ-MYC lymphomas lacking BCR expression

To test whether the antigen receptor influenced the uptake of glucose in λ-MYC lymphomas, BCR^+ and BCR^- tumor cells generated by TAT-cre transduction of 3 independent primary tumors, were grown *in vitro* under competitive conditions.

Glucose uptake was measured at the single cell level using the fluorescent labeled glucose analog 2-NBDG (2-(*N*-(7-Nitrobenz-2-oxa-1,3-diazol-4-yl)Amino)-2-Deoxyglucose) (Zhong et al., 2010).

At the earliest time when counter selection of BCR$^-$ cells was observed (Figure 42a, upper right plot), glucose uptake was not significantly affected by BCR inactivation (Figure 42a, left histograms).

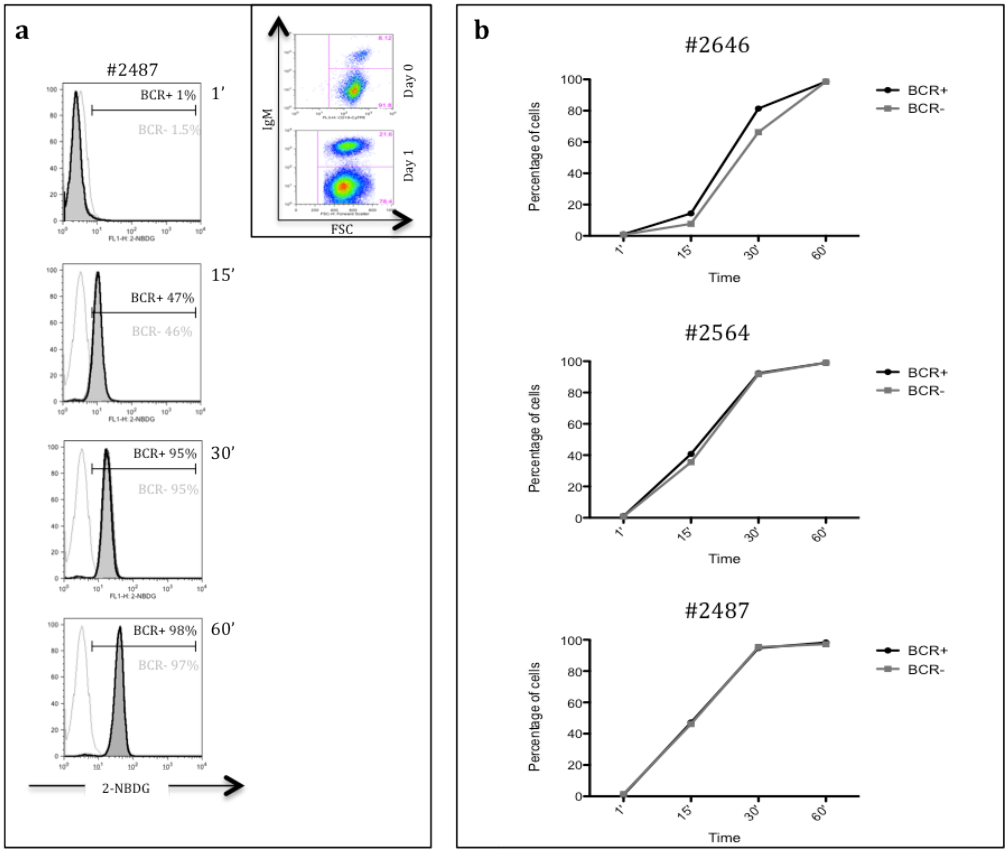

Figure 42: BCR does not influence glucose uptake in lymphoma B cells

a) Representative example of uptake of the glucose analog NBDG in BCR$^+$ (black thick histogram) and BCR$^-$ (grey filled histograms) lymphoma cells (#2487) upon 24 hours of competition. Unlabeled cells were used as negative control (grey thin line). Numbers indicate percentages of BCR$^+$ (black) and BCR$^-$ (grey) lymphomas that have up taken 2-NBDG at the indicated time points. Histograms refer to live FSC^{hi} lymphoma cells. Mixture of BCR$^+$ and BCR$^-$ cells used for the analysis were analyzed by flow cytometry at the onset of competition and 24 h later. Note the over 2-fold increase in the fraction of BCR$^+$ tumor cells, 1-day after the beginning of the competition. b) Percentages of 2-NBDG-positive BCR$^+$ (black lines) and BCR$^-$ cells, derived from three independent tumors (#2646, #2564 and #2487), measured by flow cytometry at the indicated time points. Uptake of 2-NBDG was measured after 24 hours of competition.

In particular, the percentage of BCR^+ and BCR^- lymphoma cells internalizing 2-NBDG was comparable, with saturation of the signal occurring between 30 and 60 minutes after the start of the labelling (Figure 42). In a similar fashion, no major differences in glucose uptake were scored at early time points, (between 1 and 15 minutes of labelling with 2-NBDG) (Figure 42b). These results exclude a role of the BCR in the control of glucose uptake in c-MYC transformed B cells.

7.4.4.2 Normal pyruvate to lactate conversion in BCR-deficient lymphoma cells

Pyruvic acid represents a central node in glucose metabolism. Pyruvic acid supplies energy to living cells through the citric acid cycle (also known as the Krebs cycle or TCA cycle) under conditions of normoxia (aerobic respiration). Alternatively it is reduced to lactic acid under anaerobic conditions or as a consequence of the Warburg effect.

To determine whether BCR controlled the reduction of pyruvate to lactate, Lactate De-Hydrogenase (LDH) activity was measured in tumor cells, before and after BCR inactivation. I quantified NADH levels in the conditioned media of tumor cells as a read-out of LDH activity. BCR^+ and BCR^- lymphoma cells were isolated upon Tat-Cre transduction of 2 independent tumors (#2567, #2646), grown *in vitro* for 24 hours and conditioned medium collected for NADH measurements. As shown in Figure 43 NADH levels were not significantly different between cultures of BCR-proficient and-deficient cells. This result suggests that conversion of pyruvate into lactate is not altered in BCR-negative lymphomas at least when cells are grown under non-competitive conditions.

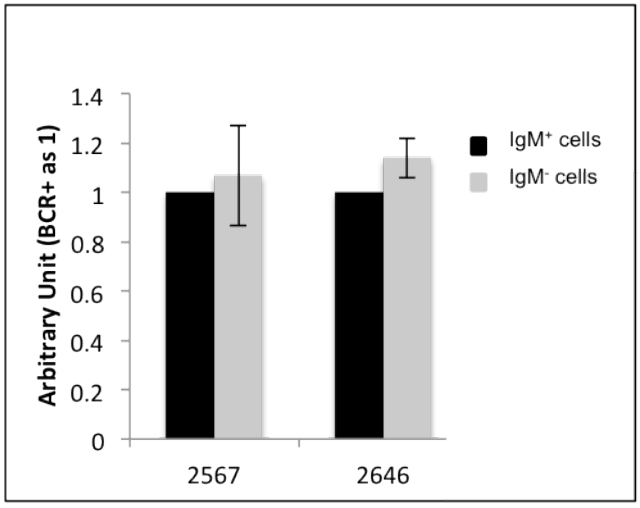

Figure 43: LDH activity is not significantly altered in response to BCR ablation

Colorimetric measurement of NADH production in supernatants collected from *in vitro* cultures of pure BCR$^+$ (black bars) and BCR$^-$ (grey bars) lymphoma cells derived from 2 independent tumors (#2567 and #2646). LDH activity normalized to BCR$^+$ lymphoma cells (± SD) is shown.

7.4.4.3 Analysis of mitochondrial function in λ-MYC B-cell lymphomas

Measurement of oxygen consumption has long been used to assess mitochondrial function (Chance and Williams, 1956). To investigate whether BCR influenced the consumption of oxygen through oxidative phosphorylation, I measured mitochondrial respiration in BCR$^+$ and BCR$^-$ tumor cells. To this aim, highly purified populations of BCR$^+$ and BCR$^-$ lymphoma cells generated from 3 independent λ–MYC;B1-8f tumors (#2567, #2646 and #2676), were expanded shortly *in vitro* and oxygen consumption of the purified cells was measured in collaboration with dr M. Giorgio (European Institute of Oncology, Milan). Both basal and uncoupled respiration was measured (Figure 44). Basal respiration is controlled by the ATP turnover of the cell (Brown, 1992), whereas uncoupled respiration represents the maximum respiration rate of a cell. The latter can be measured by addition of carbonylcyanide-4-trifluoromethoxy-phenylhydrazone (FCCP) and evaluates the integrity of the electron transport chain. Respiration rates were normalized to total protein amounts, limiting thereby the impact of differences in the amount of cells measured in the oxygraph chamber. λ-

MYC lymphomas showed a considerable degree of oxygen consumption under basal conditions thus highlighting robust oxidative phosphorylation. Importantly, BCR^+ and BCR^- lymphoma cells showed similar uncoupled-to-basal respiration ratios, thus excluding major mitochondrial alterations resulting from BCR loss.

These data suggest that the BCR neither influences glucose uptake, nor the conversion of pyruvate to lactate or mitochondrial respiration in lymphomas provided with an excess in sugar substrates and in the presence of normal/high partial pressure of oxygen.

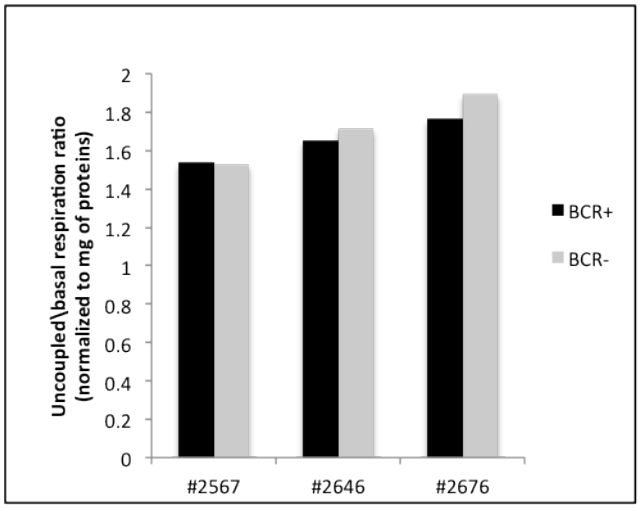

Figure 44: O_2 consumption is independent of BCR expression in λ-MYC lymphomas

Mitochondrial respiration measured in BCR^+ (black bars) and BCR^- (grey bars) lymphoma cells derived from three independent tumors (#2567, #2646 and #2676). Respiration rate is expressed as uncoupled to basal respiration ratio. Samples are normalized according to protein content.

7.4.5 BCR controls GSK3β activity in lymphoma cells

A series of studies have identified in the recent years a number of BCR effectors controlling the survival of resting mature B cells and their contribution to Burkitt lymphomagenesis (Refaeli et al., 2008; Sander et al., 2012; Schmitz et al., 2012; Srinivasan et al., 2009; Werner et al., 2010). In particular, the PI3K pathway was shown to play a central role in sustaining the survival signal emanating from the BCR in resting mature B cells (Srinivasan et al., 2009). More recently, it was demonstrated

that constitutive activation of the PI3K pathway was necessary to support c-MYC-dependent transformation of germinal center B cells leading ultimately to BL (Sander et al., 2012). Glycogen Synthase Kinase 3 beta (GSK3β) is an essential downstream effector of the PI3 kinase signalling pathway. It is phosphorylated on serine-9 by the AKT kinase causing its inactivation. I tested whether BCR could influence the phosphorylation of GSK3β in λ-MYC lymphomas. To this aim, mixtures of BCR$^+$ and BCR$^-$ lymphoma cells, obtained upon Tat-Cre transduction of four independent primary tumors (#2646, #2676, #2564 and #2487), were cultured for few days. As soon as the counter selection of BCR-deficient tumor cells became apparent, I measured by phosphoflow the levels of phosphorylated GSK3β (Ser9), in the individual tumor populations. The levels of phosphorylated GSK3β were significantly reduced in lymphoma cells that had undergone BCR loss (Figure 45a).

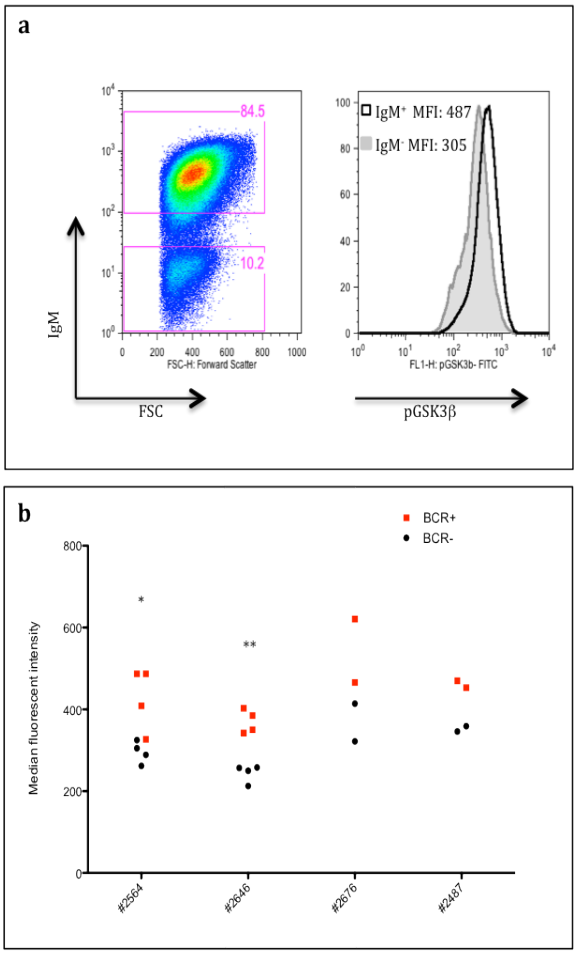

Figure 45: Reduced GSK3β phosphorylation in λ-MYC lymphomas loosing BCR expression

a) Representative flow cytometric analysis of Ser9 phosphorylated GSK3 β levels in BCR$^+$ and BCR$^-$ cells upon *in vitro* competition. In the left plot, percentages of BCR$^+$ and BCR$^-$ cells are shown. In the right panel median fluorescent intensity (MFI) of phosphorylated GSK3β (pGSK3β) in BCR$^+$ (black thick line) and BCR$^-$ (grey filled line) lymphoma cells is shown. Dot plots show FSC^{hi} live lymphoma B cells. Tumor cells were derived from λ-MYC;B1-8f lymphoma #2564; b) Median fluorescence intensity of phopshorylated GSK3β in BCR$^+$ (black circles) and BCR$^-$ (red squares) tumor B cells grown under competition. The analysis was performed on cells derived from 4 independent lymphomas (#2564, #2646, #2676 and #2487). (t-test: *p<0.05 or **p<0.01).

These results highlight the central role exerted by the BCR in the control of GSK3β activity in c-MYC transformed B cells.

7.4.6 BCR-dependent inhibition of GSK3β sustains growth of λ-MYC lymphomas

Reduced serine-9 phosphorylation is expected to increase GSK3β activity (reviewed in Cohen and Frame, 2001). To determine whether the increased activity of GSK3β was responsible for the counter selection of BCR-less lymphoma cells, we treated 1:1 mixtures of BCR^+/BCR^- tumor cells with the GSK3β-specific inhibitor CT99021 (Meijer et al., 2004). I first titrated the drug on purified BCR^+ and BCR^- lymphoma cells, addressing cell viability at different doses of CT99021 after respectively 1- and 2-days of treatment (Figure 46). The inhibitor caused a mild reduction in the growth of BCR^+ and BCR^- cells, with an extension of their doubling time when cells were exposed at the highest dose. The specificity of the inhibition was confirmed by the reduction in both BCR^+ and BCR^- lymphoma cells of c-MYC phosphorylation on threonine-58 (Thr58), a known target of GSK3β (Adhikary and Eilers, 2005) (Figure 47). Finally, four independent lymphomas (#2646, #2676, #2564 and #2487) were transduced with Tat-Cre, and 1:1 mixtures of BCR^+ and BCR^- lymphomas were grown in the presence of 1μM CT99021. Strikingly, inhibition of GSK3β activity prevented the counter selection of BCR^- lymphoma cells and in few instances favored the expansion of the BCR^- population (Figure 48a and b). Importantly, the inhibition of GSK3β upon CT99021 treatment was reversible as its withdrawal led to the preferential expansion of BCR-proficient lymphomas (Figure 48a). These results reveal the essential function of the BCR to control/limit the activity of GSK3β, necessary to sustain the growth of λ-MYC lymphomas.

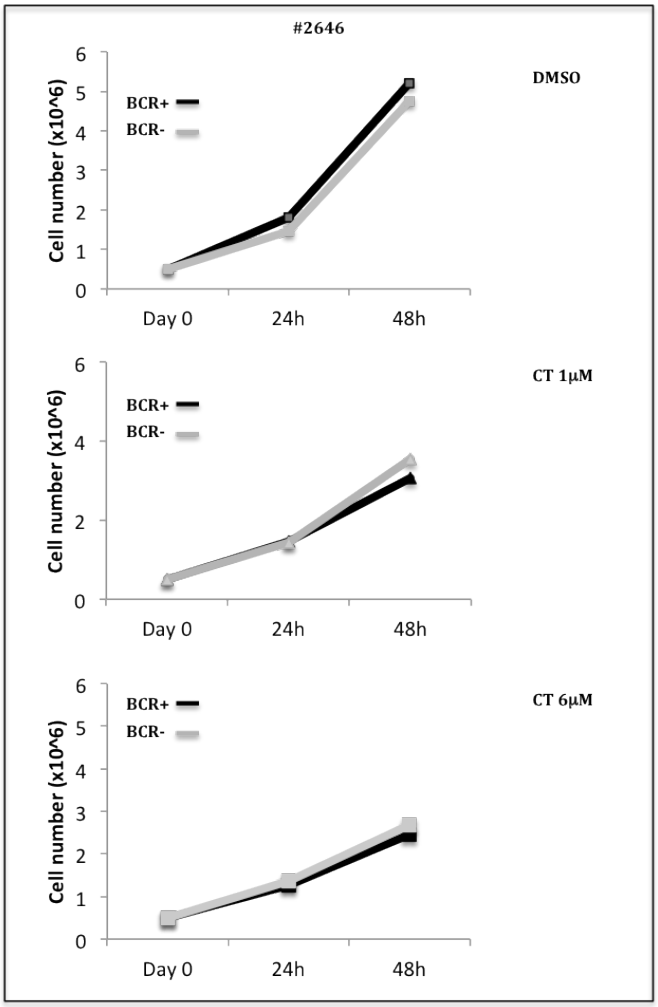

Figure 46: Effects of the GSK3β inhibitor CT99021 on *in vitro* growth of λ-MYC lymphomas

Growth curves of purified BCR$^+$ and BCR$^-$ lymphoma cells cultured in the presence of the indicated doses of the GSK3β inhibitor CT99021 for 3 days. BCR$^+$ and BCR$^-$ lymphoma cells cultured in the presence of vehicle (DMSO) were used as controls. Cells were counted every 24 hours. Each experimental point represents the average count of three replicates.

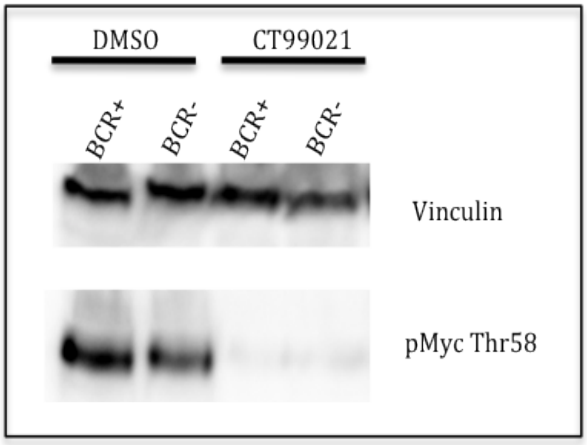

Figure 47: GSK3β inhibition through CT99021 blocks Threonine 58 c-MYC phosphorylation in λ-MYC B-lymphoma cells

Immunoblot analysis to measure Threonine 58 c-MYC phosphorylation (Thr58), in BCR$^+$ and BCR$^-$ lymphoma B cells (#2646), cultured in the presence of 1μM CT99021, or DMSO, for 48 hours. Vinculin levels were quantified to control for protein input.

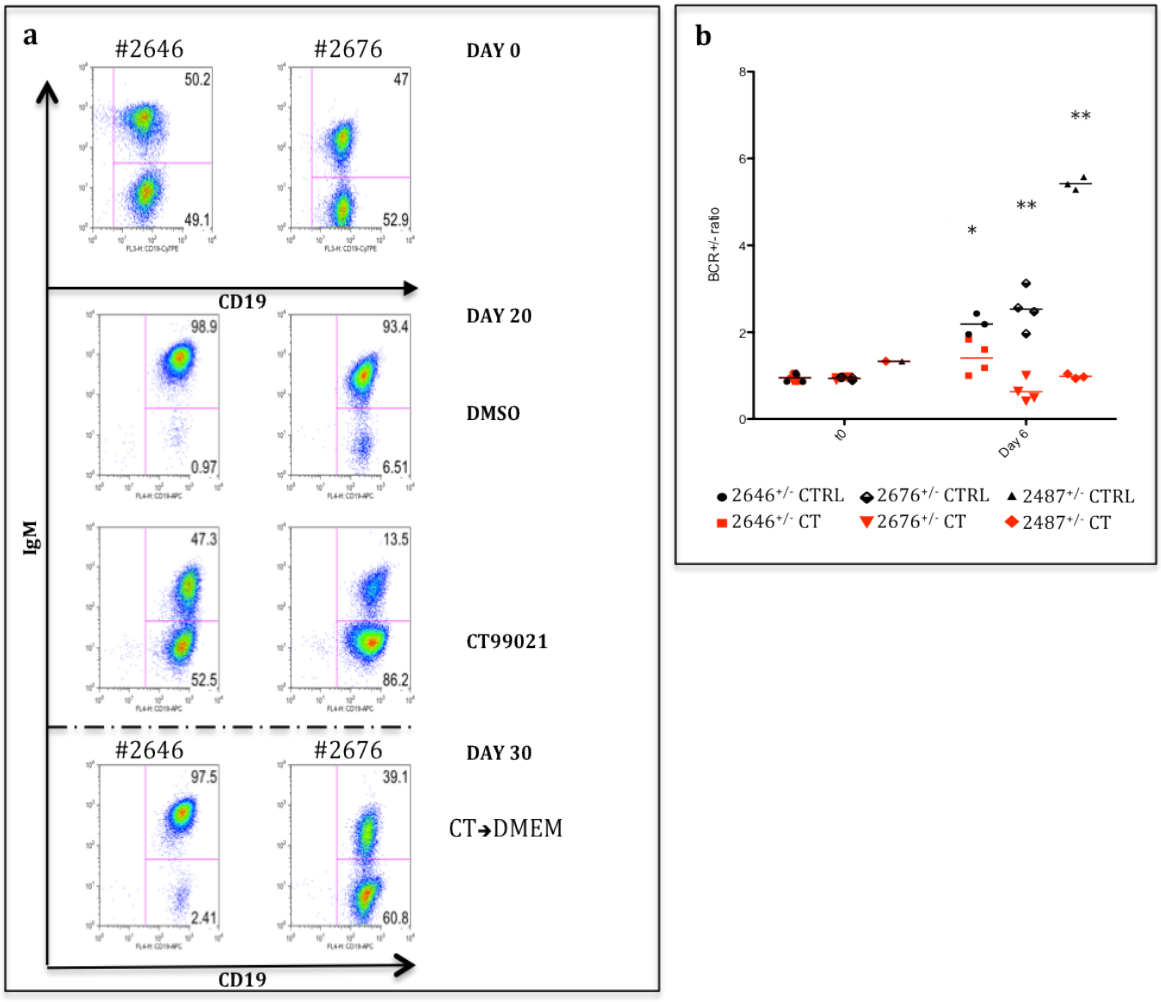

Figure 48: Modulation of GSK3β activity influences counter selection of BCR⁻ lymphoma cells

Representative flow cytometric analysis of 1:1 mixtures of BCR⁺ and BCR⁻ tumor cells cultured for 20 days in the presence (CT) or absence (DMSO) of 1 μM CT99021. Lower dot plots (CT➔DMEM) represent flow cytometric analyses of BCR$^{+/-}$ competitions 10 days after removal of the GSK3β inhibitor. Dot plots are gated on live FSC^{hi} lymphocytes. Numbers indicate percentage of BCR$^{+\backslash-}$ tumor cells. Tumor cells were derived from two independent λ-MYC;B1-8f lymphomas (#2646 and #2676); b) Summary of the data relative to *in vitro* competitions of BCR⁺ and BCR⁻ lymphoma cells, obtained from three independent λ-MYC;B1-8f lymphomas (#2646, #2676 and #2487), cultured in the presence (CT, red symbols) or absence (CTRL, black symbols) of 1μM CT99021. Ratios of BCR⁺ over BCR⁻ cells are shown before (t0) and 6 days after competition. Bars represent average of 4, 3 and 2 replicates of #2646, #2676 and #2487 tumors, respectively (t-test: *$p<0.05$ or **$p<0.01$*). Each symbol represents average of technical triplicates.

7.4.7 GSK3β inhibition restores normal cell-cycle progression in BCR$^-$ lymphomas

Loss of the BCR promotes a delay in cell cycle progression and an increase in apoptosis of BCR-deficient lymphomas when grown in competition with their BCR$^+$ counterparts (see paragraphs 7.3.6 and 7.3.7). Given the ability of the GSK3β inhibitor CT99021 to block counter selection of BCR$^-$ lymphomas, I assessed its contribution to cell–cycle progression.

Ex vivo isolated lymphoma cells were Tat-Cre transduced, expanded for few days *in vitro* and BCR$^+$ and BCR$^-$ cells cultured in a 1:1 ratio in the presence of 1μM CT99021 (or DMSO) (Figure 49a). Cell cycle analysis was performed coupling BrdU labeling with staining for DNA content (PI) and surface IgM expression (as described in paragraph 7.3.6). In the absence of the inhibitor, the percentage of BCR$^-$ lymphoma cells in G_0/G_1 was 1.5-2 fold higher than in their BCR$^+$ competitors, in accordance with previous results. Noteworthy, the normalization of BCR$^+$/BCR$^-$ ratios induced by pharmacological inhibition of GSK3β (Figure 49a) was associated to an increase in the fraction of cells in S-phase that was particularly evident among BCR$^-$ cells (Figure 49b and c). These results highlight the control exerted by GSK3β on the entry of lymphoma cells into S-phase.

7.4.8 GSK3β inhibition rescues apoptosis of BCR$^-$ lymphomas

Experiments displayed in Figure 34 and have revealed the protective role exerted by the BCR on tumor cell survival. To test whether aberrant GSK3β activation was involved in the enhanced apoptosis of BCR-deficient lymphomas, BCR$^+$ and BCR$^-$ cells generated from *ex vivo* isolated primary lymphomas as a result of Cre transduction, were cultured as 1:1 mixtures for 2 days, in the presence of 1μM CT99021. Apoptotic cells were identified according to either DNA content (fraction of hypodiplod cells), or expression of active forms of caspases (fraction of cells labeled by VAD-FMK). In the absence of the GSK3β inhibitor, the fraction of apoptotic cells was 3 to 5 fold higher in

the population of BCR$^-$ cells as compared to its BCR$^+$ counterpart (Figure 50a and Figure 51a).

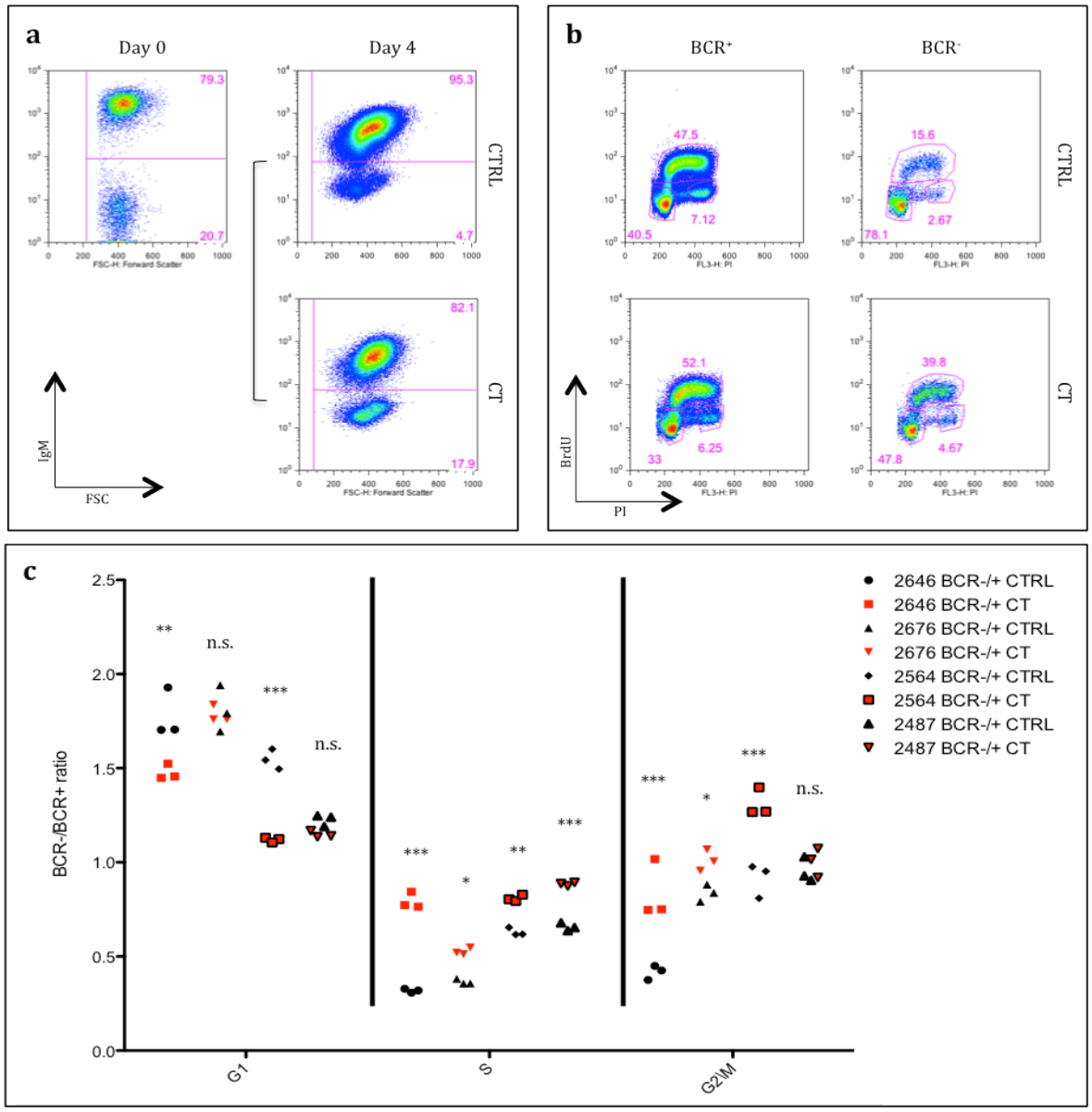

Figure 49: GSK3β inhibition facilitates G$_1$-to-S transition mainly in BCR$^-$ lymphoma cells

a) Representative flow cytometric analysis of BCR$^+$ and BCR$^-$ tumor cells (#2646) cultured for 4 days in competition, in the presence (CT) or absence (CTRL) of 1μM CT99021. Dot plots are gated on live FSC^{hi} lymphocytes. Numbers indicate percentage of BCR$^{+\backslash -}$ tumor cells; b) BrdU incorporation assays measured in BCR$^+$ and BCR$^-$ cells after 4 days of competition in the presence (CT) or absence (CTRL) of 1μM CT99021. Cell doublets were excluded from the analysis. Dot plots are gated on either IgM$^+$ (left) or IgM$^-$ (right) cells. Numbers represent percentage of cells; c) Summary of cell cycle analyses of BCR$^+$ and BCR$^-$ lymphoma cells, cultured in competition in the presence (CT, red symbols) or absence (CTRL, black symbols) of 1μM CT99021. Ratio of BCR$^-$ over BCR$^+$ cells is plotted separately for each stage of the cell-cycle (2way-Anova: *p<0.05; **p-<0.01; *** p<0.001). Tumor cells derived from four independent lymphomas (#2646, #2676, #2564 and #2487) were analyzed.

Upon treatment of BCR^{+}/BCR^{-} tumor mixtures with CT99021, I observed a significant improvement in the survival of BCR^{-} lymphoma cells (Figure 50 and Figure 51). These results indicate an essential contribution of the BCR to prevent tumor death through the inhibition of GSK3β activity.

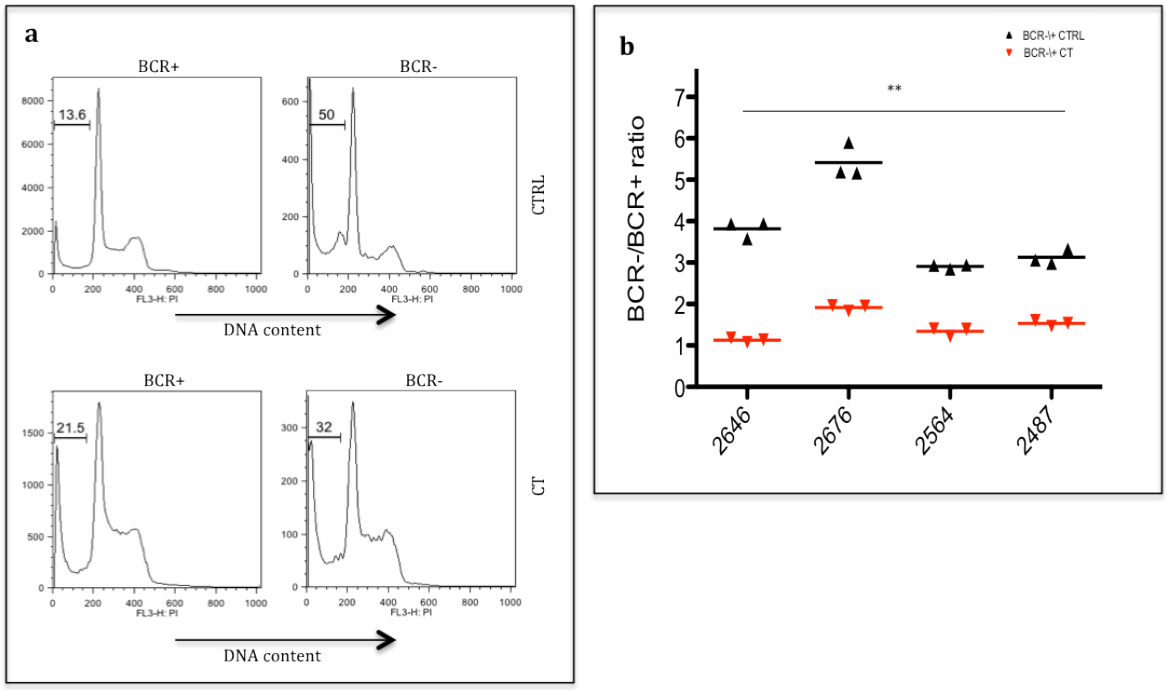

Figure 50: GSK3β inhibition improves the survival of BCR^{-} lymphoma cells

Representative flow cytometric analysis of IgM^{+} and IgM^{-} B lymphoma cells (#2487) after 2 days of competition, cultured in the presence (CT) or absence (CTRL) of μM CT99021. Numbers within histograms indicate frequencies of apoptotic cells with a hypodiploid DNA content; b) Ratio of BCR^{-} over BCR^{+} lymphoma B cells with less than *2n* DNA content measured by flow cytometry after 2 days of competition, in the presence (CT, red symbols) or absence (CTRL, black symbols) of 1μM CT99021; bars indicate the average of 3 replicates (*t-test **p<0.01*). Tumor cells were derived from four independent λ-MYC;B1-8f lymphomas (#2646, #2676, #2564 and #2487).

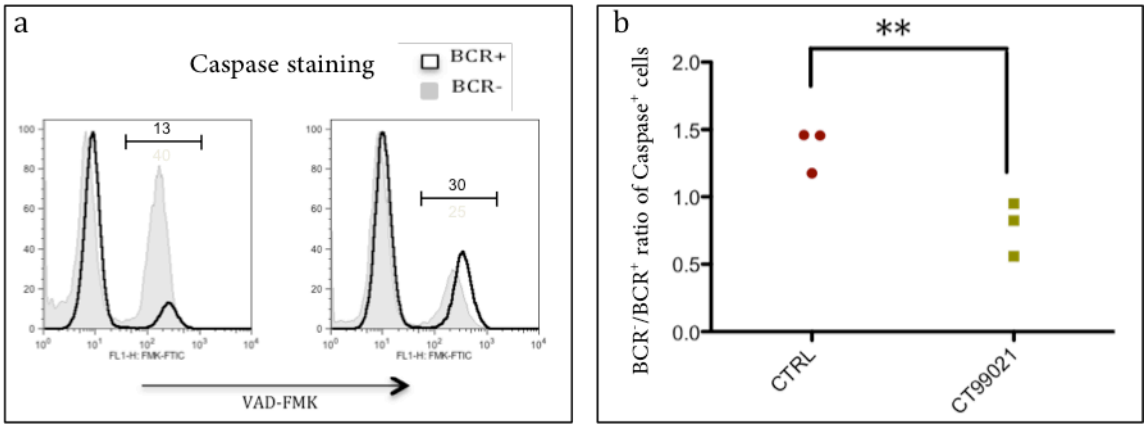

Figure 51: GSK3β inhibition prevents apoptosis in BCR- lymphoma cells

a) Flow cytometric analysis of IgM+ and IgM- lymphoma B cells after 4 days of *in vitro* competition, cultured in the presence (CT) or absence (CTRL) of 1μM CT99021. Numbers in the representative histograms indicate the frequency of apoptotic cells (VAD-FMK+) detected by flow cytometry among BCR+ (black thick line) and BCR- cells (grey filled line); b) Analysis of the ratio of BCR-/BCR+ tumor cells expressing active caspase(s) (VAD-FMK+); Tumor cells were obtained from three independent λ-MYC;B1-8f lymphomas (#2676, #2564 and #2487) (*t-test* **p<0.05)*.

7.4.9 Identification of BCR-regulated genes in λ-MYC lymphomas

To identify genes controlled by the BCR in lymphoma cells, whole transcriptome analysis of BCR+ and BCR- lymphoma cells grown in competition was performed, respectively in the presence or absence of the GSK3β inhibitor CT99021. Specifically, BCR+ and BCR- lymphoma cells obtained from 3 independent primary tumors transduced with TAT-Cre, were cultured in the presence of either CT99021 or vehicle, and cell competition was monitored by FACS. Tumor cells were sorted on the basis of surface Ig expression, at the time when BCR-deficient tumor cells started to get counter selected (in the absence of CT99021).

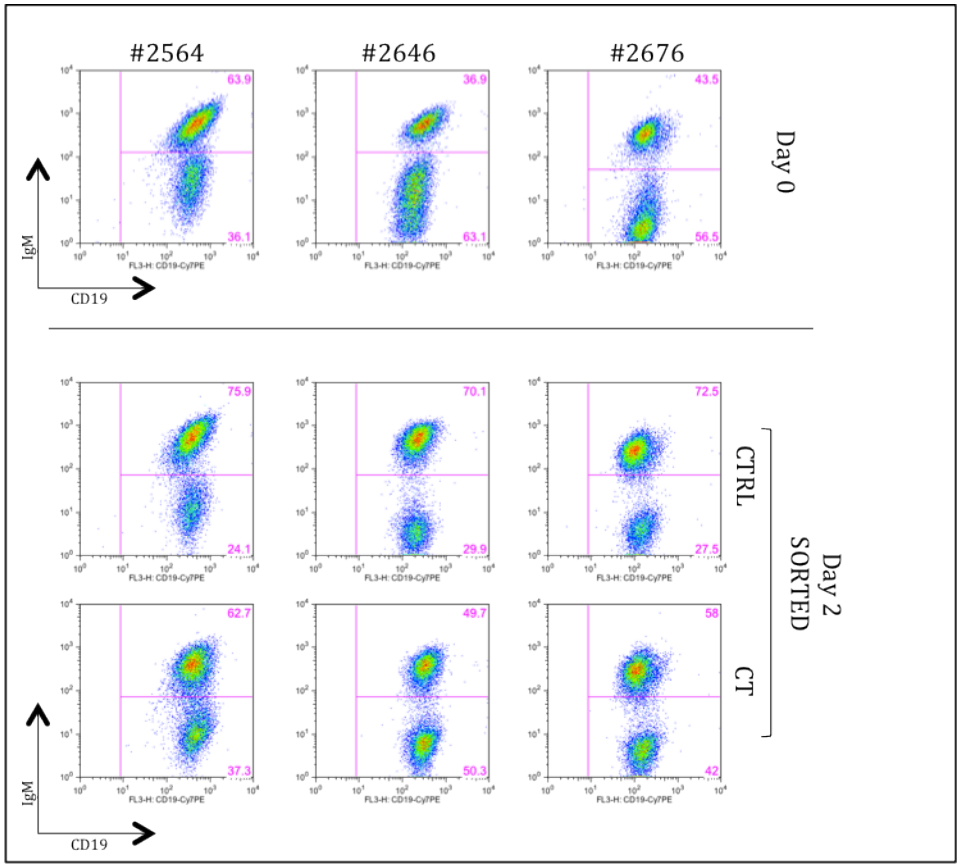

Figure 52: Purification of BCR$^+$ and BCR$^-$ lymphoma cells from mixed cultures for transcriptome analyses

Flow cytometric analysis of BCR$^+$ and BCR$^-$ lymphoma cells from three independent λ-MYC;B1-8f lymphomas (#2564, #2646 and #2676), cultured in competition in the presence (CT) or absence (CTRL) of 1μM CT99021. Numbers indicate percentages of live/FSC^{hi} cells.

The identity of sorted cells was confirmed through a quantitative assessment of B1-8f transcripts that were 10- to 100-fold reduced in BCR$^-$ lymphomas compared to their BCR$^+$ sorted counterparts (Figure 53).

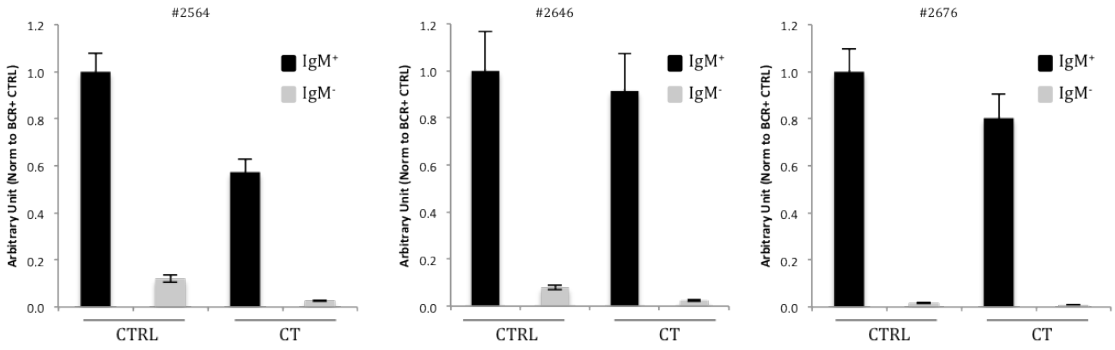

Figure 53: Analysis of B1-8 mRNA levels in sorted BCR$^+$ and BCR$^-$ λ-MYC;B1-8f lymphoma cells

Quantitative Real-Time PCR to measure B1-8 mRNA levels in BCR$^+$ (black bars) and BCR$^-$ (grey bars) tumor cells, derived from three independent lymphomas (#2564, #2646 and #2676), sorted after 2 days of *in vitro* competition in the presence (CT) or absence (CTRL) of 1μM CT99021. Columns represent average transcript levels of triplicates relative to BCR$^+$ CTRL, and normalized to the housekeeping gene RPLP0 (± SD).

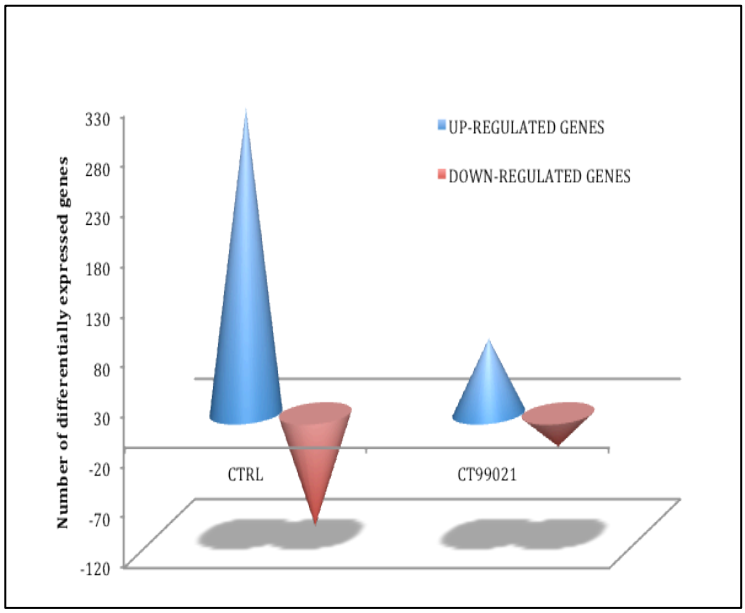

Figure 54: BCR controls target gene expression through GSK3β inhibition in λ-MYC lymphoma cells

Numbers of genes differentially expressed between BCR$^+$ and BCR$^-$ lymphoma cells, cultured in competition in the presence or absence (CTRL) of 1μM CT99021 inhibitor. Up- (blue) and down-regulated genes (red) in at least 2 independent tumors are displayed (*fold change:* ±1.5).

Affymetrix gene-chip analyses identified over 400 genes differentially expressed between BCR$^+$ and BCR$^-$ tumor cells in at least 2 out of 3 independent tumors (fold change ±1.5). In particular, 306 genes were up-regulated and 112 were down-regulated in BCR$^-$ lymphoma cells. Strikingly, almost 80% (237 among the up-regulated and 87 among the down-regulated genes) of differentially expressed genes

were normalized in BCR$^-$ lymphomas in response to the treatment with the GSK3β inhibitor CT99021 (Figure 54).

These results indicate that the BCR controls a core subset of 324 genes through GSK3β inhibition to sustain the survival and proliferation of c-MYC transformed B cells.

7.4.9.1 BCR target genes are enriched within particular categories of gene ontology

To gain insights into the relevance of BCR-regulated genes in the biology of λ-MYC B cell lymphomas, I performed gene set enrichment analysis (GEA) on genes that were either induced or repressed upon BCR loss (fold change ±1.5). As shown in Figure 55, programmed cell death was among the categories of biological processes most significantly enriched for genes up-regulated in BCR-deficient lymphoma cells (Figure 55, upper panel) (p<0.01).

The genes down-regulated in BCR-negative lymphoma cells were significantly (p<0.01) enriched in GO classes involved in lymphocyte differentiation and activation (Figure 55, bottom panel). Moreover, despite not reaching statistical significance, down-regulated genes were enriched in GO gene categories controlling cell-cycle progression. Altogether, these results suggest that the BCR plays a central role to support survival and proliferation of c-MYC transformed B cells through the inhibition of pro-apoptotic genes and the induction of cell-cycle genes. Moreover, BCR expression in lymphoma cells appears to control a B-cell program that sustains B-cell function.

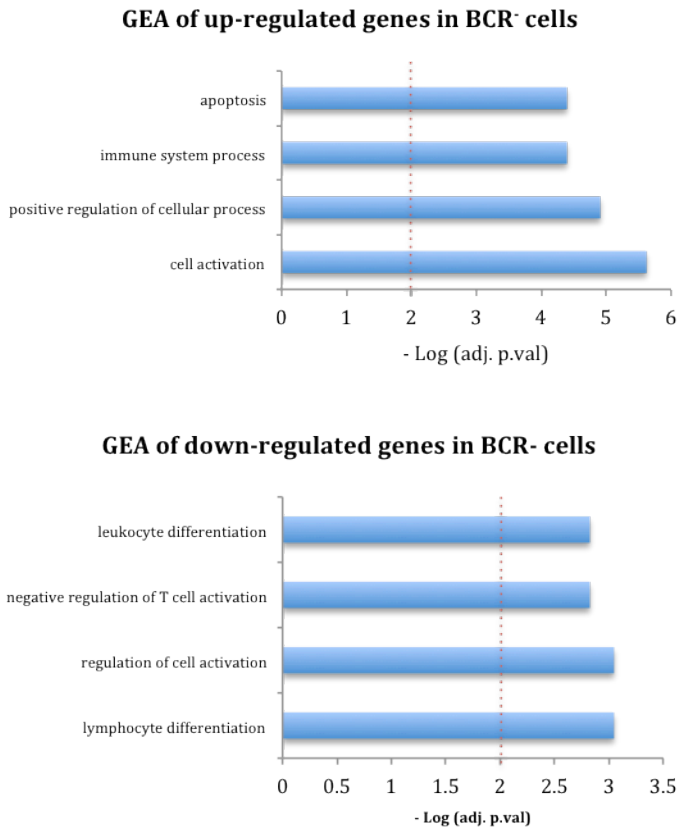

Figure 55: Gene set enrichment analysis of genes differentially expressed in BCR- lymphomas

Gene Set Enrichment analysis of up- (upper panel) and down-regulated (bottom panel) genes (fold change: ±1.5) upon BCR-deletion in at least two independent λ-MYC;B1-8f tumors.. Red dashed line indicates the threshold of significance (*p<0.01).*

7.4.9.2 BCR controls the expression of a subset of c-MYC target genes

We have shown that BCR expression limits the activity of GSK3β. GSK3β has been implicated in the phosphorylation of several substrates, including c-MYC. Phosphorylation by GSK3β of c-MYC on threonine-58, promotes its subsequent degradation through the proteasome machinery. Hence, the BCR, through the inhibition of GSK3β, may sustain c-MYC activity by preventing its degradation (Cohen and Frame, 2001). To test this hypothesis, I assessed whether genes differentially expressed between BCR^+ and BCR^- lymphoma cells were regulated by MYC. To this aim, I intersected the list of BCR-regulated genes in λ-MYC lymphomas, with a dataset of MYC ChIP-sequencing data of Eμ-MYC primary B cell lymphomas recently

generated by the group of B. Amati (European Institute of Oncology, Milan, personal communication). Importantly, BCR-regulated genes were significantly ($p<0.01$) enriched for MYC targets (70% of BCR regulated genes bound MYC, i.e. 292 out of 418 genes) (Figure 56). Both up- and down-regulated genes in BCR$^-$ lymphomas were significantly enriched for MYC binding. Interestingly, when we analyzed the subset of BCR-regulated genes, normalized in response to GSK3β inhibition (n=324), for MYC binding (n=227), only genes down-regulated in BCR$^-$ tumor cells (n=87) were significantly ($p<0.05$) enriched for MYC targets (n=60). This result points to a control exerted by the BCR on the ability of MYC to induce the expression of a core subset of its targets.

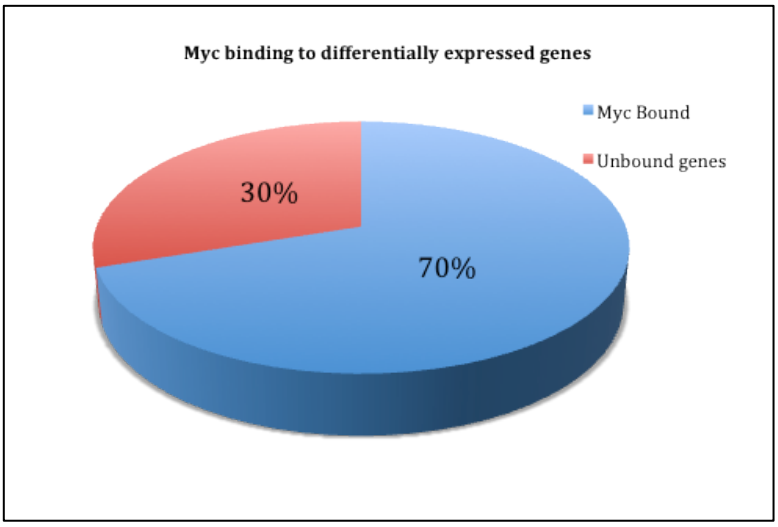

Figure 56: BCR controls the expression of a subset of MYC-targets

Pie chart representation of genes differentially expressed in BCR$^-$ lymphoma cells according to c-MYC binding status. Percentage of genes bound (blue) or not (red) by MYC is shown (*p-value*<0.01).

8 DISCUSSION

The B cell antigen receptor is required throughout B cell development, as both B cell precursors and mature B cells are under continuous selection for the expression of a functional, non auto-reactive BCR. Several genetic evidences over the course of the last 20 years support this concept. First, the failure to express a functional IgH chain in progenitor B cells was shown to prevent further development of the cells, thus establishing a B-cell lymphopenic condition (Kitamura and Rajewsky, 1992). Similar results were obtained through the disruption of other components of the pre-BCR/ BCR during early B-cell lymphopoiesis (Kitamura et al., 1992; Kraus et al., 2001). The development of conditional gene targeting approaches led subsequently to the demonstration that surface expression of the BCR complex is essential for the survival of resting mature B cells. (Kraus et al., 2004; Lam et al., 1997; Srinivasan et al., 2009). The requirement for a signal emanating from the BCR in mature B-cell survival was demonstrated with conditional inactivation of the BCR signalling effector, CD79a. (Kraus et al., 2004; Meffre and Nussenzweig, 2002). More recently, Srinivasan and colleagues have extended this work, revealing the central role of the PI3K signaling cascade in the transmission of the survival signal emanating from surface BCR (Srinivasan et al., 2009).

Several observations suggest that lymphomas and leukemias originating from mature B cells may also depend on expression and signalling competence of the BCR for survival and/or growth. Specifically:

1) The integrity of BCR components is preserved in most forms of mature of NH B-cell lymphomas and leukemia including BL, DLBCL, FL, MALT lymphomas and CLL.

2) Genetic analysis of Ig V-gene rearrangements in lymphoma B cells.

In particular:

a) Early work on BL cell lines and primary BL tumors have revealed that t(8;14) translocations involve almost exclusively the chromosome 14 bearing a germline/non-functional Ig V-gene, thereby preserving structural integrity and thus functional competence of the BCR in lymphoma cells (Cleary et al., 1986; de Jong et al., 1989; Meeker et al., 1985).

b) Analysis of the pattern of V-gene mutations in several types of NHL, including BL, FL and DLBCL have revealed a peculiar selection for replacement mutations accumulating within CDR regions. In contrast, framework regions (that are important to preserve structural integrity of the BCR) are mainly subjected to silencing mutations (Cleary et al., 1986). Furthermore, these results suggest the selection in lymphomas showing ongoing SHM, for subclones carrying improved BCR specificities.

c) Recent high throughput sequencing analyses in primary DLBCL have identified recurrent mutations in the gene coding for CD79a, an essential effector of BCR signalling in DLBCL cases (Davis et al., 2010). Importantly these mutations were found to mimic a constitutively activated BCR (Staudt, 2010). Similar approaches have allowed the recent identification in primary BL cases of genetic mutations affecting the transcription factor TCF3/E2A, which controls Ig gene transcription (Schmitz et al., 2012).

d) Work mainly performed by the group of Ron Levy has elucidated in the past 20 years the genetic basis for the acquired resistance of Follicular lymphoma B cells to the treatment with anti-BCR idiotype antibodies. The administration of anti-idiotype antibodies promoted the selection in FL patients of lymphoma subclones expressing "novel" BCRs (therefore confirming the need to express an antigen receptor) that escaped the treatment. Sequencing of the V-genes coding for the variable region of the "resistant" BCRs, revealed the presence of the original Ig V-

genes that had acquired few key mutations that escaped recognition by the anti-idiotype antibody (Meeker et al., 1985).

3) The role of antigen in triggering lymphoma B-cell survival and growth through the BCR has been suggested in several instances:

a. MALT lymphomas occurring in gastric mucosa of patients infected with Helicobacter Pylori are currently treated with antibiotics. In most cases, the eradication of the bacteria leads to a complete clinical remission. Similar observations have been provided for marginal zone B-cell malignancies affecting the ocular adnexae (Hermine et al., 2002; Wotherspoon et al., 1993).

b. Both Hodgkin and Non-Hodgkin B-cell lymphomas can develop in close association with chronic hepatitis caused by infection with Hepatitis-C Virus (HCV). Ig V-gene analysis of lymphoma B cells have revealed the selection for clones expressing unique BCRs, possibly reactive against specific viral antigens (Chan et al., 2001). Importantly, treatment of lymphoma cases associated to chronic HCV infection, with anti-viral drugs leads often to complete clinical remission.

c. Chronic Lymphocytic Leukemia is characterized by the slow outgrowth of B-cell clones expressing a limited, unique, subset of BCRs. These antigen receptors have been predicted to recognize common environmental antigens of microbial origin, possibly with some degree of cross-reactivity with self-antigens. An important recent study has contributed to shed light on the signaling property of stereotypic BCRs expressed by CLL cells. It was shown that BCRs expressed by CLL cells signal in a cell autonomous manner, in the absence of foreign antigen recognition. Instead the variable region of such BCRs recognizes an internal epitope present within all IgH chains thereby activating a downstream proliferative and survival signal (Duhren-von Minden et al., 2012).

What type of signal is delivered to B-lymphoma cells through the BCR?

Studies in Eμ-MYC lymphoma-prone mice expressing a BCR of known specificity (hen egg lysozyme) have revealed an active role of the BCR in supporting MYC-driven transformation, as a result of cognate antigen recognition (Refaeli et al., 2008). Whereas we cannot exclude a contribution of antigen to BCR-controlled growth of BL, our own study demonstrates that a "tonic", low-strength, BCR signal is sufficient, and most importantly, required for MYC-driven transformation.

In vitro studies performed on DLBCL lines have further contributed to our understanding of the signalling events active downstream of the BCR in these tumor cells. The identification of DLBCL lines sensitive to knock-down of proximal BCR signalling effectors including Cd79a, Cd79b and the kinases SYK and BTK, have proposed the existence of a "chronic" BCR signal supporting the *in vitro* growth of lymphoma cells through the downstream activation of the NF-κB transcription factors (Davis et al., 2010). Interestingly, the high sensitivity of DLBCL cells to the down regulation of effectors of BCR signalling was preferentially observed among tumor lines representing the more aggressive Activated B-Cell (ABC) type of DLBCL (Davis et al., 2010). The precise nature of the so-called "chronic" B cell signal measured *in vitro* in ABC DLBCL lines remains still to be fully elucidated. The latter signal is clearly distinct from the tonic signal emanating from the BCR that is required to sustain the survival of resting B cell, as the latter does not involve the activation of the NF-κB pathway (Srinivasan et al., 2009; Thome, 2004).

The studies listed above share several limitations including the analysis of *in vitro* cell line systems or transgenic tumor-prone lines engineered to express high-affinity BCR. Moreover, possible off-targets effects limit the interpretation of the data obtained

with the use of shRNAs. Finally the specificity of small molecule inhibitors directed against BCR effectors cannot always be experimentally validated.

With the present work, I have tried to overcome the above listed limitations. Using a genetic approach, I have addressed the contribution of the BCR in the λ-MYC model of Burkitt lymphoma. λ-MYC transgenic B cells were engineered to carry a loxP-flanked pre-rearranged V_H gene (B1-8f). This strategy enabled me to inactivate BCR expression in established BL cells by means of the Cre/loxP recombination system.

Using this approach, I provided evidence that the BCR plays an essential role in controlling the survival and proliferation of established BL both *in vitro* and *in vivo*. BCR^- BL cells, generated either by Cre-mediated recombination of λ-MYC;B1-8f mouse transgenic tumor cells, or spontaneously from the human BL cell line RAMOS (possibly due to BCR crippling mutations caused by ongoing SHM (Sale and Neuberger, 1998), were rapidly counter selected *in vitro* by their BCR^+ counterparts. In accordance with these results, competitive transplantation assays of BCR^+ and BCR^- mouse BL cells into syngeneic recipients led to the preferential outgrowth of the BCR^+ tumor subset. Surprisingly, the loss of BCR^- lymphomas was strictly dependent on the concomitant presence of their BCR^+ counterparts, as purified BCR^- tumor cells were able to expand indefinitely *in vitro* and give rise to secondary tumors *in vivo* (although with a longer latency) when grown in the absence of their BCR^+ counterparts. The presence of BCR^+ BL cells influenced the proliferation of the BCR^- counterparts, as revealed by their delay in the G_1-to-S transition of the cell-cycle. Moreover, the presence of BCR^+ BL cells rendered their BCR-deficient counterparts more prone to undergo apoptosis both in the mouse (λ-MYC;B1-8f) and human (RAMOS) system.

Importantly, complementation of BCR^- tumor cells with a novel antigen receptor promptly rescued the failure of these cells to expand *in vitro* and *in vivo* under

competitive conditions, excluding thereby the existence of additional genetic alterations contributing to the disappearance of such cells.

The biochemical analysis of proximal signalling events (phosphorylation of the Syk kinase) triggered by the antigen receptor in λ-MYC BL cells, revealed a signal of weak intensity, resembling that of small resting mature B cells. This result is compatible with a scenario whereby the basal signal emanating from BCR represents a key permissive factor to sustain survival and growth of BL cells under competitive conditions.

To investigate the contribution of the BCR to BL biology, in collaboration with the group of Dr. Bonaldi (European Institute of Oncology), we performed a quantitative proteome analysis of λ-MYC BL cells respectively before and after BCR inactivation. This experiment, the first of its kind, allowed us to quantify over 4000 proteins of which around 5% were influenced by BCR expression. A large fraction of enzymes involved in glucose metabolism were down regulated in BCR-less lymphomas, with an average 10 to 20% reduction in protein levels, that resulted statistical significant.

Tumor cells, especially MYC-transformed cells, rewire their metabolism to ensure a steady supply of metabolites to sustain the heightened anabolism, as well as for the generation of ATP. This energetic adaptation is achieved through a metabolic switch from mitochondrial respiration to a massive aerobic glycolysis, a phenomenon also known as the Warburg effect (Warburg, 1956). Consequently, the apparently modest down-modulation of the glycolytic pathway may represent a key limiting factor for the growth of BCR-less tumor cells in the presence of their BCR^+ counterparts especially under conditions of nutrient deprivation. This hypothesis was confirmed by the accelerated loss of BCR^- BL cells when BCR^+/BCR^- tumor mixtures were cultured under conditions of limited growth factor and nutrient availability, such as those achieved in serum starvation assays, or when the same tumor mixtures were

treated with Rapamycin, a specific inhibitor of the nutrient-sensitive mTOR pathway (Peng et al., 2002). At the same time, I excluded a specific defect of BCR^- tumor cells respectively in glucose uptake, LDH activity or mitochondrial respiration (however the latter two assays could not be performed under competitive conditions).

Whereas increased glucose metabolism is essential to sustain the bioenergetic needs of cancer cells, it is now becoming clear that tumor cells with a high proliferation rate (such as MYC-transformed cells) require additional supplies of biosynthetic precursors, such as glutamine, to sustain their energetic and anabolic processes. (DeBerardinis et al., 2008; DeBerardinis et al., 2007; Yuneva et al., 2007). Future experiments will reveal whether the BCR can influence the rate of glutaminolysis in c-MYC transformed B-lymphoma cells.

The use of small molecule inhibitors allowed me to identify GSK3β as an essential modulator of the survival signal triggered in BL cells by the BCR. In support of this, I observed reduced levels of the phosphorylated, inactive, form of GSK3β in BCR^- lymphomas. Synthetic inhibition of GSK3β prevented the counter selection of BCR-deficient lymphoma cells in the presence of their BCR^+ counterparts. The rescue of BCR^- lymphomas resulted from the normalization of cell cycle progression and acquired resistance to apoptosis. These data indicate that heightened GSK3β activity in BCR^- tumor cells, likely resulting from impaired PI3K activity, is the primary cause for theirs preferential loss when grown in competition with BCR^+ tumors.

GSK3β phosphorylates a variety of substrates participating to important signalling pathways that respond to environmental signals, such as growth factors, nutrients and other soluble factors including cytokines (Cohen and Frame, 2001).

GSK3β inhibits cell cycle progression and thus interferes with cell proliferation by controlling the stability of cyclin E (CcnE) and cyclin D1 (CcnD1) proteins (Xu et al.,

2009). Thus, through the inhibition of GSK3β activity, the BCR may facilitate cell cycle progression in lymphoma B cells stabilizing respectively D-type and E cyclins.

Another attractive target of GSK3β is MYC itself (Adhikary and Eilers, 2005). GSK3β phosphorylation of c-MYC on threonine-58 leads to c-MYC ubiquitylation by SCF^{Fbw7}, followed by proteosomal degradation (Adhikary and Eilers, 2005). Elegant work in Drosophila has unraveled a cell competition system regulated by c-MYC protein levels. Larval cells expressing higher dMYC levels could rapidly outcompete neighboring cells, expressing lower dMYC levels (Rhiner et al., 2010). Could BCR loss influence MYC levels (and thereby its biological function) to ultimately limit the growth of BCR-less tumor cells? I failed to observe major changes in total MYC protein levels in response to BCR inactivation. I am however aware of the relatively low sensitivity of immunoblotting analyses that may not allow the detection of subtle, yet biologically relevant, changes in MYC protein levels. I therefore decided to tackle this question measuring the effects of BCR loss on the gene expression profile of tumor cells, pointing our attention primarily to the levels of putative MYC target genes. Gene chip microarray analysis performed on three independent BL tumors identified more than 400 genes differentially expressed between BCR^+ and BCR^- tumor cells. BCR-regulated transcripts fell primarily within gene ontology categories controlling cell survival and apoptosis. Importantly, the vast majority of differentially expressed genes were normalized by the treatment of lymphoma cells with the GSK3β small molecule inhibitor, confirming the central role exerted by this kinase in the modulation of BCR-dependent gene transcription.

In collaboration with the group of B. Amati that provided us with chromatin immunoprecipitation data on the status of MYC-binding (established in Eμ-MYC lymphomas) to genes differentially expressed between BCR^+ and BCR^- lymphomas, we recognized that most of the BCR controlled genes were indeed bound by c-MYC.

These yet preliminary observations point to a possible regulation of the BCR on c-MYC function, through the inactivation of GSK3β activity in c-MYC transformed B cells. We are currently testing this possibility by chromatin immunoprecipitation assays performed on specific genes (ChIP-qPCR), and eventually extended at genome wide level (ChIP-seq). This approach will reveal the degree to which BCR expression controls MYC transcriptional activity in MYC-transformed B lymphoma cells. Finally, complementation of BCR-deficient tumor cells with a Threonine-58 mutant isoform of MYC, resistant to GSK3β induced degradation, will further demonstrate the stabilization of MYC through the BCR-GSK3β axis, and the involvement of MYC in the control of survival of transformed mature B cells.

In the past year, a series of relevant studies have improved our understanding on the genetics of BL. Work performed by the Rajewsky group have attempted to reconstruct BL in the mouse through the complementation of GC B cells with genes that are recurrently deregulated in hBL. Interestingly (and surprisingly), c-MYC deregulation induced in GC B cells was not sufficient to trigger BL. Instead, clonal outgrowth of B-cells resembling BL were observed only upon concomitant induction of deregulated c-MYC and activation of the PI3K pathway (Sander et al., 2012). Tumor B cells generated in compound mutant mice resembled closely hBL based on immunophenotype, histological appearance, gene expression profile and most importantly germinal center origin (Sander et al., 2012). These results highlight the central role exerted by the PI3K pathway in BL pathogenesis. The requirement for the PI3K signaling pathway to support BCR-mediated survival of mature B cells (Srinivasan et al., 2009) suggests a direct contribution of the BCR to BL pathogenesis.

This scenario is further supported by recent high-throughput RNA sequencing efforts performed on sporadic BL by the Staudt group. In this study, authors identified the transcription factor TCF3/E2A as frequently mutated in BL cells. TCF3 mutations

found in tumor cells altered its transcriptional activity. In accordance with a central role of TCF3 in BL pathogenesis, bi-allelic inactivating mutations in the TCF3 inhibitor ID3 were readily identified in BL cells. Deregulated TCF3 activity was associated to increased expression of Ig genes, suggesting a possible contribution of altered TCF3 activity to the enforcement of BCR function. Importantly, *in vitro* knock-down of proximal BCR signaling components (CD79a and SYK), resulted in impaired activation of the PI3K pathway and ultimately in the death of BL cell lines (Schmitz et al., 2012). Altogether these results are consistent with our own findings and confirm the central role of the BCR in sustaining the growth of BL cells. Importantly, our work implements the current understanding of the role of the BCR in BL pathogenesis identifying GSK3β as an essential downstream target of the PI3K pathway.

Interestingly, the Rajewsky group reported that mouse BL identified in c-MYC/PI3K conditional transgenic mice retained surface BCR expression (Sander et al., 2012). This result thus suggests possible additional, PI3K-independent, contributions of the BCR to BL pathogenesis.

Results from RNA sequencing efforts on hBL that were later confirmed in the c-MYC/PI3K BL mouse model identified recurrent mutations stabilizing Cyclin D_3. This result highlights the relevance of the germinal center origin of BL as Cyclin-D_3 is the main D-type cyclin expressed by these cells. It remains to be investigated why BL cells select mutations stabilizing Cyclin D_3, as MYC expression is predicted to induce other D-type cyclins that are functionally redundant with Cyclin D_3 (Musgrove et al., 2011). The importance in the regulation of G_1-to-S transition in BL cells is in accordance with our own data showing a delay in cell cycle progression of λ-MYC lymphomas as a result of Cyclin E down-regulation. The ability of the BCR to regulate G_1-type cyclins in the λ-MYC BL model revealed by our study warrants further investigations in hBL.

Schmitz and colleagues have also proposed a role for the PI3K pathway in the control the mTOR axis, to ultimately sustain BL growth. Indeed, most BL cell lines showed constitutive phosphorylation of the mTOR substrate, S6 kinase, which was reduced in response to pharmacological inhibition of PI3K. Importantly, BL lines were highly sensitive to Rapamycin indicating a strict dependence of the tumor cells on the mTOR pathway. Interestingly, this effect was also observed in BL lines that did not depend on BCR signals (Schmitz et al., 2012). Our work integrates and complements the above findings. Indeed, we could show that loss of antigen receptor expression rendered c-MYC transformed B cells particularly sensitive to Rapamycin treatment and thus preferentially dependent on the mTOR pathway. This condition led to acceleration in the counter selection of BCR^- lymphomas when grown in competition with their BCR^+ counterparts.

Based on published work and our own results, we would like to propose a model whereby BL cells depend critically on two independent pathways for their growth. The first is the BCR/PI3K pathway that is required to inhibit the activity of GSK3β facilitating the stabilization of the c-MYC oncoprotein. In the absence of BCR expression, BL cells become strictly dependent on the second main pathway supporting tumor growth centered on the nutrient-sensitive mTOR axis.

This model predicts that BL cells are able to sustain their growth through constitutive activation of the mTOR pathway as long as nutrients are unlimited. In conditions of nutrient restrictions, such as those found in lymphomas with a high proliferation rate, tonic BCR signalling may represent a crucial determinant to sustain tumor growth through the activation of the PI3K pathway, which will sustain both mTOR activation and GSK3 inhibition.

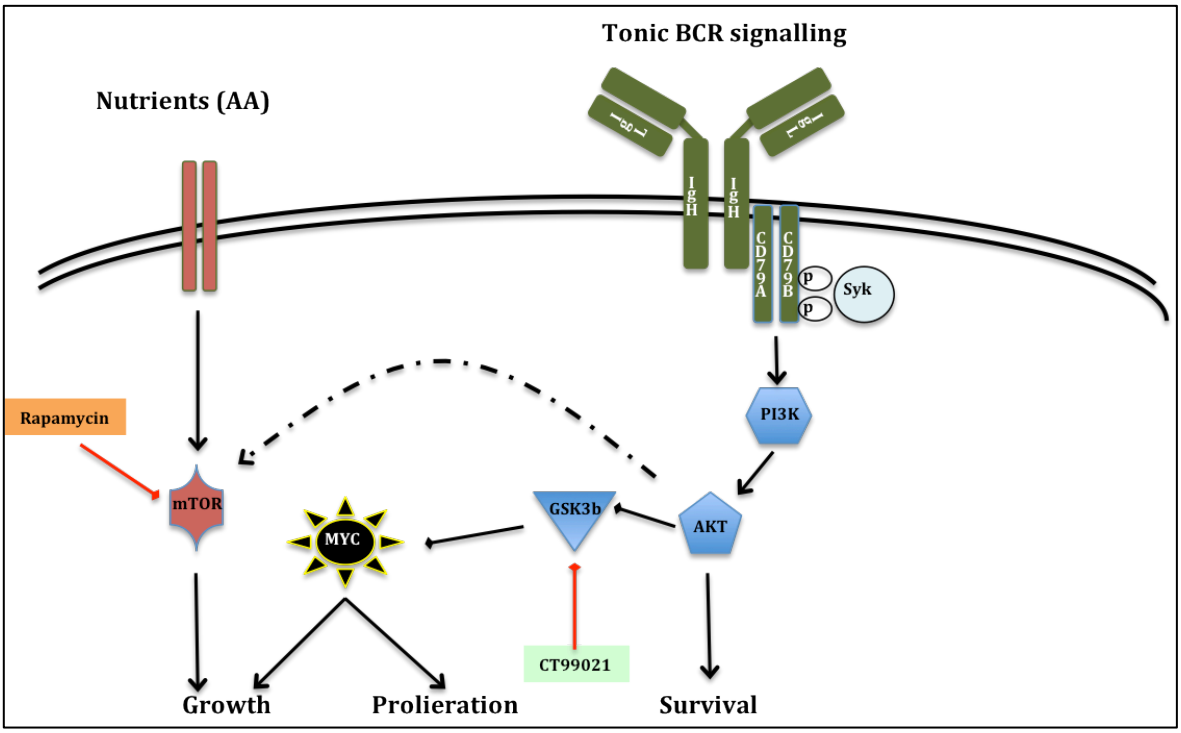

Figure 57: Pathways controlled by the BCR to sustain BL proliferation and survival

Model revealing the main pathways regulated by the BCR to support the growth of c-MYC transformed B cells. The BCR complex is depicted in green; amino acid\nutrient-sensitive receptors are depicted in red. Dashed line indicates a possible regulation of mTOR by BCR-dependent PI3K/Akt activity.

Altogether my results provide experimental evidence for an essential role of the BCR in the pathogenesis of BL. BCR signalling competence may exert its function at multiple stages of BL pathogenesis. During tumor initiation, the expression of a functional BCR is required to sustain the survival of GC B cells that acquire the t(8:14) translocation. This is confirmed by the selection, among BL precursors, of cells carrying a MYC translocation involving almost exclusively the non-functional IgH chromosome. Continuous BCR expression is then expected to sustain the survival of t(8:14) bearing BL precursors until additional mutations have been selected to give rise to a clonal malignancy. Finally, as BL cells, the continuous expression of the BCR will provide a selective growth advantage, especially under conditions of limited nutrient supply. This scenario is indeed compatible with the continuous elimination

from the tumor mass of BCR-deficient lymphoma cells generated by ongoing SHM, through the acquisition of Ig crippling mutations.

Our study has implications for the therapy of Burkitt lymphoma and possibly other mature B-cell malignancies expressing a functional BCR. Small molecule inhibitors of proximal BCR signalling components are predicted to contribute to the efficacy of current chemotherapeutic protocols used to treat aggressive forms of NHL including BL, as recently suggested (Chen et al., 2008; Honigberg et al., 2010; Young et al., 2009).

At the same time, our study provides a warning for future monotherapies based exclusively on inhibitors of BCR signalling. Indeed, these conditions are likely to promote the outgrowth of BCR-deficient lymphomas that would otherwise never be identified due to their rapid counter selection. To avoid this outcome, based on our results in the λ-MYC model, we propose a combinatorial treatment based on BCR inhibitors coupled to Rapamycin against which BCR-less lymphomas have shown a preferential sensitivity.

REFERENCES

Adams, J. M., Harris, A. W., Pinkert, C. A., Corcoran, L. M., Alexander, W. S., Cory, S., Palmiter, R. D., and Brinster, R. L. (1985). The c-myc oncogene driven by immunoglobulin enhancers induces lymphoid malignancy in transgenic mice. Nature *318*, 533-538.

Adhikary, S., and Eilers, M. (2005). Transcriptional regulation and transformation by Myc proteins. Nature reviews Molecular cell biology *6*, 635-645.

Aiba, Y., Kameyama, M., Yamazaki, T., Tedder, T. F., and Kurosaki, T. (2008). Regulation of B-cell development by BCAP and CD19 through their binding to phosphoinositide 3-kinase. Blood *111*, 1497-1503.

Akamine, R., Yamamoto, T., Watanabe, M., Yamazaki, N., Kataoka, M., Ishikawa, M., Ooie, T., Baba, Y., and Shinohara, Y. (2007). Usefulness of the 5' region of the cDNA encoding acidic ribosomal phosphoprotein P0 conserved among rats, mice, and humans as a standard probe for gene expression analysis in different tissues and animal species. J Biochem Biophys Methods *70*, 481-486.

Albihn, A., Johnsen, J. I., and Henriksson, M. A. (2010). MYC in oncogenesis and as a target for cancer therapies. Adv Cancer Res *107*, 163-224.

Alizadeh, A. A., Eisen, M. B., Davis, R. E., Ma, C., Lossos, I. S., Rosenwald, A., Boldrick, J. C., Sabet, H., Tran, T., Yu, X.*, et al.* (2000). Distinct types of diffuse large B-cell lymphoma identified by gene expression profiling. Nature *403*, 503-511.

Allen, C. D., Okada, T., Tang, H. L., and Cyster, J. G. (2007). Imaging of germinal center selection events during affinity maturation. Science *315*, 528-531.

Allman, D., Dalod, M., Asselin-Paturel, C., Delale, T., Robbins, S. H., Trinchieri, G., Biron, C. A., Kastner, P., and Chan, S. (2006). Ikaros is required for plasmacytoid dendritic cell differentiation. Blood *108*, 4025-4034.

Allman, D. M., Ferguson, S. E., Lentz, V. M., and Cancro, M. P. (1993). Peripheral B cell maturation. II. Heat-stable antigen(hi) splenic B cells are an immature developmental intermediate in the production of long-lived marrow-derived B cells. J Immunol *151*, 4431-4444.

Alt, F. W., Yancopoulos, G. D., Blackwell, T. K., Wood, C., Thomas, E., Boss, M., Coffman, R., Rosenberg, N., Tonegawa, S., and Baltimore, D. (1984). Ordered rearrangement of immunoglobulin heavy chain variable region segments. Embo J *3*, 1209-1219.

Amati, B., Brooks, M. W., Levy, N., Littlewood, T. D., Evan, G. I., and Land, H. (1993). Oncogenic activity of the c-Myc protein requires dimerization with Max. Cell *72*, 233-245.

Amati, B., Dalton, S., Brooks, M. W., Littlewood, T. D., Evan, G. I., and Land, H. (1992). Transcriptional activation by the human c-Myc oncoprotein in yeast requires interaction with Max. Nature *359*, 423-426.

Avet-Loiseau, H., Li, J. Y., Facon, T., Brigaudeau, C., Morineau, N., Maloisel, F., Rapp, M. J., Talmant, P., Trimoreau, F., Jaccard, A.*, et al.* (1998). High incidence of translocations t(11;14)(q13;q32) and t(4;14)(p16;q32) in patients with plasma cell malignancies. Cancer Res *58*, 5640-5645.

Bahram, F., von der Lehr, N., Cetinkaya, C., and Larsson, L. G. (2000). c-Myc hot spot mutations in lymphomas result in inefficient ubiquitination and decreased proteasome-mediated turnover. Blood *95*, 2104-2110.

Bannish, G., Fuentes-Panana, E. M., Cambier, J. C., Pear, W. S., and Monroe, J. G. (2001). Ligand-independent signaling functions for the B lymphocyte antigen receptor and their role in positive selection during B lymphopoiesis. The Journal of experimental medicine *194*, 1583-1596.

Baron, B. W., Nucifora, G., McCabe, N., Espinosa, R., 3rd, Le Beau, M. M., and McKeithan, T. W. (1993). Identification of the gene associated with the recurring chromosomal translocations t(3;14)(q27;q32) and t(3;22)(q27;q11) in B-cell lymphomas. Proc Natl Acad Sci U S A *90*, 5262-5266.

Blackwood, E. M., Lugo, T. G., Kretzner, L., King, M. W., Street, A. J., Witte, O. N., and Eisenman, R. N. (1994). Functional analysis of the AUG- and CUG-initiated forms of the c-Myc protein. Mol Biol Cell *5*, 597-609.

Blum, K. A., Lozanski, G., and Byrd, J. C. (2004). Adult Burkitt leukemia and lymphoma. Blood *104*, 3009-3020.

Boffetta, P. (2011). Epidemiology of adult non-Hodgkin lymphoma. Ann Oncol *22*, iv27–iv31.

Bottaro, A., Lansford, R., Xu, L., Zhang, J., Rothman, P., and Alt, F. W. (1994). S region transcription per se promotes basal IgE class switch recombination but additional factors regulate the efficiency of the process. Embo J *13*, 665-674.

Braeuninger, A., Kuppers, R., Strickler, J. G., Wacker, H. H., Rajewsky, K., and Hansmann, M. L. (1997). Hodgkin and Reed-Sternberg cells in lymphocyte predominant Hodgkin disease represent clonal populations of germinal center-derived tumor B cells. Proceedings of the National Academy of Sciences of the United States of America *94*, 9337-9342.

Brezski, R. J., and Monroe, J. G. (2008). B-cell receptor. In Advances in experimental medicine and biology, pp. 12-21.

Brooks, T. A., and Hurley, L. H. (2010). Targeting MYC Expression through G-Quadruplexes. Genes Cancer *1*, 641-649.

Brown, G. C. (1992). Control of respiration and ATP synthesis in mammalian mitochondria and cells. Biochem J *284 (Pt 1)*, 1-13.

Burkitt, D. (1958). A sarcoma involving the jaws in African children. Br J Surg *46*, 218-223.

Burkitt, D. (1962). A lymphoma syndrome in African children. Ann R Coll Surg Engl *30*, 211-219.

Casola, S., Otipoby, K. L., Alimzhanov, M., Humme, S., Uyttersprot, N., Kutok, J. L., Carroll, M. C., and Rajewsky, K. (2004). B cell receptor signal strength determines B cell fate. Nature immunology *5*, 317-327.

Chan, C. H., Hadlock, K. G., Foung, S. K., and Levy, S. (2001). V(H)1-69 gene is preferentially used by hepatitis C virus-associated B cell lymphomas and by normal B cells responding to the E2 viral antigen. Blood *97*, 1023-1026.

Chance, B., and Williams, G. R. (1956). The respiratory chain and oxidative phosphorylation. Adv Enzymol Relat Subj Biochem *17*, 65-134.

Chang, T. C., Yu, D., Lee, Y. S., Wentzel, E. A., Arking, D. E., West, K. M., Dang, C. V., Thomas-Tikhonenko, A., and Mendell, J. T. (2008). Widespread microRNA repression by Myc contributes to tumorigenesis. Nature genetics *40*, 43-50.

Chapman, C. J., Zhou, J. X., Gregory, C., Rickinson, A. B., and Stevenson, F. K. (1996). VH and VL gene analysis in sporadic Burkitt's lymphoma shows somatic hypermutation, intraclonal heterogeneity, and a role for antigen selection. Blood *88*, 3562-3568.

Chen, L., Monti, S., Juszczynski, P., Daley, J., Chen, W., Witzig, T. E., Habermann, T. M., Kutok, J. L., and Shipp, M. A. (2008). SYK-dependent tonic B-cell receptor signaling is a rational treatment target in diffuse large B-cell lymphoma. Blood *111*, 2230-2237.

Christoffersen, N. R., Shalgi, R., Frankel, L. B., Leucci, E., Lees, M., Klausen, M., Pilpel, Y., Nielsen, F. C., Oren, M., and Lund, A. H. (2010). p53-independent upregulation of miR-34a during oncogene-induced senescence represses MYC. Cell Death Differ *17*, 236-245.

Cleary, M. L., Meeker, T. C., Levy, S., Lee, E., Trela, M., Sklar, J., and Levy, R. (1986). Clustering of extensive somatic mutations in the variable region of an immunoglobulin heavy chain gene from a human B cell lymphoma. Cell *44*, 97-106.

Coffer, P. J., and Burgering, B. M. (2004). Forkhead-box transcription factors and their role in the immune system. Nature reviews Immunology *4*, 889-899.

Cohen, P., and Frame, S. (2001). The renaissance of GSK3. Nature reviews Molecular cell biology *2*, 769-776.

Cole, M. D., and Cowling, V. H. (2008). Transcription-independent functions of MYC: regulation of translation and DNA replication. Nature reviews Molecular cell biology *9*, 810-815.

Cox, J., and Mann, M. (2008). MaxQuant enables high peptide identification rates, individualized p.p.b.-range mass accuracies and proteome-wide protein quantification. Nature biotechnology *26*, 1367-1372.

Cox, J., Neuhauser, N., Michalski, A., Scheltema, R. A., Olsen, J. V., and Mann, M. (2011). Andromeda: a peptide search engine integrated into the MaxQuant environment. J Proteome Res *10*, 1794-1805.

Cyster, J. G. (2010). B cell follicles and antigen encounters of the third kind. Nature immunology *11*, 989-996.

Dalla-Favera, R., Bregni, M., Erikson, J., Patterson, D., Gallo, R. C., and Croce, C. M. (1982). Human c-myc onc gene is located on the region of chromosome 8 that is translocated in Burkitt lymphoma cells. Proc Natl Acad Sci U S A *79*, 7824-7827.

Davis, R. E., Ngo, V. N., Lenz, G., Tolar, P., Young, R. M., Romesser, P. B., Kohlhammer, H., Lamy, L., Zhao, H., Yang, Y.*, et al.* (2010). Chronic active B-cell-receptor signalling in diffuse large B-cell lymphoma. Nature *463*, 88-92.

de Jong, D., Voetdijk, B. M., Van Ommen, G. J., Kluin-Nelemans, J. C., Beverstock, G. C., and Kluin, P. M. (1989). Translocation t(14;18) in B cell lymphomas as a cause for defective immunoglobulin production. The Journal of experimental medicine *169*, 613-624.

Deane, J. A., and Fruman, D. A. (2004). Phosphoinositide 3-kinase: diverse roles in immune cell activation. Annual review of immunology *22*, 563-598.

DeBerardinis, R. J., Lum, J. J., Hatzivassiliou, G., and Thompson, C. B. (2008). The biology of cancer: metabolic reprogramming fuels cell growth and proliferation. Cell metabolism *7*, 11-20.

DeBerardinis, R. J., Mancuso, A., Daikhin, E., Nissim, I., Yudkoff, M., Wehrli, S., and Thompson, C. B. (2007). Beyond aerobic glycolysis: transformed cells can engage in glutamine metabolism that exceeds the requirement for protein and nucleotide synthesis. Proceedings of the National Academy of Sciences of the United States of America *104*, 19345-19350.

Dengler, H. S., Baracho, G. V., Omori, S. A., Bruckner, S., Arden, K. C., Castrillon, D. H., DePinho, R. A., and Rickert, R. C. (2008). Distinct functions for the transcription factor Foxo1 at various stages of B cell differentiation. Nature immunology *9*, 1388-1398.

Di Noia, J., and Neuberger, M. S. (2002). Altering the pathway of immunoglobulin hypermutation by inhibiting uracil-DNA glycosylase. Nature *419*, 43-48.

Di Noia, J. M., and Neuberger, M. S. (2007). Molecular mechanisms of antibody somatic hypermutation. Annu Rev Biochem *76*, 1-22.

Dominguez-Sola, D., Ying, C. Y., Grandori, C., Ruggiero, L., Chen, B., Li, M., Galloway, D. A., Gu, W., Gautier, J., and Dalla-Favera, R. (2007). Non-transcriptional control of DNA replication by c-Myc. Nature *448*, 445-451.

Dong, C., Davis, R. J., and Flavell, R. A. (2002). MAP kinases in the immune response. Annual review of immunology *20*, 55-72.

Duhren-von Minden, M., Ubelhart, R., Schneider, D., Wossning, T., Bach, M. P., Buchner, M., Hofmann, D., Surova, E., Follo, M., Kohler, F.*, et al.* (2012). Chronic lymphocytic leukaemia is driven by antigen-independent cell-autonomous signalling. Nature *489*, 309-312.

Durrieu, F., Belloc, F., Lacoste, L., Dumain, P., Chabrol, J., Dachary-Prigent, J., Morjani, H., Boisseau, M. R., Reiffers, J., Bernard, P., and Lacombe, F. (1998). Caspase activation is an early event in anthracycline-induced apoptosis and allows detection of apoptotic cells before they are ingested by phagocytes. Exp Cell Res *240*, 165-175.

Eilers, M., and Eisenman, R. N. (2008). Myc's broad reach. Genes & development *22*, 2755-2766.

Foon, K. A., Takeshita, K., and Zinzani, P. L. (2012). Novel therapies for aggressive B-cell lymphoma. Adv Hematol *2012*, 302570.

Fulop, G., Gordon, J., and Osmond, D. G. (1983). Regulation of lymphocyte production in the bone marrow. I. Turnover of small lymphocytes in mice depleted of B lymphocytes by treatment with anti-IgM antibodies. J Immunol *130*, 644-648.

Gabrea, A., Bergsagel, P. L., Chesi, M., Shou, Y., and Kuehl, W. M. (1999). Insertion of excised IgH switch sequences causes overexpression of cyclin D1 in a myeloma tumor cell. Mol Cell *3*, 119-123.

Gautier, L., Cope, L., Bolstad, B. M., and Irizarry, R. A. (2004). affy--analysis of Affymetrix GeneChip data at the probe level. Bioinformatics *20*, 307-315.

Goodnow, C. C., Crosbie, J., Adelstein, S., Lavoie, T. B., Smith-Gill, S. J., Brink, R. A., Pritchard-Briscoe, H., Wotherspoon, J. S., Loblay, R. H., Raphael, K., and et al. (1988). Altered immunoglobulin expression and functional silencing of self-reactive B lymphocytes in transgenic mice. Nature *334*, 676-682.

Grande, S. M., Bannish, G., Fuentes-Panana, E. M., Katz, E., and Monroe, J. G. (2007). Tonic B-cell and viral ITAM signaling: context is everything. Immunological reviews *218*, 214-234.

Gregory, M. A., and Hann, S. R. (2000). c-Myc proteolysis by the ubiquitin-proteasome pathway: stabilization of c-Myc in Burkitt's lymphoma cells. Molecular and cellular biology *20*, 2423-2435.

Gregory, M. A., Qi, Y., and Hann, S. R. (2003). Phosphorylation by glycogen synthase kinase-3 controls c-myc proteolysis and subnuclear localization. J Biol Chem *278*, 51606-51612.

Hann, S. R., King, M. W., Bentley, D. L., Anderson, C. W., and Eisenman, R. N. (1988). A non-AUG translational initiation in c-myc exon 1 generates an N-terminally distinct protein whose synthesis is disrupted in Burkitt's lymphomas. Cell *52*, 185-195.

Hao, Z., and Rajewsky, K. (2001). Homeostasis of peripheral B cells in the absence of B cell influx from the bone marrow. The Journal of experimental medicine *194*, 1151-1164.

Hardy, R. R., and Hayakawa, K. (2001). B cell development pathways. Annual review of immunology *19*, 595-621.

Harriman, G. R., Bradley, A., Das, S., Rogers-Fani, P., and Davis, A. C. (1996). IgA class switch in I alpha exon-deficient mice. Role of germline transcription in class switch recombination. J Clin Invest *97*, 477-485.

Hecht, J. L., and Aster, J. C. (2000a). Molecular biology of Burkitt's lymphoma. J Clin Oncol *18*, 3707-3721.

Hermine, O., Lefrere, F., Bronowicki, J. P., Mariette, X., Jondeau, K., Eclache-Saudreau, V., Delmas, B., Valensi, F., Cacoub, P., Brechot, C.*, et al.* (2002). Regression of splenic lymphoma with villous lymphocytes after treatment of hepatitis C virus infection. N Engl J Med *347*, 89-94.

Herzog, S., Hug, E., Meixlsperger, S., Paik, J. H., DePinho, R. A., Reth, M., and Jumaa, H. (2008). SLP-65 regulates immunoglobulin light chain gene recombination through the PI(3)K-PKB-Foxo pathway. Nature immunology *9*, 623-631.

Higashi, A. Y., Ikawa, T., Muramatsu, M., Economides, A. N., Niwa, A., Okuda, T., Murphy, A. J., Rojas, J., Heike, T., Nakahata, T.*, et al.* (2009). Direct hematological toxicity and illegitimate chromosomal recombination caused by the systemic activation of CreERT2. J Immunol *182*, 5633-5640.

Honigberg, L. A., Smith, A. M., Sirisawad, M., Verner, E., Loury, D., Chang, B., Li, S., Pan, Z., Thamm, D. H., Miller, R. A., and Buggy, J. J. (2010). The Bruton tyrosine kinase inhibitor PCI-32765 blocks B-cell activation and is efficacious in models of autoimmune disease and B-cell malignancy. Proceedings of the National Academy of Sciences of the United States of America *107*, 13075-13080.

Honjo, T., Kinoshita, K., and Muramatsu, M. (2002). Molecular mechanism of class switch recombination: linkage with somatic hypermutation. Annual review of immunology *20*, 165-196.

Hubner, N. C., Ren, S., and Mann, M. (2008). Peptide separation with immobilized pI strips is an attractive alternative to in-gel protein digestion for proteome analysis. Proteomics *8*, 4862-4872.

Hurley, L. H., Von Hoff, D. D., Siddiqui-Jain, A., and Yang, D. (2006). Drug targeting of the c-MYC promoter to repress gene expression via a G-quadruplex silencer element. Semin Oncol *33*, 498-512.

Iwasato, T., Shimizu, A., Honjo, T., and Yamagishi, H. (1990). Circular DNA is excised by immunoglobulin class switch recombination. Cell *62*, 143-149.

Jaffe, E. S., and Pittaluga, S. (2011). Aggressive B-cell lymphomas: a review of new and old entities in the WHO classification. Hematology Am Soc Hematol Educ Program *2011*, 506-514.

Jager, U., Bocskor, S., Le, T., Mitterbauer, G., Bolz, I., Chott, A., Kneba, M., Mannhalter, C., and Nadel, B. (2000). Follicular lymphomas' BCL-2/IgH junctions contain templated nucleotide insertions: novel insights into the mechanism of t(14;18) translocation. Blood *95*, 3520-3529.

Joshi, S. K., Hashimoto, K., and Koni, P. A. (2002). Induced DNA recombination by Cre recombinase protein transduction. Genesis *33*, 48-54.

Jun, J. E., and Goodnow, C. C. (2003). Scaffolding of antigen receptors for immunogenic versus tolerogenic signaling. Nature immunology *4*, 1057-1064.

Jung, S., Rajewsky, K., and Radbruch, A. (1993). Shutdown of class switch recombination by deletion of a switch region control element. Science *259*, 984-987.

Karasuyama, H., Kudo, A., and Melchers, F. (1990). The proteins encoded by the VpreB and lambda 5 pre-B cell-specific genes can associate with each other and with mu heavy chain. J Exp Med *172*, 969-972.

Kelly, G. L., Long, H. M., Stylianou, J., Thomas, W. A., Leese, A., Bell, A. I., Bornkamm, G. W., Mautner, J., Rickinson, A. B., and Rowe, M. (2009). An Epstein-Barr virus anti-apoptotic protein constitutively expressed in transformed cells and implicated in burkitt lymphomagenesis: the Wp/BHRF1 link. PLoS Pathog *5*, e1000341.

Kitamura, D., Kudo, A., Schaal, S., Muller, W., Melchers, F., and Rajewsky, K. (1992). A critical role of lambda 5 protein in B cell development. Cell *69*, 823-831.

Kitamura, D., and Rajewsky, K. (1992). Targeted disruption of mu chain membrane exon causes loss of heavy-chain allelic exclusion. Nature *356*, 154-156.

Kitamura, D., Roes, J., Kuhn, R., and Rajewsky, K. (1991). A B cell-deficient mouse by targeted disruption of the membrane exon of the immunoglobulin mu chain gene. Nature *350*, 423-426.

Klein, U., and Dalla-Favera, R. (2008). Germinal centres: role in B-cell physiology and malignancy. Nature reviews Immunology *8*, 22-33.

Klein, U., Klein, G., Ehlin-Henriksson, B., Rajewsky, K., and Kuppers, R. (1995). Burkitt's lymphoma is a malignancy of mature B cells expressing somatically mutated V region genes. Mol Med *1*, 495-505.

Klein, U., Tu, Y., Stolovitzky, G. A., Keller, J. L., Haddad, J., Jr., Miljkovic, V., Cattoretti, G., Califano, A., and Dalla-Favera, R. (2003a). Gene expression dynamics during germinal center transit in B cells. Ann N Y Acad Sci *987*, 166-172.

Kocks, C., and Rajewsky, K. (1988). Stepwise intraclonal maturation of antibody affinity through somatic hypermutation. Proc Natl Acad Sci U S A *85*, 8206-8210.

Kosco-Vilbois, M. H., and Scheidegger, D. (1995). Follicular dendritic cells: antigen retention, B cell activation, and cytokine production. Curr Top Microbiol Immunol *201*, 69-82.

Kovalchuk, A. L., Qi, C. F., Torrey, T. A., Taddesse-Heath, L., Feigenbaum, L., Park, S. S., Gerbitz, A., Klobeck, G., Hoertnagel, K., Polack, A*., et al.* (2000). Burkitt lymphoma in the mouse. The Journal of experimental medicine *192*, 1183-1190.

Kraus, M., Alimzhanov, M. B., Rajewsky, N., and Rajewsky, K. (2004). Survival of resting mature B lymphocytes depends on BCR signaling via the Igalpha/beta heterodimer. Cell *117*, 787-800.

Kraus, M., Pao, L. I., Reichlin, A., Hu, Y., Canono, B., Cambier, J. C., Nussenzweig, M. C., and Rajewsky, K. (2001). Interference with immunoglobulin (Ig)alpha immunoreceptor tyrosine-based activation motif (ITAM) phosphorylation modulates or blocks B cell development, depending on the availability of an Igbeta cytoplasmic tail. The Journal of experimental medicine *194*, 455-469.

Kress, T. R., Cannell, I. G., Brenkman, A. B., Samans, B., Gaestel, M., Roepman, P., Burgering, B. M., Bushell, M., Rosenwald, A., and Eilers, M. (2011). The MK5/PRAK kinase and Myc form a negative feedback loop that is disrupted during colorectal tumorigenesis. Molecular cell *41*, 445-457.

Küppers, R. (2005). Mechanisms of B-cell lymphoma pathogenesis. Nature reviews Cancer *5*, 251-262.

Kuppers, R., and Dalla-Favera, R. (2001). Mechanisms of chromosomal translocations in B cell lymphomas. Oncogene *20*, 5580-5594.

Kuppers, R., Klein, U., Hansmann, M. L., and Rajewsky, K. (1999). Cellular origin of human B-cell lymphomas. N Engl J Med *341*, 1520-1529.

Kurosaki, T. (2011). Regulation of BCR signaling. Molecular immunology *48*, 1287-1291.

Kurosaki, T., Shinohara, H., and Baba, Y. (2010). B cell signaling and fate decision. Annual review of immunology *28*, 21-55.

Laborda, J. (1991). 36B4 cDNA used as an estradiol-independent mRNA control is the cDNA for human acidic ribosomal phosphoprotein PO. Nucleic Acids Res *19*, 3998.

Lam, K. P., Kuhn, R., and Rajewsky, K. (1997). In vivo ablation of surface immunoglobulin on mature B cells by inducible gene targeting results in rapid cell death. Cell *90*, 1073-1083.

Levens, D. (2010). You Don't Muck with MYC. Genes Cancer *1*, 547-554.

Li, Q., and Verma, I. M. (2002). NF-kappaB regulation in the immune system. Nature reviews Immunology *2*, 725-734.

Lin, C. Y., Loven, J., Rahl, P. B., Paranal, R. M., Burge, C. B., Bradner, J. E., Lee, T. I., and Young, R. A. (2012). Transcriptional Amplification in Tumor Cells with Elevated c-Myc. Cell *151*, 56-67.

Livak, K. J., and Schmittgen, T. D. (2001). Analysis of relative gene expression data using real-time quantitative PCR and the 2(-Delta Delta C(T)) Method. Methods *25*, 402-408.

Lopes-Carvalho, T., Foote, J., and Kearney, J. F. (2005). Marginal zone B cells in lymphocyte activation and regulation. Curr Opin Immunol *17*, 244-250.

Lossos, I. S., Alizadeh, A. A., Eisen, M. B., Chan, W. C., Brown, P. O., Botstein, D., Staudt, L. M., and Levy, R. (2000). Ongoing immunoglobulin somatic mutation in germinal center B cell-like but not in activated B cell-like diffuse large cell lymphomas. Proceedings of the National Academy of Sciences of the United States of America *97*, 10209-10213.

Lyons, A. B., and Parish, C. R. (1994). Determination of lymphocyte division by flow cytometry. J Immunol Methods *171*, 131-137.

MacLennan, I. C., Toellner, K. M., Cunningham, A. F., Serre, K., Sze, D. M., Zuniga, E., Cook, M. C., and Vinuesa, C. G. (2003). Extrafollicular antibody responses. Immunol Rev *194*, 8-18.

Manis, J. P., van der Stoep, N., Tian, M., Ferrini, R., Davidson, L., Bottaro, A., and Alt, F. W. (1998). Class switching in B cells lacking 3' immunoglobulin heavy chain enhancers. The Journal of experimental medicine *188*, 1421-1431.

Manning, B. D., and Cantley, L. C. (2007). AKT/PKB signaling: navigating downstream. Cell *129*, 1261-1274.

Martin, F., and Kearney, J. F. (2002). Marginal-zone B cells. Nat Rev Immunol *2*, 323-335.

Matsuoka, M., Yoshida, K., Maeda, T., Usuda, S., and Sakano, H. (1990). Switch circular DNA formed in cytokine-treated mouse splenocytes: evidence for intramolecular DNA deletion in immunoglobulin class switching. Cell *62*, 135-142.

McHeyzer-Williams, L. J., Pelletier, N., Mark, L., Fazilleau, N., and McHeyzer-Williams, M. G. (2009). Follicular helper T cells as cognate regulators of B cell immunity. Current opinion in immunology *21*, 266-273.

McHeyzer-Williams, M., and Nussenzweig, M. C. (2009). Introduction to the section on lymphocyte activation and effector function. Current opinion in immunology *21*, 241-243.

McKean, D., Huppi, K., Bell, M., Staudt, L., Gerhard, W., and Weigert, M. (1984). Generation of antibody diversity in the immune response of BALB/c mice to influenza virus hemagglutinin. Proc Natl Acad Sci U S A *81*, 3180-3184.

Meeker, T., Lowder, J., Cleary, M. L., Stewart, S., Warnke, R., Sklar, J., and Levy, R. (1985). Emergence of idiotype variants during treatment of B-cell lymphoma with anti-idiotype antibodies. N Engl J Med *312*, 1658-1665.

Meffre, E., and Nussenzweig, M. C. (2002). Deletion of immunoglobulin beta in developing B cells leads to cell death. Proceedings of the National Academy of Sciences of the United States of America *99*, 11334-11339.

Meijer, L., Flajolet, M., and Greengard, P. (2004). Pharmacological inhibitors of glycogen synthase kinase 3. Trends Pharmacol Sci *25*, 471-480.

Mezzanzanica, D., Balladore, E., Turatti, F., Luison, E., Alberti, P., Bagnoli, M., Figini, M., Mazzoni, A., Raspagliesi, F., Oggionni, M*., et al.* (2004). CD95-mediated apoptosis is impaired at receptor level by cellular FLICE-inhibitory protein (long form) in wild-type p53 human ovarian carcinoma. Clin Cancer Res *10*, 5202-5214.

Miltenburger, H. G., Sachse, G., and Schliermann, M. (1987). S-phase cell detection with a monoclonal antibody. Dev Biol Stand *66*, 91-99.

Miltenyi, S., Muller, W., Weichel, W., and Radbruch, A. (1990). High gradient magnetic cell separation with MACS. Cytometry *11*, 231-238.

Molyneux, E. M., Rochford, R., Griffin, B., Newton, R., Jackson, G., Menon, G., Harrison, C. J., Israels, T., and Bailey, S. (2012). Burkitt's lymphoma. Lancet *379*, 1234-1244.

Muramatsu, M., Kinoshita, K., Fagarasan, S., Yamada, S., Shinkai, Y., and Honjo, T. (2000). Class switch recombination and hypermutation require activation-induced cytidine deaminase (AID), a potential RNA editing enzyme. Cell *102*, 553-563.

Musgrove, E. A., Caldon, C. E., Barraclough, J., Stone, A., and Sutherland, R. L. (2011). Cyclin D as a therapeutic target in cancer. Nature reviews Cancer *11*, 558-572.

Nasi, S., Ciarapica, R., Jucker, R., Rosati, J., and Soucek, L. (2001). Making decisions through Myc. FEBS Lett *490*, 153-162.

Neuberger, M. S., Ehrenstein, M. R., Klix, N., Jolly, C. J., Yelamos, J., Rada, C., and Milstein, C. (1998). Monitoring and interpreting the intrinsic features of somatic hypermutation. Immunol Rev *162*, 107-116.

Nie, Z., Hu, G., Wei, G., Cui, K., Yamane, A., Resch, W., Wang, R., Green, D. R., Tessarollo, L., Casellas, R.*, et al.* (2012). c-Myc Is a Universal Amplifier of Expressed Genes in Lymphocytes and Embryonic Stem Cells. Cell *151*, 68-79.

Okkenhaug, K., and Vanhaesebroeck, B. (2003). PI3K in lymphocyte development, differentiation and activation. Nature reviews Immunology *3*, 317-330.

Ong, S. E., Blagoev, B., Kratchmarova, I., Kristensen, D. B., Steen, H., Pandey, A., and Mann, M. (2002). Stable isotope labeling by amino acids in cell culture, SILAC, as a simple and accurate approach to expression proteomics. Mol Cell Proteomics *1*, 376-386.

Ong, S. E., and Mann, M. (2007). Stable isotope labeling by amino acids in cell culture for quantitative proteomics. Methods Mol Biol *359*, 37-52.

Papavasiliou, F. N., and Schatz, D. G. (2002). Somatic hypermutation of immunoglobulin genes: merging mechanisms for genetic diversity. Cell *109 Suppl*, S35-44.

Park, S., Chung, S., Kim, K. M., Jung, K. C., Park, C., Hahm, E. R., and Yang, C. H. (2004). Determination of binding constant of transcription factor myc-max/max-max and E-box DNA: the effect of inhibitors on the binding. Biochim Biophys Acta *1670*, 217-228.

Peitz, M., Pfannkuche, K., Rajewsky, K., and Edenhofer, F. (2002). Ability of the hydrophobic FGF and basic TAT peptides to promote cellular uptake of recombinant Cre recombinase: a tool for efficient genetic engineering of mammalian genomes. Proceedings of the National Academy of Sciences of the United States of America *99*, 4489-4494.

Pelicci, P. G., Knowles, D. M., 2nd, Magrath, I., and Dalla-Favera, R. (1986). Chromosomal breakpoints and structural alterations of the c-myc locus differ in endemic and sporadic forms of Burkitt lymphoma. Proceedings of the National Academy of Sciences of the United States of America *83*, 2984-2988.

Peng, T., Golub, T. R., and Sabatini, D. M. (2002). The immunosuppressant rapamycin mimics a starvation-like signal distinct from amino acid and glucose deprivation. Molecular and cellular biology *22*, 5575-5584.

Petersen-Mahrt, S. K., Harris, R. S., and Neuberger, M. S. (2002). AID mutates E. coli suggesting a DNA deamination mechanism for antibody diversification. Nature *418*, 99-103.

Pham, P., Bransteitter, R., Petruska, J., and Goodman, M. F. (2003). Processive AID-catalysed cytosine deamination on single-stranded DNA simulates somatic hypermutation. Nature *424*, 103-107.

Pillai, S., Cariappa, A., and Moran, S. T. (2004). Positive selection and lineage commitment during peripheral B-lymphocyte development. Immunological reviews *197*, 206-218.

Pomerantz, J. L., and Baltimore, D. (2002). Two pathways to NF-kappaB. Molecular cell *10*, 693-695.

Radtke, F., Fasnacht, N., and Macdonald, H. R. (2010). Notch signaling in the immune system. Immunity *32*, 14-27.

Rajewsky, K. (1996). Clonal selection and learning in the antibody system. Nature *381*, 751-758.

Rappsilber, J., Mann, M., and Ishihama, Y. (2007). Protocol for micro-purification, enrichment, pre-fractionation and storage of peptides for proteomics using StageTips. Nat Protoc *2*, 1896-1906.

Reaban, M. E., Lebowitz, J., and Griffin, J. A. (1994). Transcription induces the formation of a stable RNA.DNA hybrid in the immunoglobulin alpha switch region. J Biol Chem *269*, 21850-21857.

Refaeli, Y., Young, R. M., Turner, B. C., Duda, J., Field, K. A., and Bishop, J. M. (2008). The B cell antigen receptor and overexpression of MYC can cooperate in the genesis of B cell lymphomas. PLoS biology *6*, e152.

Reth, M., Hombach, J., Wienands, J., Campbell, K. S., Chien, N., Justement, L. B., and Cambier, J. C. (1991). The B-cell antigen receptor complex. Immunol Today *12*, 196-201.

Retter, M. W., and Nemazee, D. (1998). Receptor editing occurs frequently during normal B cell development. J Exp Med *188*, 1231-1238.

Revy, P., Muto, T., Levy, Y., Geissmann, F., Plebani, A., Sanal, O., Catalan, N., Forveille, M., Dufourcq-Labelouse, R., Gennery, A.*, et al.* (2000). Activation-induced cytidine deaminase (AID) deficiency causes the autosomal recessive form of the Hyper-IgM syndrome (HIGM2). Cell *102*, 565-575.

Rhiner, C., Lopez-Gay, J. M., Soldini, D., Casas-Tinto, S., Martin, F. A., Lombardia, L., and Moreno, E. (2010). Flower forms an extracellular code that reveals the fitness of a cell to its neighbors in Drosophila. Developmental cell *18*, 985-998.

Richter, J., Schlesner, M., Hoffmann, S., Kreuz, M., Leich, E., Burkhardt, B., Rosolowski, M., Ammerpohl, O., Wagener, R., Bernhart, S. H.*, et al.* (2012). Recurrent mutation of the ID3 gene in Burkitt lymphoma identified by integrated genome, exome and transcriptome sequencing. Nature genetics.

Rockwood, L. D., Torrey, T. A., Kim, J. S., Coleman, A. E., Kovalchuk, A. L., Xiang, S., Ried, T., Morse, H. C., 3rd, and Janz, S. (2002). Genomic instability in mouse Burkitt

lymphoma is dominated by illegitimate genetic recombinations, not point mutations. Oncogene *21*, 7235-7240.

Rowe, M., Kelly, G. L., Bell, A. I., and Rickinson, A. B. (2009). Burkitt's lymphoma: the Rosetta Stone deciphering Epstein-Barr virus biology. Semin Cancer Biol *19*, 377-388.

Rowley, R. B., Burkhardt, A. L., Chao, H. G., Matsueda, G. R., and Bolen, J. B. (1995). Syk protein-tyrosine kinase is regulated by tyrosine-phosphorylated Ig alpha/Ig beta immunoreceptor tyrosine activation motif binding and autophosphorylation. J Biol Chem *270*, 11590-11594.

Ruland, J., and Mak, T. W. (2003). Transducing signals from antigen receptors to nuclear factor kappaB. Immunological reviews *193*, 93-100.

Saijo, K., Schmedt, C., Su, I. H., Karasuyama, H., Lowell, C. A., Reth, M., Adachi, T., Patke, A., Santana, A., and Tarakhovsky, A. (2003). Essential role of Src-family protein tyrosine kinases in NF-kappaB activation during B cell development. Nature immunology *4*, 274-279.

Sale, J. E., and Neuberger, M. S. (1998). TdT-accessible breaks are scattered over the immunoglobulin V domain in a constitutively hypermutating B cell line. Immunity *9*, 859-869.

Sambrook, J., and Russell, D. W. (2001). Molecular cloning : a laboratory manual, 3rd edn (Cold Spring Harbor, N.Y.: Cold Spring Harbor Laboratory Press).

Sander, S., Calado, D. P., Srinivasan, L., Kochert, K., Zhang, B., Rosolowski, M., Rodig, S. J., Holzmann, K., Stilgenbauer, S., Siebert, R.*, et al.* (2012). Synergy between PI3K signaling and MYC in Burkitt lymphomagenesis. Cancer Cell *22*, 167-179.

Sasaki, K., Murakami, T., and Takahashi, M. (1989). [Flow cytometric analysis of cell proliferation kinetics using the anti-BrdUrd antibody]. Gan To Kagaku Ryoho *16*, 2338-2344.

Schmidt-Supprian, M., and Rajewsky, K. (2007). Vagaries of conditional gene targeting. Nature immunology *8*, 665-668.

Schmitt, C. A., McCurrach, M. E., de Stanchina, E., Wallace-Brodeur, R. R., and Lowe, S. W. (1999). INK4a/ARF mutations accelerate lymphomagenesis and promote chemoresistance by disabling p53. Genes & development *13*, 2670-2677.

Schmitz, R., Young, R. M., Ceribelli, M., Jhavar, S., Xiao, W., Zhang, M., Wright, G., Shaffer, A. L., Hodson, D. J., Buras, E.*, et al.* (2012). Burkitt lymphoma pathogenesis and therapeutic targets from structural and functional genomics. Nature *490*, 116-120.

Schwarze, S. R., Hruska, K. A., and Dowdy, S. F. (2000). Protein transduction: unrestricted delivery into all cells? Trends Cell Biol *10*, 290-295.

Schwickert, T. A., Lindquist, R. L., Shakhar, G., Livshits, G., Skokos, D., Kosco-Vilbois, M. H., Dustin, M. L., and Nussenzweig, M. C. (2007). In vivo imaging of germinal centres reveals a dynamic open structure. Nature *446*, 83-87.

Shinohara, H., Yasuda, T., Aiba, Y., Sanjo, H., Hamadate, M., Watarai, H., Sakurai, H., and Kurosaki, T. (2005). PKC beta regulates BCR-mediated IKK activation by facilitating the interaction between TAK1 and CARMA1. The Journal of experimental medicine *202*, 1423-1431.

Silver, D. P., and Livingston, D. M. (2001). Self-excising retroviral vectors encoding the Cre recombinase overcome Cre-mediated cellular toxicity. Molecular cell *8*, 233-243.

Smith, K. G., Hewitson, T. D., Nossal, G. J., and Tarlinton, D. M. (1996). The phenotype and fate of the antibody-forming cells of the splenic foci. Eur J Immunol *26*, 444-448.

Smolewski, P., Grabarek, J., Halicka, H. D., and Darzynkiewicz, Z. (2002). Assay of caspase activation in situ combined with probing plasma membrane integrity to detect three distinct stages of apoptosis. J Immunol Methods *265*, 111-121.

Srinivasan, L., Sasaki, Y., Calado, D. P., Zhang, B., Paik, J. H., DePinho, R. A., Kutok, J. L., Kearney, J. F., Otipoby, K. L., and Rajewsky, K. (2009). PI3 kinase signals BCR-dependent mature B cell survival. Cell *139*, 573-586.

Staudt, L. M. (2010). Oncogenic activation of NF-kappaB. Cold Spring Harb Perspect Biol *2*, a000109.

Stevenson, F., Sahota, S., Zhu, D., Ottensmeier, C., Chapman, C., Oscier, D., and Hamblin, T. (1998). Insight into the origin and clonal history of B-cell tumors as revealed by analysis of immunoglobulin variable region genes. Immunological reviews *162*, 247-259.

Su, I., and Tarakhovsky, A. (2000). B-1 cells: orthodox or conformist? Curr Opin Immunol *12*, 191-194.

Taub, R., Kirsch, I., Morton, C., Lenoir, G., Swan, D., Tronick, S., Aaronson, S., and Leder, P. (1982). Translocation of the c-myc gene into the immunoglobulin heavy chain locus in human Burkitt lymphoma and murine plasmacytoma cells. Proc Natl Acad Sci U S A *79*, 7837-7841.

Thome, M. (2004). CARMA1, BCL-10 and MALT1 in lymphocyte development and activation. Nature reviews Immunology *4*, 348-359.

Thome, M., and Tschopp, J. (2003). TCR-induced NF-kappaB activation: a crucial role for Carma1, Bcl10 and MALT1. Trends in immunology *24*, 419-424.

Tiegs, S. L., Russell, D. M., and Nemazee, D. (1993). Receptor editing in self-reactive bone marrow B cells. J Exp Med *177*, 1009-1020.

Torres, R. M., Flaswinkel, H., Reth, M., and Rajewsky, K. (1996). Aberrant B cell development and immune response in mice with a compromised BCR complex. Science *272*, 1804-1808.

Tsubata, T., and Reth, M. (1990). The products of pre-B cell-specific genes (lambda 5 and VpreB) and the immunoglobulin mu chain form a complex that is transported onto the cell surface. J Exp Med *172*, 973-976.

Tsujimoto, Y., Gorham, J., Cossman, J., Jaffe, E., and Croce, C. M. (1985). The t(14;18) chromosome translocations involved in B-cell neoplasms result from mistakes in VDJ joining. Science *229*, 1390-1393.

Turner, M., Mee, P. J., Costello, P. S., Williams, O., Price, A. A., Duddy, L. P., Furlong, M. T., Geahlen, R. L., and Tybulewicz, V. L. (1995). Perinatal lethality and blocked B-cell development in mice lacking the tyrosine kinase Syk. Nature *378*, 298-302.

Vanderlaan, M., and Thomas, C. B. (1985). Characterization of monoclonal antibodies to bromodeoxyuridine. Cytometry *6*, 501-505.

Vereide, D. T., and Sugden, B. (2011). Lymphomas differ in their dependence on Epstein-Barr virus. Blood *117*, 1977-1985.

Verkoczy, L., Duong, B., Skog, P., Ait-Azzouzene, D., Puri, K., Vela, J. L., and Nemazee, D. (2007). Basal B cell receptor-directed phosphatidylinositol 3-kinase signaling turns off RAGs and promotes B cell-positive selection. J Immunol *178*, 6332-6341.

Victora, G. D., and Nussenzweig, M. C. (2012). Germinal centers. Annual review of immunology *30*, 429-457.

Victora, G. D., Schwickert, T. A., Fooksman, D. R., Kamphorst, A. O., Meyer-Hermann, M., Dustin, M. L., and Nussenzweig, M. C. (2010). Germinal center dynamics revealed by multiphoton microscopy with a photoactivatable fluorescent reporter. Cell *143*, 592-605.

Vogt, P. K., Jiang, H., and Aoki, M. (2005). Triple layer control: phosphorylation, acetylation and ubiquitination of FOXO proteins. Cell Cycle *4*, 908-913.

Wade, M., and Wahl, G. M. (2006). c-Myc, genome instability, and tumorigenesis: the devil is in the details. Curr Top Microbiol Immunol *302*, 169-203.

Wagner, S. D., and Neuberger, M. S. (1996). Somatic hypermutation of immunoglobulin genes. Annu Rev Immunol *14*, 441-457.

Warburg, O. (1956). On the origin of cancer cells. Science *123*, 309-314.

Welcker, M., Orian, A., Grim, J. E., Eisenman, R. N., and Clurman, B. E. (2004). A nucleolar isoform of the Fbw7 ubiquitin ligase regulates c-Myc and cell size. Current biology : CB *14*, 1852-1857.

Werner, M., Hobeika, E., and Jumaa, H. (2010). Role of PI3K in the generation and survival of B cells. Immunological reviews *237*, 55-71.

Willis, T. G., and Dyer, M. J. (2000). The role of immunoglobulin translocations in the pathogenesis of B-cell malignancies. Blood *96*, 808-822.

Wotherspoon, A. C., Doglioni, C., Diss, T. C., Pan, L., Moschini, A., de Boni, M., and Isaacson, P. G. (1993). Regression of primary low-grade B-cell gastric lymphoma of mucosa-associated lymphoid tissue type after eradication of Helicobacter pylori. Lancet *342*, 575-577.

Xu, C., Kim, N. G., and Gumbiner, B. M. (2009). Regulation of protein stability by GSK3 mediated phosphorylation. Cell Cycle *8*, 4032-4039.

Yada, M., Hatakeyama, S., Kamura, T., Nishiyama, M., Tsunematsu, R., Imaki, H., Ishida, N., Okumura, F., Nakayama, K., and Nakayama, K. I. (2004). Phosphorylation-dependent degradation of c-Myc is mediated by the F-box protein Fbw7. Embo J *23*, 2116-2125.

Ye, B. H., Rao, P. H., Chaganti, R. S., and Dalla-Favera, R. (1993). Cloning of bcl-6, the locus involved in chromosome translocations affecting band 3q27 in B-cell lymphoma. Cancer Res *53*, 2732-2735.

Young, R. M., Hardy, I. R., Clarke, R. L., Lundy, N., Pine, P., Turner, B. C., Potter, T. A., and Refaeli, Y. (2009). Mouse models of non-Hodgkin lymphoma reveal Syk as an important therapeutic target. Blood *113*, 2508-2516.

Yu, K., Chedin, F., Hsieh, C. L., Wilson, T. E., and Lieber, M. R. (2003). R-loops at immunoglobulin class switch regions in the chromosomes of stimulated B cells. Nat Immunol *4*, 442-451.

Yuneva, M., Zamboni, N., Oefner, P., Sachidanandam, R., and Lazebnik, Y. (2007). Deficiency in glutamine but not glucose induces MYC-dependent apoptosis in human cells. The Journal of cell biology *178*, 93-105.

Zhang, B., Kirov, S., and Snoddy, J. (2005). WebGestalt: an integrated system for exploring gene sets in various biological contexts. Nucleic Acids Res *33*, W741-748.

Zhang, J., Bottaro, A., Li, S., Stewart, V., and Alt, F. W. (1993). A selective defect in IgG2b switching as a result of targeted mutation of the I gamma 2b promoter and exon. Embo J *12*, 3529-3537.

Zhang, W., Bardwell, P. D., Woo, C. J., Poltoratsky, V., Scharff, M. D., and Martin, A. (2001). Clonal instability of V region hypermutation in the Ramos Burkitt's lymphoma cell line. Int Immunol *13*, 1175-1184.

Zhong, L., D'Urso, A., Toiber, D., Sebastian, C., Henry, R. E., Vadysirisack, D. D., Guimaraes, A., Marinelli, B., Wikstrom, J. D., Nir, T.*, et al.* (2010). The histone deacetylase Sirt6 regulates glucose homeostasis via Hif1alpha. Cell *140*, 280-293.